UNIVERSITY OF WARMIA AND MAZURY IN OLSZTYN

Technical Sciences

10

PUBLISHER UWM

OLSZTYN 2007

EDITORIAL BOARD
Leszek Mieszkalski (Editor-in-Chief) – University of Warmia and Mazury in Olsztyn,
Stefan Cenkowski – University of Manitoba, Canada, Adam Chrzanowski – University of New Brunswick, Canada, Janusz Laskowski – University of Agriculture in Lublin,
Władimir Nikołajewicz Tilipałow – University of Technical in Kaliningrad, Russia,
Alojzy Wasilewski – University of Warmia and Mazury in Olsztyn

Executive Editor
Mariola Jezierska

The Journal is also available in electronic form.
The online edition is hosted by Metapress (www.metapress.com)
in partnership with Versita (www.versita.com)

PL ISSN 1505–4675

© Copyright by Wydawnictwo UWM • Olsztyn 2007

Address
ul. Jana Heweliusza 14
10-718 Olsztyn-Kortowo, Poland
tel.: (48) 089 523 36 61
fax: (48) 089 523 34 38
e-mail: wydawca@uwm.edu.pl

Ark. wyd. 8,31, ark. druk. 6,75
Druk: Zakład Poligraficzny UWM, zam. nr 669

Contents

Agricultural Engineering

A. Ciupak, I. Szczurowska, B. Gładyszewska, S. Pietruszewski – *Impact of Laser Light and Magnetic Field Stimulation on the Process of Buckwheat Seed Germination* 1
A. Ciupak, I. Szczurowska, B. Gładyszewska, S. Pietruszewski – *Germination of Buckwheat Seeds Subject to Storage Time and Electromagnetic Stimulation Methods* 11
J. Pawlak – *Model Method for Economically Reasonable Choice of Agricultural Machine* 19

Mechanical Sciences

S. Zeman, Ľ. Kubík – *Permeability of Polymeric Packaging Materials* 26
S. Zeman – *Mechanical Properties to Measure Resistance of Food Packaging Materials to External Influences* 35
J. Domański, G. Żywica – *Optimization of the Construction of a Pressure Tank using CAD/CAE Systems* 41
J. Pršan, M. Kučera – *Possibilities of Application of Stochastic Process Theory in Evaluation of Tribological Experiment* 59
J. Dobriański, M. Duda – *An Algorithm for Handling Experimental Data of PERiodical Processes with Microsoft EXCEL* 69
A. Molchanov, A. Wróblewski – *Study of Negative Pressure in Suction PROPeller and Tube Agitators* 81
A. Mazurkiewicz, T. Topoliński – *Relations Among Strength and Structure Osteoporotic and Coxarthrotic Trabecular Bone* 87
A. Wieromiej-Ostrowska – *The Singularities at the Vicinity of the Triple Point of Contact of Three Orthotropic Wedges in Plane Elasticity* 95

Spis treści

Inżynieria rolnicza

A. Ciupak, I. Szczurowska, B. Gładyszewska, S. Pietruszewski – *Analiza wpływu światła laserowego i pola magnetycznego na proces kiełkowania nasion gryki* 1
A. Ciupak, I. Szczurowska, B. Gładyszewska, S. Pietruszewski – *Przebieg procesu kiełkowania nasion gryki w zależności od czasu przechowywania oraz elektromagnetycznych metod stymulacji* 11
J. Pawlak – *Metoda modelowa ekonomicznie uzasadnionego doboru maszyn rolniczych* 19

Mechanika

S. Zeman, Ľ. Kubík – *Przepuszczalność polimerowych materiałów opakowaniowych* 26
S. Zeman – *Właściwości mechaniczne opakowań i ich odporność na obciążenia zewnętrzne* 35
J. Domański, G. Żywica – *Optymalizacja konstrukcji zbiornika ciśnieniowego z wykorzystaniem systemów CAD/CAE* 41
J. Pršan, M. Kučera – *Możliwości wykorzystania teorii procesów stochastycznych do oceny eksperymentu tribologicznego* 59
J. Dobriański, M. Duda – *Algorytm opracowania w EXCELU danych eksperymentalnych procesów okresowych* 69
A. Molchanov, A. Wróblewski – *Badanie podciśnienia w mieszadłach samozasysających śmigłowych i rurkowych* 81
A. Mazurkiewicz, T. Topoliński – *Relacje między wytrzymałością a strukturą osteoporotycznej i koksartrycznej kości beleczkowej* 87
A. Wieromiej-Ostrowska – *Rząd osobliwości w otoczeniu wierzchołka potrójnego punktu kontaktu trzech klinów w płaskim zagadnieniu teorii sprężystości* 95

TECHNICAL SCIENCES
Abbrev.: Techn. Sc., No 10, Y 2007

DOI 10.2478/v10022-007-0002-8

IMPACT OF LASER LIGHT AND MAGNETIC FIELD STIMULATION ON THE PROCESS OF BUCKWHEAT SEED GERMINATION

Anna Ciupak, Izabela Szczurowska, Bożena Gładyszewska, Stanisław Pietruszewski

Department of Physics
Agricultural University in Lublin

Key words: buckwheat, germination, laser stimulation, magnetic field, simulation model.

Abstract

This paper presents the results of research on the influence of laser and magnetic field stimulation and the combination of both stimulants on the process of germination of buckwheat cv. "Kora" seeds. Germination tests were carried out in a controlled environment chamber with a stable temperature of 21°C, stable humidity and without a source of light. The curves obtained during the experiment were described based on a simulation model. The applied physical stimulation factors affected the germination rate of buckwheat seeds, but they did not increase the final number of germinated seeds.

ANALIZA WPŁYWU ŚWIATŁA LASEROWEGO I POLA MAGNETYCZNEGO NA PROCES KIEŁKOWANIA NASION GRYKI

Anna Ciupak, Izabela Szczurowska, Bożena Gładyszewska, Stanisław Pietruszewski

Katedra Fizyki
Akademia Rolnicza w Lublinie

Słowa kluczowe: gryka, kiełkowanie, stymulacja laserowa, pole magnetyczne, model symulacyjny.

Streszczenie

W pracy przedstawiono wyniki badań nad wpływem światła laserowego, pola magnetycznego oraz kombinacji tych czynników na proces kiełkowania nasion gryki odmiany Kora. Testy kiełkowania przeprowadzono w komorze klimatycznej w stabilnej temperaturze 21°C, stałej wilgotności i bez dostępu światła. Krzywe doświadczalne otrzymane na podstawie eksperymentu opisano za pomocą modelu symulacyjnego. Poddanie badanych nasion działaniu fizycznych czynników stymulacyjnych wywarło wpływ na tempo ich kiełkowania, jednak nie odnotowano zwiększenia końcowej liczby wykiełkowanych nasion.

Introduction

Plant production requires seeds which meet adequate qualitative standards. The obtained seeds are both the means of the production process and its goal (Grzesiuk, Kulka 1981), which is why the use of good quality material determines the germination process and affects the height and quality of the yield. Factors which play the most important role in the germination process include genetic and environmental conditions (hydration, access to air, adequate temperature) as well as seed growth conditions. Seeds have to be adequately prepared prior to sowing with the application of chemical agents (seed dressing, growth regulators) or physical factors (Vasilewski 2003) (magnetic and electric field, ionizing, microwave and laser radiation) which usually have a positive effect on the germination process and the yield.

The authors of this study aimed to analyze the impact of stimulation with a He-Ne laser beam (Ciupak i in. 2006), magnetic field and a combination of the above factors on the process of buckwheat seed germination. Physical stimulation factors have already been applied to various vegetables, including tomatoes (Gładyszewska 1998, Gładyszewska, Koper 2002a, Gładyszewska, Koper 2002b, Koper i in. 2001) onions (Pietruszewski i in. 2002a, Prokop i in. 2001, Prokop i in. 2002), cabbage (Pietruszewski i in. 2002b), radishes (Pietruszewski i in. 2002c, Prokop i in. 2002a), spinach (Pietruszewski i in. 2002c), sugar beets (Koper i in. 2002, Pietruszewski 2000), pulse crops – faba beans (Podleśny 2002, Podleśny, Podleśna 2007, Podleśny, Podleśna 2004), cereals – wheat (Kordas 2002, Komarzyński i in. 2004, Pietruszewski 1999, Pietruszewski i in. 2002c), barley (Rybiński i in 2004, Rybiński i in 2002), oat (Drozd i in. 2004), maize (Rochalska 1997, Rochalska 2002), flax (Olchowik, Gawda 2002) and plants of the family Brassicaceae, including thale cress (Qin i in. 2006) and woad (used in the production of indigo pigment) (Yi-Ping Chena i in 2005). The results of many research studies indicate that vegetable seeds are more susceptible to stimulation. The effect of pre-sowing simulation on the germination of buckwheat seeds (which is classified as a cereal only due to a similar farming technology) and the extent to which it affects the germination process have not been investigated to date.

The objective of this study was to determine the impact of laser beam and magnetic field stimulation on the process of buckwheat seed germination and to verify the possibility of applying the simulation model to the description of the germination process.

Materials and methods

The experimental material comprising buckwheat cv. Kora seeds (harvested in 2003) was subjected to laser stimulation (in 3 series during the free fall of seeds from the charging hopper chute) with a He-Ne laser beam with

a wavelength of λ=630 nm and density power of 4 mW/cm^2 (group L), magnetic field stimulation with an intensity of 30 mT (group M) and a combination of the above factors (groups LM and ML). The time of exposure to a variable magnetic field with a frequency of 50 Hz was 8 seconds. The germination of buckwheat seeds (placed in a controlled environment chamber) was observed at a stable temperature of 21°C, with stable humidity and without a source of light. Each group was represented by 400 seeds sown on Petri dishes (on stimulation day) in 4 samples of 100 seeds each. Germinated seeds (showing germs with a minimum length of 2 mm) were counted every 1–2 hours beginning from the appearance of the first germ (when germination was most intense). The time intervals in which germs were counted were gradually extended due to decreasing germination intensity. As a point of reference for further analysis, the study involved control groups of non-stimulated buckwheat seeds. Based on the obtained results, the percentage of germinated seeds N_k was calculated with the use of the below formula:

$$N_k = \frac{n_k}{n_c} \cdot 100\%$$

where:
n_k – number of germinated seeds,
n_c – total number of sown seeds

The germination rate S_k (seed/h) of buckwheat seeds was calculated with the use of the below formula:

$$S_k = \frac{n_{\max}}{\Delta t}$$

where:
$n_{\max}$ – maximum number of germinated seeds recorded during the count,
Δt – time interval between two successive counts.

The relative germination rate coefficient W_k was determined with the use of the below formula:

$$W_k = \frac{n(t)}{n_{\text{control}}}$$

where:
$n(t)$ – number of seeds germinated in time t,
n_{control} – number of control group seeds germinated in given time t.

A simulation model (Gładyszewska 1998, Gładyszewska, Koper 2002a, Gładyszewska, Koper 2002b) was applied for the mathematical description of experimental results. The change in the $n(t)$ number of germinated seeds in a given time interval is described with the following formula:

$$n(t) = n_k \cdot \left(1 - \frac{\alpha \cdot e^{-\lambda_1 (t-t_0)} + \beta \cdot e^{-\lambda_2 (t-t_0)} + \gamma \cdot e^{-\lambda_3 (t-t_0)}}{\alpha + \beta + \gamma} \right)$$

where:

$$\alpha = \lambda_2 \cdot \lambda_3 \cdot (\lambda_2 - \lambda_3)$$

$$\beta = \lambda_3 \cdot \lambda_1 \cdot (\lambda_3 - \lambda_1)$$

$$\gamma = \lambda_1 \cdot \lambda_2 \cdot (\lambda_1 - \lambda_2)$$

Parameters λ_1, λ_2, λ_3 indicate the probability of seed evolution from one growth phase to another; n_k is the final number of germinated seeds; t is the germination time (h); t_0 is time between the end of the latent development phase and the beginning of germ formation phase.

Results and discussion

Common buckwheat (Fagopyrum esculentum Moench) is characterized by high heat requirements and frost sensitivity. According to professional literature (Grzesiuk, Kulka 1981), the most favorable growth environment for the common buckwheat is at a temperature range of 20–25°C. For this reason, the authors of this study decided to adopt the optimal temperature for the analysis of the germination process. When conducted at the above temperature range, the experiment produces results already after 24 hours from sowing.

The obtained data were applied to determine the final number of germinated buckwheat seeds N_k (in %) and to calculate the germination rate S_k. Five special time points (corresponding to successive germination days) were also identified in the observed process for which the change in the percentage of germinated seeds relative to the control group was analyzed. A comparison of the obtained results indicates that none of the applied stimulation methods reduced the time of germination of the first seeds. Germination time in all groups was 24 hours. As of that moment, an increase in the number of germinated seeds (Fig. 1) was also observed, and a 7% increase in that number was reported on the second day after sowing in respect of seeds which were subjected to laser beam stimulation followed by magnetic field stimulation (group LM) in comparison with control (71%). The number of germinated seeds was 11.5% higher for the same combination of stimulating factors (LM) than in the group of seeds where magnetic field was applied as the first stimulant – ML (66.5%). At the third point indicated on the time axis (hour 72 after sowing), the number of germs increased by 6% within 24 hours in the control group and group LM, and by 8.5% in group ML. The number of germinated seeds in group LM was also higher in comparison with the control group (77%) at the same time point (second

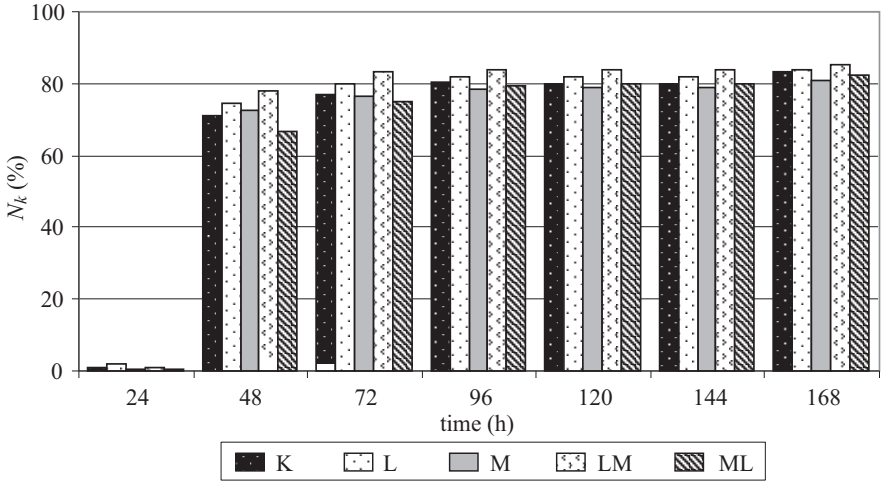

Fig. 1. Number of germinated seeds N_k (%) as a function of germination time

germination day). This was confirmed by a statistical analysis based on testing the hypothesis of the difference between two means (at a significance level of α=0.05). With a combination of factors where laser beam stimulation was followed by magnetic field stimulation (group LM), the final value N_k reached 84% as soon as in hour 48 of the germination process.

A minimum percentage increase in the number of germinated seeds was observed on the third day after the appearance of the first germs, i.e. in hour 96 after sowing, both in the group of stimulated seeds and in the control group. At the fifth time point, which marks the moment when the last germinated seeds were counted (sixth germination day), the final number of germinated seeds was determined. The obtained results indicate that the rate of the germination process was uniform at the end of the experiment (Fig. 1) and that none of the applied stimulation factors increased the final number of germinated seeds.

Based on observation data obtained in the first 24 hours of the germination process, the value of the relative germination rate coefficient W_k (Tab. 1)

Table 1

Relative germination rate coefficients

Hour	L	M	LM	ML
26	1.09	1	1.09	0.36
28	0.87	0.8	0.97	0.83
30	1.23	1.31	0.77	1.14
32	0.73	0.87	0.83	0.79
33	1.83	1.17	1.52	1.00
35	1.37	1.3	1.43	1.07
48	0.9	0.93	1.43	1.05

was determined and changes in that coefficient as a function of seed germination time were presented in graphic form (Fig. 2).

The highest germination intensity (42 germinated seeds in 1 hour) was reported in the group of seeds stimulated with a He-Ne laser beam in hour

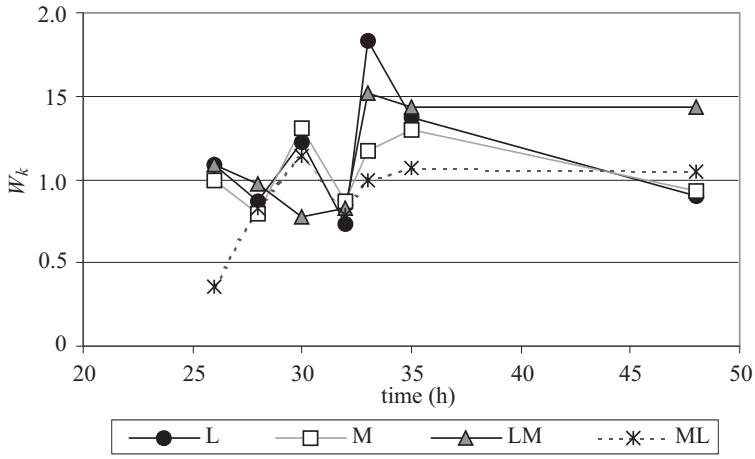

Fig. 2. Relative germination rate coefficient as a function of seed germination time

9 after the appearance of the first germs (the relative germination rate coefficient for that group of seeds relevant to control was 1.83). The value of W_k for seeds stimulated with a laser beam and, subsequently, a magnetic field reached 1.52 at the same time, and it remained at the highest level among all groups stimulated in successive hours of the count (Tab. 1).

Figure 3 presents the germination rate S_k of buckwheat seeds subject to the applied stimulation method. The curves representing particular seed groups illustrate changes in the number of germinated seeds in every time interval. They can be used for a detailed analysis of the initial phase of the germination process.

In comparison with the description of the control group, the shape of the presented curves points to certain changes which resulted from the applied stimulating factors. The maximum germination rate in the control group and in groups M and ML decreased in hour 8 of the analyzed process. A higher number of germinated seeds at that point was observed only in the control group. Nine hours after the appearance of the first germs, the highest S_k value was reported in the group of seeds stimulated with laser and in the laser and magnetic field combination group. In hour 24 of the process (48 hours after sowing), the germination rate was similar in all groups.

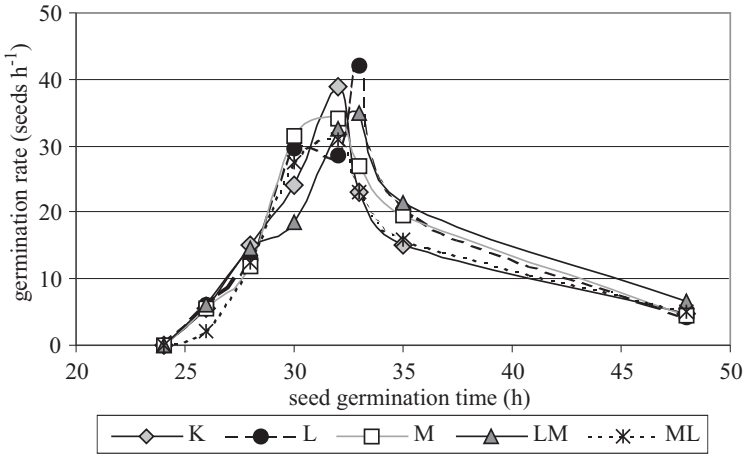

Fig 3. Seed germination rate

Table 2 presents curve parameters which describe the experimental data from the simulation process. The analysis of the course of the curves presented in Figure 4 indicates that the applied model adequately represents the germination process of buckwheat seeds, including both the stimulated and control groups.

Table 2.

Parameters for adjusting the simulation curve to experimental points at a temperature of 21°C

Simulation model					
Stimulation factor	λ_1	λ_2	λ_3	t_o (h)	n_k
Control	0.100	0.96	0.98	23.8	324
Laser	0.120	0.78	0.82	23.8	331
Magnetic field	0.140	0.92	0.96	24.4	316
Laser + Magnetic field	0.140	0.50	0.52	24.4	341
Magnetic field + Laser	0.086	0.96	0.98	24.0	320

A statistical analysis based on testing the hypothesis of the difference between two means with the use of Student's t-test (at a significance level of α=0.05) showed that the applied stimulating factors did not increase the final number of germinated buckwheat seeds.

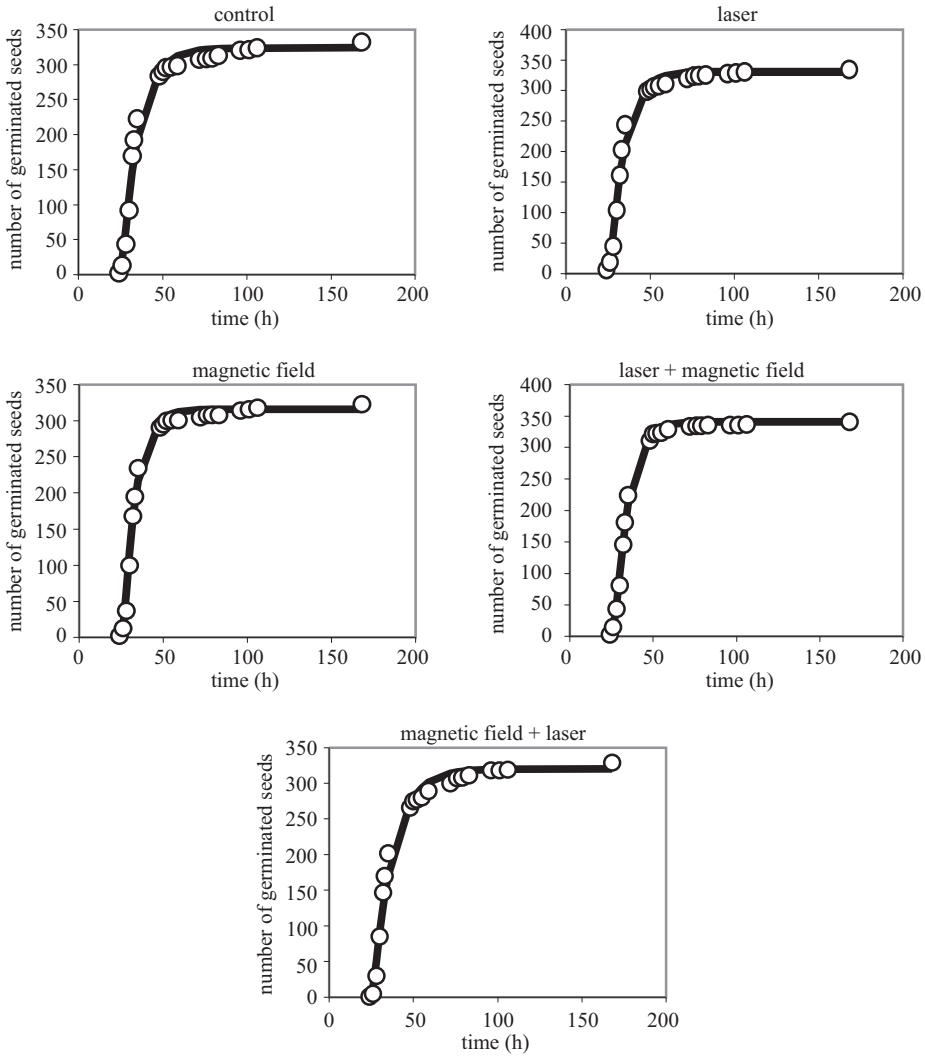

Fig. 4. Experimental germination curves (o) and model curves (-) generated based on the simulation model at a temperature of 21°C

Conclusions

1. The course of curves mapping the germination rate of stimulated seeds point to a certain dependency on the applied physical factors.

2. None of the applied stimulating factors accelerated the beginning of the germination process of buckwheat seeds.

3. There were no statistically significant differences in the final number of germinated seeds which were subjected to stimulation.

4. A 7% increase in the number of germinated seeds subjected to laser stimulation followed by magnetic stimulation was observed (in comparison with control) at the initial germination stage (48 hours after sowing).

5. The highest germination intensity expressed by the value of coefficient W_k was observed in hour 33 and 35 after sowing.

6. The applied simulation model is highly effective in describing experimental points for both the control and stimulated seed groups.

References

Ciupak A., Gładyszewska B., Pietruszewski S. 2006. *Wpływ stymulacji laserowej i temperatury na proces kiełkowania nasion gryki odmiany Kora.* Fragmenta Agronomica, 1: 23–35,.

Drozd D., Szajsner H., Bieniek J., Banasiak J. 2004. *Wpływ stymulacji laserowej na zdolność kiełkowania i cechy siewek różnych odmian owsa*. Acta Agrophysica, 4(3): 637–643.

Gładyszewska B. 1998. *Ocena wpływu przedsiewnej laserowej biostymulacji nasion pomidorów na proces ich kiełkowania*. Rozprawa doktorska, Lublin.

Gładyszewska B., Koper R. 2002a. *Zastosowanie modelowania matematycznego w ocenie żywotności nasion*. Inżynieria Rolnicza, 7: 51–57.

Gładyszewska B., Koper R. 2002b. *Symulacyjny model procesu kiełkowania nasion w ujęciu analitycznym*. Inżynieria Rolnicza, 7: 59–63.

Grzesiuk S., Kulka K. 1981. *Fizjologia i biochemia nasion.* PWRiL, Warszawa.

Hryncewicz Z. 1992. *Uprawa roślin rolniczych.* PWRiL, Warszawa.

Kopcewicz J., Lewak S. 2002. *Fizjologia roślin*. Wydawnictwo Naukowe PWN, Warszawa.

Koper R., Kornas-Czuczwar B., Budzyński T. 2001. *Wpływ przedsiewnej biostymulacji laserowej nasion pomidorów gruntowych na właściwości fizykochemiczne owoców*. Inżynieria Rolnicza, 2: 131–135

Koper R., Kornas-Czuczwar B., Truchliński J., Zarębski W. 2002. *Przedsiewna biostymulacja światłem białym nasion buraków cukrowych*. Acta Agrophysica, 62: 41–47.

Kordas L. 2002. *The Effect of magnetic field on growth, development and the yield of spring wheat*. Polish Journal of Environmental Studies, 11(5): 527–530.

Kornarzyński K., Pietruszewski S., Segit Z. 2004. *Wstępne badania wpływu zmiennego pola magnetycznego na szybkość wzrostu kiełków pszenicy.* Acta Agrophysica, 3(3): 521–528.

Olchowik G., Gawda H. 2002. *Influence of microwave radiation on germination capacity of flax seeds*. Acta Agrophysica, 62: 63–68.

Pietruszewski S. 2000. *Wpływ pola magnetycznego na plony buraka cukrowego odmian Kalwia i Polko*. Inżynieria Rolnicza, 5: 207–214.

Pietruszewski S. 1999. *Magnetyczna biostymulacja materiału siewnego pszenicy jarej.* Rozprawy Naukowe, 220, Akademia Rolnicza, Lublin.

Pietruszewski S., Kornarzyński K., Prokop M. 2002a. *Kiełkowanie nasion cebuli odmiany Sochaczewska w stałym polu magnetycznym.* Acta Agrophysica, 62: 69–74.

Pietruszewski S., Kornarzyński K., Prokop M. 2002b. *Kiełkowanie nasion kapusty białej w stałym polu magnetycznym*. Acta Agrophysica, 62: 75–82.

Pietruszewski S., Kornarzyński K., Łacek R. 2002c. *Porównanie kiełkowania nasion roślin uprawnych eksponowanych w polu magnesu stałego*. Inżynieria Rolnicza, 7. 111–115.

Podleśny J. 2002. *Effect of laser irradiation on the biochemical changes in seeds and the accumulation of dry matter in the faba bean.* Int. Agrophysics, 16: 209–213.

Podleśny J., Podleśna A. 2004. *Wpływ traktowania nasion polem magnetycznym na wzrost, rozwój i dynamikę gromadzenia masy bobiku (Vicia faba minor).* Acta Agrophysica, 4(3): 787–801.

Podleśny J., Podleśna A., Koper R. 2001. *Wykorzystanie światła laserowego do przedsiewnej biostymulacji nasion bobiku (Vicia faba minor).* Inżynieria Rolnicza, 2: 315–321.

Prokop M., Kornarzyński K., Pietruszewski S. 2001. *Wstępne badania wpływu biostymulacji zmiennym polem magnetycznym na kiełkowanie nasion cebuli.* Inżynieria Rolnicza, 2: 324–327.

PROKOP M., PIETRUSZEWSKI S., KORNARZYŃSKI K. 2002a. *Wstępne badania wpływu zmiennych pól magnetycznych i elektrycznych na kiełkowanie, plony oraz cechy mechaniczne korzeni rzodkiewki i rzodkwi.* Acta Agrophysica, 62: 83–93.

PROKOP M., PIETRUSZEWSKI S., KORNARZYŃSKI K. 2002b. O*cena biostymulacji zmiennym polem magnetycznym nasion cebuli odmiany Sochaczewska.* Acta Agrophysica, 62: 95–102.

QIN H.L. , XUE J.M., LAI J.N. 2006. *Energy related germination and survival rates of water-imbibed Arabidopsis seeds irradiated with protons*. Nuclear Instruments and Methods in Physics Research B, 245: 314–317.

ROCHALSKA M. 2002. *Pole magnetyczne jako środek poprawy wigoru nasion.* Acta Agrophysica, 62: 103–111.

ROCHALSKA M. 1997. *Wpływ zmiennego pola magnetycznego na kiełkowanie nasion kukurydzy (Zea mays L.) w niskiej temperaturze*. Roczniki Nauk Rolniczych, s. A. T 112, z. 3–4: 91–99.

RYBIŃSKI W., PIETRUSZEWSKI S., KORNARZYŃSKI K. 2004. *Analiza wpływu pola magnetycznego i promieni gamma na zmienność elementów plonowania jęczmienia jarego (Hordeum vulgare L)*. Acta Agrophysica, 3(3): 579–591.

RYBIŃSKI W., PIETRUSZEWSKI S., KORNARZYŃSKI K. 2002. *Ocena oddziaływania pola magnetycznego i traktowania chemomutagenem na zmienność cech jęczmienia jarego (Hordeum vulgare L.)*. Acta Agrophysica, 62: 135–145.

YI-PING CHENA, MING YUEA, XUN-LING WANGA 2005. I*nfluence of He–Ne laser irradiation on seeds thermodynamic parameters and seedlings growth of Isatis indogotica.* Plant Science, 168: 601–606.

VASILEVSKI G. 2003. *Perspectives of the application of biophysical methods in sustainable agriculture.* Bulg. J. Plant Physiol., Special Issue, pp. 179–186.

Accepted for print 4.10.2007

TECHNICAL SCIENCES
Abbrev.: Techn. Sc., No 10, Y 2007

DOI 10.2478/v10022-007-0003-7

GERMINATION OF BUCKWHEAT SEEDS SUBJECT TO STORAGE TIME AND ELECTROMAGNETIC STIMULATION METHODS

Anna Ciupak, Izabela Szczurowska, Bożena Gładyszewska, Stanisław Pietruszewski

Department of Physics
Agricultural University in Lublin

Key words: buckwheat, storage time, physical stimulating factors.

Abstract

This paper presents the results of research on the influence of storage time, laser beam and magnetic field stimulation on the final number of germinated buckwheat cv. "Kora" seeds. Germination tests were carried out in a controlled environment chamber at a stable temperature of 21°C, stable humidity and without a source of light. Significant differences were reported in respect of values determining the percentage of germinated seed subject to the year of harvest. The impact of physical stimulation factors on seeds (harvested in 1993 and 2002) did not increase the final number of germinated seeds in those groups.

PRZEBIEG PROCESU KIEŁKOWANIA NASION GRYKI W ZALEŻNOŚCI OD CZASU PRZECHOWYWANIA ORAZ ELEKTROMAGNETYCZNYCH METOD STYMULACJI

Anna Ciupak, Izabela Szczurowska, Bożena Gładyszewska, Stanisław Pietruszewski

Katedra Fizyki
Akademia Rolnicza w Lublinie

Słowa kluczowe: gryka, czas przechowywania, fizyczne czynniki stymulacyjne.

Streszczenie

W pracy przedstawiono wyniki badań nad wpływem czasu przechowywania oraz działania światła laserowego i pola magnetycznego na końcową liczbę wykiełkowanych nasion gryki odmiany Kora. Testy kiełkowania przeprowadzono w komorze klimatycznej w stabilnej temperaturze 21°C, stałej wilgotności i bez dostępu światła. Stwierdzono znaczne różnice w wartościach określających procent wykiełkowanych nasion w zależności od lat zbioru. Poddanie badanych nasion (roczniki 1993 i 2003) działaniu fizycznych czynników stymulacyjnych nie miało wpływu na zwiększenie końcowej liczby wykiełkowanych nasion w tych grupach.

Introduction

Seeds are stored to keep them in a state of anabiosis until the moment when the right environmental conditions (adequate hydration level, access to air, adequate temperature) allow for the germination process to begin. The period of storage and the storing conditions are also important factors which affect germination. The process of seed aging is accompanied by (usually irreversible) degenerative changes in the structure and physiological and biochemical functions of the protoplast (Lityński 1977). Seeds lose their viability for various reasons, mainly due to the loss of enzymatic activity, depletion of reserve substances, changes in the structure of embryo cytoplasm, disturbances in protein metabolism, degree of degeneration of embryo's cell nuclei, accumulation of toxic metabolites and changes in the structure of nucleic acids (Zurzycki, Michniewicz 1985). Numerous research studies (Lityński 1977) have shown that seeds stored under adequate conditions maintain their germinating capacity at a level similar to the initial value for around three years, after which seed viability is subject to a sudden and irreversible drop. Those irreversible degenerative changes are directly responsible for decreasing crop yields. Various substances and methods are presently applied to stimulate the seed germination process and, consequently, increase the yield. The application of pre-sowing chemical agents, such as seed dressings, growth regulators and physical stimulants, supports the germination process and contributes to yield increase. The beneficial effect of a variable magnetic field as a factor which supports other processing methods was observed by Rochalska (2002) in respect of soybean and maize seeds germinated under temperature stress. Physical stimulation factors (magnetic and electric field, ionizing, microwave and laser radiation) have already been applied to various vegetables, pulse crops and cereals, including tomatoes (Gładyszewska 1998, Gładyszewska, Koper 2002a, b, Koper i in. 2001) onions (Pietruszewski 2000, Prokop i in. 2001, Prokop i in. 2002), cabbage (Pietruszewski i in. 2002), radishes (Pietruszewski i in. 2002, Prokop i in. 2002), spinach (Pietruszewski i in. 2002), sugar beets (Koper i in. 2002, Pietruszewski 2000), faba beans (Podleśny 2001, Podleśny, Podlesna 2004, Podleśny i in. 2001), wheat (Kordas 2002, Kornarzyński i in. 2004, Pietruszewski 1999), barley (Rybiński i in. 2002, Rybiński i in. 2004), oat (Drozd i in. 2004), maize (Rochalska 2002), flax (Olchowik, Gawda 2002) and plants of the family Brassicaceae, including thale cress (Qin i in. 2006) and woad (Yi-Ping Chena i in. 2005). In general, research results indicate that the impact of the above factors differs subject to the applied parameters which determine their properties.

The objective of this study was to analyze the effect of laser light stimulation and variable magnetic field stimulation on the percentage of germinated buckwheat cv. Kora seeds, subject to the period of seed storage.

Materials and methods

The experimental material comprising seeds harvested in 1993 and 2003 was subjected to laser stimulation (in 3 series during the free fall of seeds from the charging hopper chute) with a He-Ne laser beam with a wavelength of λ=630 nm and density power of 4 mW/cm^2 (group L) (Ciupak i in. 2006) or magnetic field stimulation with an intensity of 30 mT and frequency of 50 Hz (group M) with exposure time of 8 seconds. A combination of the above stimulating factors was also applied to form group LM (laser + magnetic field). The control group in the experiment were non-stimulated buckwheat seeds (group C). Every group was represented by 400 seeds sown on Petri dishes (on stimulation day) in 4 samples of 100 seeds each. The prepared seeds were placed in a controlled environment chamber at a stable temperature of 21°C, stable humidity and without a source of light. The above temperature (which was within the optimum range for buckwheat seed germination (Hryncewicz 1992) enabled to obtain results within a shorter time and created a more favorable environment for the germination of older seeds (1993). Germinated seeds (showing germs with a minimum length of 2 mm) were counted every 1–2 hours beginning from the appearance of the first germ (when germination was most intense). The time intervals in which germs were counted were gradually extended due to decreasing germination intensity. Germination rate S_k, the final number of germinated seeds N_k (indicated in %) and the time required for the germination of 50% of all sown seeds (t_{50}) were calculated based on the obtained results.

Results and discussion

The data defining the final number of germinated buckwheat seeds N_k (standard deviation values are indicated in parenthesis), subject to storage time and the applied stimulation factors, are presented in Table 1. Figure 1 additionally presents curves which represent the number of germinated seeds (in %) as a function of time. When analyzed, the obtained results indicate significant differences in N_k values of seeds harvested in 1993 and

Table 1

Number of germinated seeds N_k (in %) subject to the harvest year and the applied stimulation method

Number of germinated seeds (%)			
1993			
K	L	M	LM
69 (5.9)	64.75 (7.37)	62.5 (9.54)	71.25 (13.96)
2003			
83.25 (3.3)	84 (8.6)	81 (2.2)	85 (8.7)

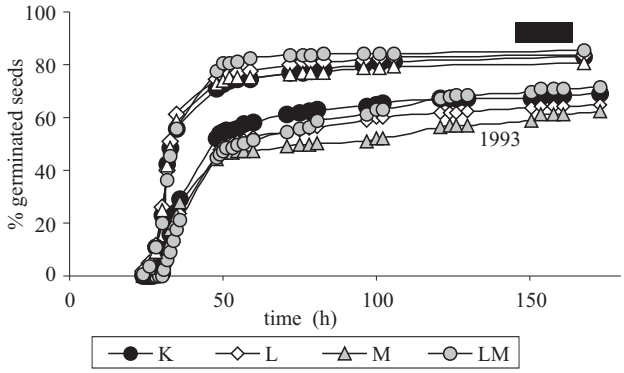

Fig. 1. Final number of germinated seeds N_k (%) harvested in 1993 and 2003, subject to stimulation method

2003. A comparison of control groups (C) representing both harvest years shows that N_k values were more than 14% lower in older seeds.

The greatest difference between stimulated groups (more than 19%) in the final N_k value was observed with regard to seeds which were subjected to laser simulation. None of the applied physical stimulation factors contributed to an increase in the number of germinated seeds from both harvest years. The above was confirmed by a statistical analysis based on testing the hypothesis of the difference between two means with the use of Student's t-test (at a significance level of α=0.05). Statistically significant negative effects of stimulation were observed in older seeds (1993) which were subjected to a variable magnetic field (group M).

The data for the beginning of the germination processes in every seed group are presented in Table 2, and significant differences in the time of the beginning of germination are illustrated by Figure 1. The obtained results

Table 2

Time of the beginning of germination process t_p and time of germination of 50% of all sown seeds t_{50}

Time of germination beginning t_p (h)			
K	L	M	LM
1993			
28	28	27	31
2003			
24	24	24	24
Time of germination of 50% of all sown seeds t_{50} (h)			
K	L	M	LM
1993			
48	53	78	57
2003			
34	33	33	34

indicate that regardless of the applied stimulation method, the germination of the seeds harvested in 2003 began at the same moment (hour 24 after sowing). Older seeds (1993) germinated later (Table 2). As regards group LM, the germination process started in hour 31 after sowing, i.e. 7 hours later than the group of seeds harvested in 2003.

Table 2 also indicates the time required for 50% of all sown seeds to germinate. An analysis of the above data indicates that the seeds harvested in 2003 needed 33 hours from sowing to germinate. Older seeds (1993) needed more than twice that time to attain the same germination level. As regards magnetic field stimulation, the time required for the germination of 50% of buckwheat seeds harvested in 1993 was more than five times longer than that observed in the group of seeds from 2003. The data obtained from the observation of the initial germination phase was used to set the value of the relative germination rate coefficient W_k (against control) of buckwheat seeds with the use of the below formula:

$$W_k = \frac{n(t)}{n_{\text{control}}}$$

where:
$n(t)$ – number of seeds germinated in time t,
$n_{control}$ – number of control group seeds germinated in given time t, and the corresponding change in the number of germinated seeds N_k as per the below formula:

$$N_k = \frac{n_k}{n_c} \cdot 100\%$$

where:
n_k – number of germinated seeds,
n_c – total number of sown seeds.

The comparative diagrams in Figure 2 indicate the germination rate S_k of buckwheat seeds, subject to the applied stimulation method and harvest time. The germination rate S_k (seed/h) of buckwheat seeds was calculated based on the below formula:

$$S_k = \frac{n_{\max}}{\Delta t}$$

where:
$n_{\max}$ – maximum number of germinated seeds recorded during the count,
Δt – time interval between two successive counts.

The curves representing 1993 harvest groups differ significantly from the curves which illustrate the 2003 harvest group. This difference is most likely due to a longer period of storage. The curves in Figures 2 also present the maximum germination rate by indicating the number of seeds which germinated within 1 hour after sowing.

Table 3

Value of relative germination rate coefficient W_k and number of germinated seeds N_k

1993							
	K	L		M		LM	
Time from sowing (h)	N_k (%)	W_k	N_k (%)	W_k	N_k (%)	W_k	N_k (%)
28	0.5	0.5	0.25	0.5	0.75	0	0
29	0.75	0	0.25	1	1	0	0
30	1.25	0.5	0.5	5	3.5	0	0
31	5.25	0.56	2.75	0.56	5.75	0.56	2.25
32	10.5	0.67	6.25	1	11	0.71	6
33	15.5	0.75	10	1.3	17.5	0.65	9.25
34	19.8	0.65	12.8	0.53	19.8	1	13.5
35	24	1.18	17.75	0.7	22.75	1	17.75
36	29	1.15	23.5	1	27.75	0.75	21.5
48	52.25	0.96	45.75	0.72	44.5	1.01	45
49	53.75	1.33	47.75	1.33	46.5	0.83	46.25
50	54.5	1.67	49	0	46.5	1	47
	K	L		M		LM	
Time from sowing (h)	N_k (%)	W_k	N_k %)	W_k	N_k (%)	W_k	N_k (%)
26	3.5	1.09	4.75	1	3.3	1.09	3.8
28	11	0.87	11.3	0.8	9.3	0.97	11
30	23	1.23	26	1.31	25	0.77	20
32	42.5	0.73	40.3	0.87	42	0.83	37
33	48.25	1.83	50.8	1.17	49	1.52	45
35	55.75	1.37	61	1.3	59	1.43	56
48	71	0.9	74.8	0.93	73	1.43	78
50	72.75	0.43	75.5	0.57	74	1.57	81

A detailed analysis of the obtained curves indicates that the highest germination rate of seeds harvested in 2003 was observed in hour 8–9 of the process (hour 32–33 after sowing). Maximum S_k values for seeds harvested in 1993 were reported from hour 5 to 9 of the germination process (hour 32–36 after sowing) The highest S_k values for older seeds (1993) were nearly half the maximum germination rate values reported for seeds with a shorter storage period (2003 harvest).

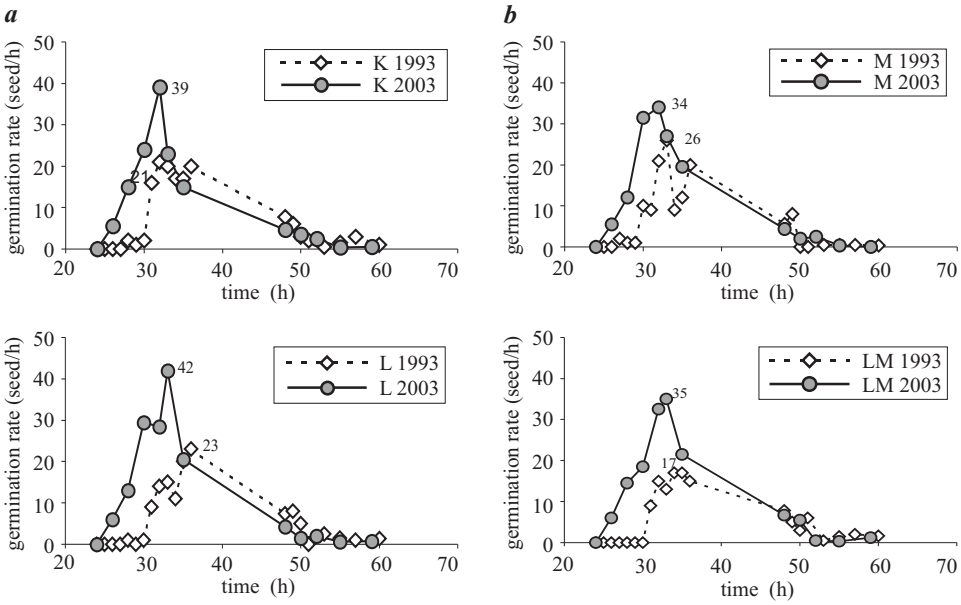

Fig. 2. Seed germination rate subject to harvest year and the applied stimulation method

Conclusions

1. Considerable differences were observed in the final number of germinated seeds which were harvested in 1993 and 2003.

2. The applied stimulating factors did not increase the final number of germinated buckwheat seeds.

3. A statistically significant, negative effect of stimulation was reported for the group of seeds harvested in 1993 which were stimulated with a magnetic field.

4. A longer storage period (for seeds harvested in 1993) extended the time required for the germination process to begin and it reduced the germination rate of seeds.

References

Ciupak A., Gładyszewska B., Pietruszewski S. 2006. *Wpływ stymulacji laserowej i temperatury na proces kiełkowania nasion gryki odmiany Kora.* Fragmenta Agronomica, 1: 23:35.

Drozd D., Szajsner H., Bieniek J., Banasiak J. 2004. *Wpływ stymulacji laserowej na zdolność kiełkowania i cechy siewek różnych odmian owsa.* Acta Agrophysica, 4(3): 637–643.

Gładyszewska B. 1998. *Ocena wpływu przedsiewnej laserowej biostymulacji nasion pomidorów na proces ich kiełkowania.* Rozprawa doktorska, Lublin.

Gładyszewska B., Koper R. 2002a. *Zastosowanie modelowania matematycznego w ocenie żywotności nasion.* Inżynieria Rolnicza, 7: 51–57.

Gładyszewska B., Koper R. 2002b. *Symulacyjny model procesu kiełkowania nasion w ujęciu analitycznym.* Inżynieria Rolnicza, 7: 59–63.

HRYNCEWICZ Z. 1992. *Uprawa roślin rolniczych*. PWRiL, Warszawa.

KOPER R., KORNAS-CZUCZWAR B., BUDZYŃSKI T. 2001. *Wpływ przedsiewnej biostymulacji laserowej nasion pomidorów gruntowych na właściwości fizykochemiczne owoców*. Inżynieria Rolnicza, 2. 131–135.

KOPER R., KORNAS-CZUCZWAR B., TRUCHLIŃSKI J., ZARĘBSKI W. 2002. *Przedsiewna biostymulacja światłem białym nasion buraków cukrowych*. Acta Agrophysica, 62: 41:47.

KORDAS L. 2002. *The Effect of magnetic field on growth, development and the yield of spring wheat*. Polish Journal of Environmental Studies, 11(5): 527–530.

KORNARZYŃSKI K., PIETRUSZEWSKI S., SEGIT Z. 2004. *Wstępne badania wpływu zmiennego pola magnetycznego na szybkość wzrostu kiełków pszenicy*. Acta Agrophysica, 3(3): 521–528.

LITYŃSKI M. 1977. *Biologiczne podstawy nasiennictwa*. PWN, Warszawa.

OLCHOWIK G., GAWDA H. 2002. *Influence of microwave radiation on germination capacity of flax seeds*. Acta Agrophysica, 62: 63–68.

PIETRUSZEWSKI S. 2000. *Wpływ pola magnetycznego na plony buraka cukrowego odmian Kalwia i Polko*. Inżynieria Rolnicza, 5: 207–214.

PIETRUSZEWSKI S. 1999. *Magnetyczna biostymulacja materiału siewnego pszenicy jarej*. Rozprawy Naukowe, 220, Akademia Rolnicza, Lublin.

PIETRUSZEWSKI S., KORNARZYŃSKI K., PROKOP M. 2002. *Kiełkowanie nasion cebuli odmiany Sochaczewska w stałym polu magnetycznym*. Acta Agrophysica, 62: 69–74.

PIETRUSZEWSKI S., KORNARZYŃSKI K., PROKOP M. 2002. *Kiełkowanie nasion kapusty białej w stałym polu magnetycznym*. Acta Agrophysica, 62. 75–82.

PIETRUSZEWSKI S., KORNARZYŃSKI K., ŁACEK R. 2002. *Porównanie kiełkowania nasion roślin uprawnych eksponowanych w polu magnesu stałego*. Inżynieria Rolnicza, 7: 111–115.

PODLEŚNY J. 2002. *Effect of laser irradiation on the biochemical changes in seeds and the accumulation of dry matter in the faba bean*. Int. Agrophysics, 16. 209–213.

PODLEŚNY J., PODLEŚNA A. 2004. *Wpływ traktowania nasion polem magnetycznym na wzrost, rozwój i dynamikę gromadzenia masy bobiku (Vicia faba minor)*. Acta Agrophysica, 4(3): 787–801.

PODLEŚNY J., PODLEŚNA A., KOPER R. 2001. *Wykorzystanie światła laserowego do przedsiewnej biostymulacji nasion bobiku (Vicia faba minor)*. Inżynieria Rolnicza, 2: 315–321.

PROKOP M., KORNARZYŃSKI K., PIETRUSZEWSKI S. 2001. *Wstępne badania wpływu biostymulacji zmiennym polem magnetycznym na kiełkowanie nasion cebuli*. Inżynieria Rolnicza, 2: 324–327.

PROKOP M., PIETRUSZEWSKI S., KORNARZYŃSKI K. 2002. *Ocena biostymulacji zmiennym polem magnetycznym nasion cebuli odmiany Sochaczewska*. Acta Agrophysica, 62: 95–102.

PROKOP M., PIETRUSZEWSKI S., KORNARZYŃSKI K. 2002. *Wstępne badania wpływu zmiennych pól magnetycznych i elektrycznych na kiełkowanie, plony oraz cechy mechaniczne korzeni rzodkiewki i rzodkwi*. Acta Agrophysica, 62: 83–93.

QIN H.L., XUE J.M., LAI J.N. 2006. *Energy related germination and survival rates of water-imbibed Arabidopsis seeds irradiated with protons*. Nuclear Instruments and Methods in Physics Research B, 245: 314–317.

ROCHALSKA M. 1997. *Wpływ zmiennego pola magnetycznego na kiełkowanie nasion kukurydzy (Zea mays L.) w niskiej temperaturze*. Roczniki Nauk Rolniczych, s. A. T 112, z. 3–4: 91–99.

ROCHALSKA M. 2002. *Pole magnetyczne jako środek poprawy wigoru nasion*. Acta Agrophysica, 62: 103–111.

RYBIŃSKI W., PIETRUSZEWSKI S., KORNARZYŃSKI K. 2002. *Ocena oddziaływania pola magnetycznego i traktowania chemomutagenem na zmienność cech jęczmienia jarego (Hordeum vulgare L.)*. Acta Agrophysica, 62: 135–145.

RYBIŃSKI W., PIETRUSZEWSKI S., KORNARZYŃSKI K. 2004. *Analiza wpływu pola magnetycznego i promieni gamma na zmienność elementów plonowania jęczmienia jarego (Hordeum vulgare L)*. Acta Agrophysica, 3(3): 579–591.

YI-PING CHENA, MING YUEA, XUN-LING WANGA 2005. *Influence of He–Ne laser irradiation on seeds thermodynamic parameters and seedlings growth of Isatis indogotica*. Plant Science, 168: 601–606.

ZURZYCKI J., MICHNIEWICZ M. 1985. *Fizjologia roślin*. PWRiL, Warszawa.

Accepted for print 4.10.2007

TECHNICAL SCIENCES
Abbrev.: Techn. Sc., No 10, Y 2007

DOI 10.2478/v10022-007-0009-1

MODEL METHOD FOR ECONOMICALLY REASONABLE CHOICE OF AGRICULTURAL MACHINE

Jan Pawlak

Chair of Electricity and Power Engineering
University of Warmia and Mazury in Olsztyn

Keywords: model, simulation studies, harvester thresher, operation cost, choice, method.

Abstract

The model for estimation the operation costs of machine according to the price of machine, its repair costs and working capacity has been elaborated. The model enables to determine the effect of amount of work and the machine parameters like working capacity and rate of repair costs on operation cost of machines. Simulation studies carried on for 5 different types of harvester threshers have shown that the operation cost per hour of the work of machine growths as the working capacity and price of machine increases. The operation cost per hectare of cereal harvested decreases as the working capacity increases even if price of machine growths, but only under condition of sufficient annual use. Decrease of the area to be harvested cause that operation costs grow, both per one hour and per hectare. The rate of growth is the higher the higher is the working capacity of machines. Amount of work to be done is a significant factor that should be taken into consideration when choosing the type of machine for particular farm. Use of high capacity and expensive machines is economically justified only in a case of possibility to achieve their sufficient annual use.

METODA MODELOWA EKONOMICZNIE UZASADNIONEGO DOBORU MASZYN ROLNICZYCH

Jan Pawlak

Katedra Elektrotechniki i Energetyki
Uniwersytet Warmińsko-Mazurski w Olsztynie

Słowa kluczowe: model, studia symulacyjne, kombajn zbożowy, koszt eksploatacji, dobór, metoda.

Streszczenie

Opracowano model umożliwiający szacowanie kosztów eksploatacji maszyn w zależności od ich cen, kosztów napraw i wydajności eksploatacyjnych. Studia symulacyjne przeprowadzone na przykładzie 5 różnych typów kombajnów zbożowych wykazały, że koszt eksploatacji odniesiony do godziny pracy maszyny rośnie w miarę zwiększania wydajności i ceny maszyny. Koszt eksploatacji w przeliczeniu na hektar powierzchni zbioru zbóż maleje w miarę wzrostu

wydajności pracy mimo wyższej ceny maszyny, jednak pod warunkiem dostatecznego rocznego jej wykorzystania. Zmniejszanie powierzchni przeznaczonej do zbioru powoduje, że rosną koszty, zarówno w przeliczeniu na godzinę, jak i na hektar wykonanej pracy. Stopień tego wzrostu jest tym większy, im wyższa jest wydajność maszyn. Ilość pracy do wykonania jest znaczącym czynnikiem, który powinien być brany pod uwagę przy doborze typu maszyny dla konkretnego gospodarstwa. Zastosowanie wysokowydajnej i drogiej maszyny jest ekonomicznie uzasadnione tylko w przypadku możliwości uzyskania dostatecznie wysokiego jej rocznego wykorzystania.

Introduction

Rational choice of agricultural machines is necessary as a condition of high efficiency of farm mechanization. When making decision about purchasing of machine the potential buyer takes into consideration several factors. One of most important is the price of the machine. The price determines first of all the investment cost, but it also effects such elements of operation costs like depreciation, interest and storage. However, not always more expensive machine creates higher unitary costs. Sometimes operation costs of advanced, more reliable and productive machine are lower as compared to a less expensive, but also less reliable and less productive one. Therefore, the choice of machine should be preceded by a careful economic analysis.

The purpose of this paper is to present the model for estimation the operation costs of machine according to the price of machine, its repair costs and working capacity. Simulation studies will be carried on and discussed, using this model. Exemplary calculations will be made for 5 different types of the harvester thresher.

The model

Choice of machines suited to the needs of the farm concerned is an important step to successful mechanization. Therefore, before making decision about purchase of a machine the careful analysis of future results has to be made. Proper equipment in farm machinery is one of conditions to achieve high efficiency of the technological advance (Michałek, Kowalski 1993, Michałek et al. 1998). To make this analysis easier, the model basing on cost calculation methods (Buckett 1988, Muzalewski 2004, 2005, Pawlak 2006) has been elaborated. Operation costs of agricultural machines are the sum of depreciation, interest, storage and conservation, insurance, repair and maintenance and energy. They can be described by the following formula:

$$KE = \frac{Cm}{Tn} + \frac{0.5o \cdot Cm}{100Tr} + \frac{m \cdot Cm}{Tr} + \frac{p \cdot ks}{Tr} + \frac{U}{Tr} + \frac{k \cdot Cm}{Tn} + Zp \cdot Cp \cdot M \quad \text{(PLN/h)} \tag{1}$$

where:
KE – operation costs, PLN/h,
Cm – price of the machine, PLN,
Tn – hours of work during the useful life of the machine, hours,

Tr – yearly use of the machine, hours,
o – the interest rate, %,
m – coefficient of the conservation cost related to the price of the machine,
p – space occupied by the machine in the storage place, m^2 ,
ks – cost of the unit of surface of the storage place, PLN/m^2,
k – coefficient of repair costs related to the price of the machine,
U – rate of insurance, PLN/year,
Zp – unitary consumption of the fuel, kg/kWh,
Cp – price of the fuel, PLN/kg,
M – power of engine, kW.

The formula (1) can be simplified as follows:

$$KE = Cm\left(\frac{1}{Tn} + \frac{0.5o}{100Tr} + \frac{m}{Tr} + \frac{k}{Tn}\right) + \left(\frac{p \cdot ks + U}{Tr}\right) + Zp \cdot Cp \cdot M \text{ (PLN/h)} \tag{2}$$

Following assumptions have been made when building the model. The maximal hours of machine work during the useful life (*Tn*) amounts to 3000. 15 years standard useful life (*n*) has been assumed. Therefore, the annual use (*Wr*) of at least 200 hours was necessary so that each machine could work out 3000 hours during its useful life. In a case of annual use higher than 200 hours, the number of years of the useful life becomes relatively lower. Instead, in a case of a lower annual use of machines, the useful life can be prolonged up to maximum 30 years, followed by the increase of the coefficient *k* by 30%. This increase has to be assumed so that the growth of repair costs as a result of prolonging the useful life of machine could be taken into account. In the range from 15 to 30 years of the useful life the increase of value of the coefficient *k* fluctuates between 0% and 30%. The increase is proportional to the prolongation of the useful life. In a case of annual use lower than 100 hours, the cost of depreciation grows.

There are two reasons of the wear of machines. One is a waste of elements and damages during the work. Decrease of hours worked causes costs related to this factor to decrease. This fact has been taken into account in the model in the form of reduction of the value of the coefficient k, proportionally to the decrease of the annual use of the machine. Another reason is the deterioration of materials caused by environment factors. This has also been taken into account by above-mentioned increasing the value of coefficient *k* in a case of prolonging the useful life of machines.

Results and discussion

The model has been used for simulation studies of harvest unitary costs using different types of harvester threshers. Five types of harvester threshers have been taken into consideration. Their characteristics are presented in Table 1.

Table 1

Characteristics of harvester threshers

Specification	Harvester thresher				
	A	*B*	*C*	*D*	*E*
Price, PLN	207 000	248 400	289 800	372 600	414 000
Engine power, kW	58	74	88	99	15
Fuel consumption, kg/kWh	0.215	0.198	0.176	0.165	0.151
Value of the coefficient *k*	1.0	1.0	1.0	0.85	0.85
Operational capacity, W_{07}	0.40	0.66	0.87	1.13	1.35

Source: own assumptions

Three variants of situation have been analyzed. The only difference between them is yearly use of particular harvester threshers, assumed for calculations. In the first scenario (variant I) all types of machines could achieve the annual use of 200 hours. In the second (variant II) the assumption has been made that the amount of work to be done in all cases was equal: 80 hectares. As the particular harvester threshers have different working capacity, the annual use of each of them is also different. In the third variant the area of cereals to be harvested is equal, but it is by 50% lower as compared to the variant II.

Analysis of the first scenario shows that the operation cost per hour of the work of harvester thresher growths as the working capacity and price of machine increases. However, in a case of machines *D* and E the dynamic of growth of the cost is by 15 per cent lower than the rate of the increase of price. It is a result of the lower repair costs rate for harvester threshers *D* and *E* due to their higher quality. The operation cost per hectare of cereal harvested decreases as the working capacity and price of machine growths (Fig. 1).

When the area of cereals to be harvested is limited, the annual use of machines decreases as their operational capacity W_{07} growths (Table 2).

Drop of the annual use causes the useful life (n) of machines (in years) to increase and changes of values of the coefficient k. This was taken into account in the list of input data for calculations (Table 3).

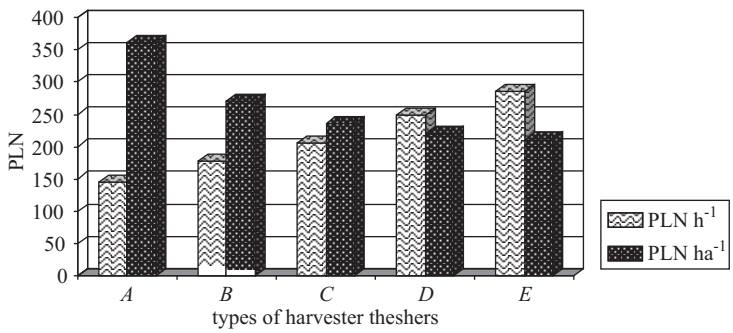

Fig. 1. Unitary operation costs of particular harvester thresher with annual use of 200 hours

Table 2

Annual use of harvester threshers in cases when area of cereals to be harvested is nit limited (variant I), when it is limited to 80 hectares (variant II) and when it is limited to 40 hectares (variant III)

Variants	Annual use in hours for harvester threshers				
	A (W_{07}=0.40)	*B* (W_{07}=0.66)	*C* (W_{07}=0.87)	*D* (W_{07}=1.13)	*E* (W_{07}=1.35)
I	200	200	200	200	200
II	200	121	92	71	59
III	100	61	46	35	30

Source: own calculations

Table 3

Input data for calculations

Symbols of data	Variants	Harvester threshers				
		A	*B*	*C*	*D*	*E*
n, years	I	15	15	15	15	15
	II	15	25	30	30	30
	III	30	30	30	30	30
k	I	1.00	1.00	1.00	0.85	0.85
	II	1.00	1.21	1.20	0.78	0.65
	III	1.30	0.79	0.60	0.39	0.33
o, %	I, II, III	5	5	5	5	5
m	I, II, III	0.04	0.04	0.04	0.04	0.04
p	I, II, III	24	34	36	40	45
ks, PLN	I, II, III	100	100	100	100	100

Source: own assumptions and calculations

Analysis of changes caused by 80 hectares limit of the harvested area (variant II) shows that operation costs both per one hour and per hectare grows. The rate of growth is the higher the higher is the working capacity of machines. The increase of the cost by 3% was registered in a case of the harvester thresher *C* and by 21% in a case of the harvester thresher *E*. Further decrease of the harvested area (variant III) causes increase of operation costs per hectare by 26% (machine *A*) and by 122% (machine *E*).

In all cases the cost per hour of the work of harvester thresher growths as the working capacity and price of machine increases. Still in the variant II the use of harvester threshers *B* and *C* creates operation costs by 13% and 12% lower as compared to the harvester thresher *A*. However, the use of machines *D* and *E* cause increase of the cost respectively by 3% and 14% (Fig. 2).

When the area of cereals to be harvested is limited to only 40 hectares, the increase of costs both per hour of work and per hectare increases as the working capacities and the prices of machines grow. The operation cost per hectare of the harvested area is in a case of harvester thresher *E* by 67% higher as in a case of the harvester thresher *A* (Fig. 3).

Above example show that the amount of work to be done is a significant factor that should be taken into consideration when choosing the type of

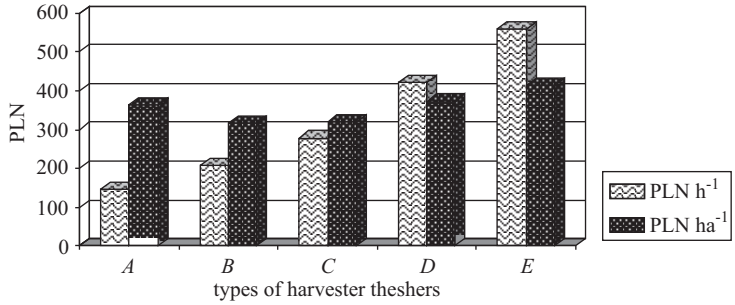

Fig. 2. Unitary operation costs of particular harvester thresher on farms with 80 ha of cereals and technologically similar crops

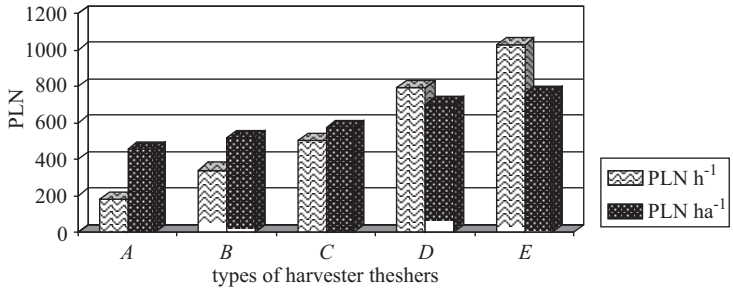

Fig. 3. Unitary operation costs of particular harvester thresher on farms with 80 ha of cereals and technologically similar crops

machine for particular farm. Use of high capacity and expensive machines is economically justified only in a case of possibility to achieve their sufficient annual use.

Conclusion

Examples of application of the proposed model for simulation studies show that it is useful for determination interdependencies between price and working capacity of machine and costs of its operation per hour as well as per unit of a work done. The model enables to determine the effect of amount of work and the machine parameters like working capacity and rate of repair costs on operation cost of machines.

Cost of operation per hour of work depends on price, rate of repair costs and the annual use of machine. Cost of operation per hectare of work depends on price, rate of repair costs, the annual use and working capacity of machine.

The operation cost per hour of the work of harvester thresher growths as the working capacity and price of machine increases.

The operation cost per hectare of cereal harvested decreases as the working capacity increases even if price of machine growths, but only under condition of sufficient annual use. Decrease of the area to be harvested cause that operation costs grow, both per one hour and per hectare. The rate of growth is the higher the higher is the working capacity of machines.

Amount of work to be done is a significant factor that should be taken into consideration when choosing the type of machine for particular farm. Use of high capacity and expensive machines is economically justified only in a case of possibility to achieve their high annual use.

References

BUCKETT M. 1988: *An introduction to farm organization and management*. 2nd edition. Pergamon Press.

MICHAŁEK R., KOWALSKI J. 1993. *Metodyczne aspekty określania postępu naukowo-technicznego w rolnictwie*. Część II: *Próba określenia syntetycznych mierników oceny postępu i jego efektywności w rolnictwie*. Roczn. Nauk Roln. C-79-4.

MICHAŁEK R. i in. 1998. *Uwarunkowania technicznej rekonstrukcji rolnictwa*. Polskie Towarzystwo Inżynierii Rolniczej, Kraków.

MUZALEWSKI A. 2004. *Koszty eksploatacji maszyn*. Wskaźniki eksploatacyjno-ekonomiczne maszyn i ciągników rolniczych stosowanych w gospodarstwach indywidualnych, 19. Wydawnictwo IBMER, Warszawa.

MUZALEWSKI A. 2005. *Koszty eksploatacji maszyn*. Wskaźniki eksploatacyjno-ekonomiczne maszyn i ciągników rolniczych stosowanych w gospodarstwach indywidualnych, 20. Wydawnictwo IBMER, Warszawa.

PAWLAK J. 2006. *Ekonomiczne i organizacyjne problemy mechanizacji i energetyki rolnictwa*. Wydawnictwo IBMER, Warszawa.

WÓJCICKI Z. 1997. *Dobór i wykorzystanie środków technicznych oraz koszty produkcji w rozwojowych gospodarstwach rodzinnych*. Wydawnictwo IBMER, Warszawa.

Accepted for print 21.09.2007

TECHNICAL SCIENCES
Abbrev.: Techn. Sc., No 10, Y 2007

DOI 10.2478/v10022-007-0004-6

PERMEABILITY OF POLYMERIC PACKAGING MATERIALS

Stanislav Zeman[1], Ľubomír Kubík[2]

[1]Department of Animal Husbandry and Food Production Mechanization
[2]Department of Physics
Slovak University of Agriculture in Nitra

Key words: gas diffusion, Fick's laws, methods of permeability determination.

Abstract

The paper deals with study of permeability of polymeric packaging materials. The review of gas diffusion through polymeric membrane is presented. The signification of the quantities attached in corresponding equations is analyzed. Permeability coefficient at thermodynamic equilibrium is equal a product of diffusion and solubility coefficients. It depends on polymeric structure of material and also on the properties of diffusive molecules. The experimental methods of determination of polymer barrier properties suitable of permeability determination are also presented in the paper.

WŁAŚCIWOŚCI MECHANICZNE OPAKOWAŃ I ICH ODPORNOŚĆ NA OBCIĄŻENIA ZEWNĘTRZNE

Stanislav Zeman, Ľubomír Kubík

Słowacki Uniwersytet Rolniczy w Nitrze

Słowa kluczowe: dyfuzja gazów, prawa Ficka, metody wyznaczania przepuszczalności.

Streszczenie

Polimery są materiałem, który często jest stosowany do produkcji opakowań produktów spożywczych. W artykule przedstawiono analizę dyfuzji gazów przez polimerową membranę, podkreślając fizykalne znaczenie poszczególnych wielkości występujących w odpowiednich zależnościach matematycznych. Współczynnik przepuszczalności, który przy termodynamicznej równowadze jest równy dyfuzji i rozpuszczalności, zależy zarówno od struktury polimeru, jak i od właściwości dyfuzyjnych molekuł. W artykule przedstawiono metody eksperymentalnego badania „barierowych" właściwości polimerów zdeterminowanych ich przepuszczalnością.

Introduction

The role of plastic packaging materials, which we apply to packaging of foodstuff, is preservation of original quality of foodstuff from external unfavorable influences. We can achieve it by means of the barrier properties of

packaging material. The required protection of the foodstuff may be achieved with a single layer of polymer or necessitates the use of multilayered films including different polymers, coatings and metal foils. The barrier properties of the packaging material mainly originate from its permeability to gases and vapors that are noxious to the quality of product. For the majority of foods, the gains and loss of moisture leads to the destruction or noxious biological defects (Jase et al. 1994, Ashley 1985, Pye et al. 1976).

The choice of a packaging material should take into account all components of the foods as well as packaging material in consequence its interactions by influence of different storage conditions. The polymeric materials are so varied that we an always find an appropriate film or laminate for a given application. However, the absolute barrier does not exist. It is necessary to adapt barrier properties to the real life. One of the crutial criteria of choice is the knowledge of the permeability of the polymeric packaging to the gases and vapors which are crucial of preservation of food quality. The permeability of gases and vapors depends mainly on the polymer structure.

Basic principles of permeability of packaging materials

Steady state

Transfer of gases and vapors in polymers is realized by mechanisms of diffusion. Diffusion is a flow of matter which originates as consequence of chemical potential difference of migrant material in different location of the system. The amount of substance flow is defined as

$$\lim_{\Delta t \to 0} \frac{dn}{dt} \tag{1}$$

then the density flux J of gases and vapors is given by:

$$J = \frac{Q}{S\,t} \tag{2}$$

where:
Q is the amount of substance of gases or vapors (mol),
S is the surface of packaging material and t is the time.

The First Fick's law is defined:

$$J = \frac{1}{S}\frac{dn}{dt} = -D\frac{\partial c}{\partial x} \tag{3}$$

where:
n is amount of substance,
D is diffusivity coefficient and $\frac{\partial c}{\partial x}$ is concentration gradient in direction of axis x.

Permeability of gases and vapors in the steady state, assuming that J=const. and $D \neq f(c)$, by integration trough of thickness of film from x_1 to x_2 and from c_1 to c_2 we obtain:

$$J\,x = -D\left(c_2 - c_1\right) \tag{4}$$

and

$$J = D\,\frac{c_1 - c_2}{x} \tag{5}$$

Substituting instead of J From relation (2) we obtain:

$$\frac{Q}{S\,t} = \frac{D\left(c_1 - c_2\right)}{x} \tag{6}$$

and

$$Q = \frac{D\left(c_1 - c_2\right)}{x} S\,t \tag{7}$$

In the case the concentration is sufficiently low the Henry's law is valid:

$$c = \sigma\,p \tag{8}$$

where:
p is the pressure of the diffused gas
σ is a gas solubility coefficient (Henry's constant).

By substituting instead of c in relation (7) form relation (8) we obtain:

$$Q = \frac{D\sigma\left(p_1 - p_2\right) S\,t}{x} \tag{9}$$

At thermodynamic equilibrium the gas permeability coefficient P is given by relation:

$$P = D\sigma \tag{10}$$

Permeability is depended on solubility and diffusivity. These quantities are functions of optional volume, cohesive energy and polymer morphology (McBride et al. 1979). Than permeability is defined:

$$P = \frac{Q\,x}{S\left(p_1 - p_2\right) t} \tag{11}$$

Permeability of unit thickness of the film is:

$$P_x = \frac{P}{x}\text{, then from relation (11)} \quad P_x = \frac{Q}{S\,\Delta p\,t} \tag{12}$$

and diffusion is realized only one direction.

Non-steady state

Speed of diffusion in the polymer is limited. Density flux of gases and vapors is given by Second Fick's law. We define the amount of substance of gases and vapors as

$$Q=\frac{D\,c_1}{x}\left(t-\frac{x^2}{6\,D}\right)=\frac{D\,c_1\,t}{x}-\frac{c_1\,x}{6} \tag{13}$$

where Q is linear function of t.

When we assuming that Q=0 and t=L, from the Figure 1 results after extrapolation

$$\frac{D\,c_1\,L}{x}=\frac{c_1\,x}{6} \tag{14}$$

and than

$$D=\frac{x^2}{6\,L} \quad \text{and} \quad L=\frac{x^2}{6\,D} \tag{15), (16}$$

where x is thickness of the foil.

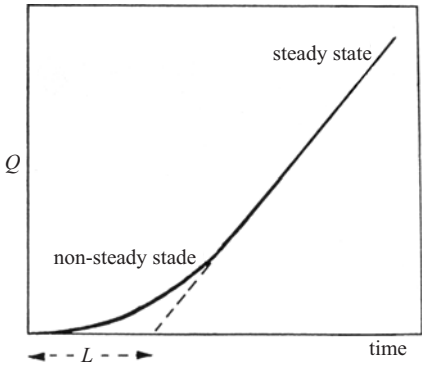

Fig. 1. Typical permeation and time lag curve by JASSE et al. (1994)

In the case the polymers include dispersed porous particles with vast surface and the solubility of gases don't agree with Henry's law the sorption (or penetrant concentration) c_H is calculated according to Langmuir isotherm (SOHAIL et al. 1997, JASSE et al. 1994, KOROS et al.1992, HACE et al. 2004):

$$c_H=\frac{c_H^{'}\,b\,p}{1+b\,p} \tag{17}$$

Here c_H is the penetrant concentration in microcavities or holes in the polymer matrix, $c_{H'}$ is saturation concentration of the penetrant species in the microvoids, p is the equilibrium pressure and b is Langmuir's hole-capacity constant.

The coefficients permeability P and P_x are function of temperature and may be expressed by Arrhenius relation (JASSE et al 1994):

$$P_x = P_0 \exp\left(-\frac{E_d}{RT}\right) \tag{18}$$

where:
P_0 is permeability at infinity temperature,
E_d activation energy for permeation,
R is universal gas constant and
T is absolute temperature.

Permeability of multilayer packaging material

Provided that total thickness of foil is

$$h_c = h_1 + h_2 + h_3 + \cdots + h_n \tag{19}$$

steady flow of gases is constant

$$Q_c = Q_1 = Q_2 = Q_3 = \cdots = Q_n \tag{20}$$

and surface of all layers is the same

$$S_c = S_1 = S_2 = S_3 = \cdots = S_n \tag{21}$$

Than we substitute in relation

$$\frac{Q}{t} = \frac{P}{x} S\left(p_1 - p_2\right) \tag{22}$$

and we obtain:

$$\frac{Q_T}{t} = \frac{P_1}{h_1} S_1\left(p_1 - p_2\right) = \frac{P_2}{h_2} S_2\left(p_2 - p_3\right) = \frac{P_3}{h_3} S_3\left(p_3 - p_4\right) \tag{23}$$

For multilayer foil we can obtain:

$$\frac{Q_T\, h_c}{t\, S_c\, P_c} = p_1 - p_4 = \Delta p_i \tag{24}$$

where:

$$\Delta p_i = \left(p_1 - p_4\right) = \left(p_1 - p_2\right) = \left(p_2 - p_3\right) = \left(p_3 - p_4\right) \tag{25}$$

than

$$\frac{Q_T\, h_c}{t\, S_c\, P_c} = \Delta p_i = \frac{Q_T}{t\, S_c}\left(\frac{h_1}{P_1} + \frac{h_2}{P_2} + \frac{h_3}{P_3}\right) \tag{26}$$

and if

$$\frac{h_c}{P_c} = \left(\frac{h_1}{P_1} + \frac{h_2}{P_2} + \frac{h_3}{P_3}\right) \tag{27}$$

than

$$P_c = \frac{h_c}{\frac{h_1}{P_1} + \frac{h_2}{P_2} + \frac{h_3}{P_3}} \tag{28}$$

Methods of determination of permeability packaging materials

Variable pressure method

Jasse et all (1994) present the equipment consisting of testing chamber divided by testing foil on two parts. Testing gas is transported at specific pressure p_1 in the first part of the chamber. The second part is evacuated on the pressure p_2. The experimental conditions are such that $p_1 p_2 \sim 0$ so that $\Delta Q/\Delta t$ can be calculated from $\Delta p_2/\Delta t$. The permeability is given by relation:

$$P = \frac{\Delta Q\, x}{S\, \Delta t\, p} \tag{29}$$

where:
ΔQ is amount of gas penetrated in the time interval Δt in the steady flow,
S is effective area of the and
x is the thickness of the packaging.

The spectrometer may be used on the measurement. The time lag L we can obtain from the samples. This quantity is related to the diffusivity coefficient D by $D=h^2/6L$. From the values of P and D we may calculate the solubility coefficient $\sigma=P/D$.

Differential methods

In these methods the gas streams on one side of the polymer film. The gas crossing the film being carried out towards a detector by helium to produce a signal proportional to the diffusion rate. The analysis may be realized using different techniques such as thermic conductivity detector, flame ionic detection, a gas chromatograph or mass spectrometer. Absorption and desorption runs can be done as illustrated in Figure 2 in the case of a thermic conductivity detector. In this case the permeability is given by:

$$P = \frac{f\, \sigma\, k\, \alpha\, S_\infty\, h}{S\, p} \tag{30}$$

where:
f is gas flow rate,
σ detector sensitivity,
k a molecular factor,
α the detector attenuation,
S_∞ the steady state signal intensity,
h the film thickness.
S is the pressure area and
p is pressure of the gas.

The diffusion constant D is given by:

$$D = \frac{h^2}{7.2 \cdot t_{1/2}} \tag{31}$$

where $t_{1/2}$ is half time necessary to obtain the steady state.

The use of a gas chromatograph as well a mass spectrometer allows us to determine the individual diffusion characteristics of each gas present in the mixture.

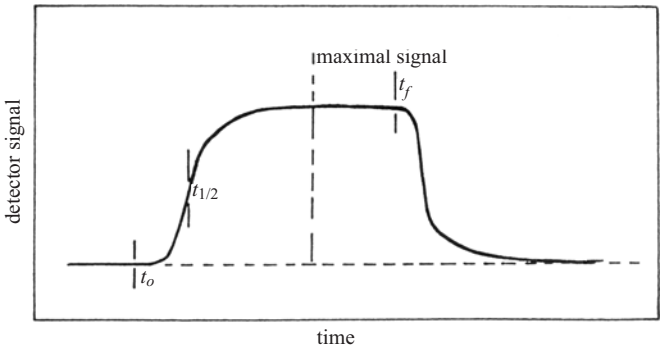

Fig. 2. Thermal conductivity detector output as function of time by Pye et al. (1976)

Parameters affecting packaging permeability

Polymeric materials present a wide range of structures and properties depending on their chemical structure, method of preparation and processing conditions. The presence of additives or use of polymer blends affect barrier properties towards carbon dioxide, oxygen, nitrogen or water vapor. Some permeability data for various polymers are given in Table 1.

Lee (1980), Mojun (2003), Paul et al. (1973) described the permeation of a gas trough different polymer using the expression:

$$P = A e^{-B(V - V_0)} \tag{32}$$

where:
A and B are constants characteristics of the gas,
V is the specific volume measured experimentally and
V_0 is an estimation of the specific volume at absolute zero.

Barbari (1993), Koros et al. (1980) using sorption and expansion data determined the molar volumes of CO_2 and CH_4 in silicon rubber and calculated the mobile gas concentration for CO_2 and CH_4. The influence of free volume on diffusivity coefficient D and permeability P was described by a study of (Maeda, Paul 1987).

During the last period, an increasing interest in polymer blends arose to improve mechanical and barrier properties of packaging materials. Usually polymers are incompatible and only few systems can be considered as compa-

Table 1

Cofficientts of permeability for various polymers by Ashley (1985)

Polymer	P(ml mm cm^{-2} s^{-1} cm Hg^{-1})				$\frac{PO_2}{PN_2}$	$\frac{PCO_2}{PO_2}$	$\frac{PCO_2}{PN_2}$	Structure of polymer
	N_2 30°C	O_2 30°C	CO_2 30°C	H_2O, 90% RH 25°C				
Low density polyethylene	19	55	352	800	2.9	6.4	18.5	Some crystallinity
High density polyethylene	2.7	10.6	35	130	3.9	3.3	13	Crystalline
Polypropylene	–	23	92	680	–	4.0	–	Crystalline
Unplasticized PVC	0.4	1.2	10	1 560	3.0	8.3	25	Slightly crystaline
Cellulose acetate	2.8	7.8	68	75 000	2.8	8.7	24	Glassy amorphous
Polystyrene	2.9	11	88	12 000	3.8	8.0	30	Glassy
Nylon 6	0.1	0.38	1.6	7 000	3.8	4.2	16	Crystalline
Polyethylene terephthalate	0.05	0.22	1.53	1 300	4.4	7.0	31	Crystalline
Plyvinylidene chloride	0.0094	0.053	0.29	14	5.6	5.5	31	Crystalline

tible either completely or in narrow range of concentration. LEE (1980) assuming the free volume of the blend equal to the sum of the free volumes of the components obtained, in incompatible blends, the following expression:

$$\ln\frac{P}{S}=\left[\frac{\Phi_1}{\ln\frac{P_1}{S}}+\frac{\Phi_2}{\ln\frac{P_2}{S}}\right]^{-1} \tag{33}$$

where:
S is a constant characteristic of the gas and
Φ_1, Φ_2 are the volume fractions of components 1 and 2.

The thickness of the film also affected on the permeability. The increased thickness reduces gas flow. One of the goals in film manufacture is to obtain as thin a film as possible with good mechanical and transport properties. In practice a thickness of 25 μm is common. Critical value the thickness of the film is 10 μm.

Conclusion

As a permeability of polymeric packaging materials depends on the sorption and diffusion of gases and vapors, it is of relevance to recall the models that apply for prediction of these parameters in the polymers. The

experimental techniques used to measure permeability are based on volumetric, gravimetric or differential methods. These permeability coefficients are influenced by the chemical structure as well as by method of preparation and processing conditions. Some of the structural parameters play a major role in their effect on permeability. The gases and vapors particularly important in food packaging and preservation are O_2 and CO_2 and water vapor. The effect of their shape and size, interaction with the polymer and the influence of temperature and pressure on their sorption and diffusion behaviour may be helpful in the understanding of the variation of their permeation through polymeric packages.

Acknowledgement

We appreciate the support of Scientific Grant Agency of the Ministry of Education of Slovak Republic and the Slovak Academy of Sciences of the project: Research of Packaging Materials and their Influence on Increasing of the Food Quality and Safety, No. 1/4437/07.

References

Ashley R.J. 1985. *Permeability and plastics packaging.* In*: Polymer Permeability*. Ed. J. Comyn Elsevier, Applied, London, p. 269–308.

Barbari T. A. 1993. *On the amount of free volume in gas-polymer mixtures.* Journal Polymer Sci. Part B, Polymer physics, 31: 501–504.

Hace J., Golob J. 2004. *Diffusion coefficient of diallyl terephthalate monomer into plymer film.* Chem. Biochem. Eng. Q., 18: 73–76.

Jasse B., Seuvre A.M., Mathlouthi M. 1994. *Food Packakging and Preservation.* Blakie Academic and Professional an imprint of Champan & Hall, Glasgov, London, 1994, p. 275, ISBN 0 7514 01182 X.

Koros W.J., Coleman M.R., Walker D.R.B. 1992. *Controlled permeability polymer membranes*. Annu. Rev. Mater. Sci., 22: 47.

Koros W.J. Paul D.R. 1980. *Sorption and transport of CO_2 above and below the glass transition of poly(ethylene terephthalate)*. Poly. Engr. and Sci., 20:14.

Lee W.M. 1980. *Selection of Barrier Materials from Molecular Structure.* Poly.Eng. Sci., 20: 65–69.

McBride J.S., Massaro T.A., Cooper S.L. 1979. *Diffusion of Gases through Polyurethane Block Polymers*. Appl. Poly. Sci., 23: 201-214.

Maeda Y., Paul D.R. 1987. *Effect of Antiplasticization on Gas Sorption and Transport*. Part II: Journal Polym. Sci.: Part B, Polym. Phys., 25: 981.

Mojun L. 2003. *Study on diffusion behavior of water in epoxy resins cured by active aster*. Phys.Chem. 5: 1848–1852.

Paul D.R., Kemp D.R. 1973. *The diffusion time lang in polymer membranes containing adsorptive fillers.* Journal Polymer, Sci., 41: 79–93.

Pye D.G., Hoen H.H, Panar M. 1976. *Measurement of gas permeability of polymers*. Journal Appl. Polym. Sci., 20: 287–301.

Sohail H., Jack Y. 1997. A*TR-FTIR spectroscopic studies of the structure and permeability of sulfonated poly(ether sulfone) membranes*. Journal Chem. Soc., Faraday Trans., 93: 1613–1620.

Accepted for print 12.06.2007

TECHNICAL SCIENCES
Abbrev.: Techn. Sc., No 10, Y 2007

DOI 10.2478/v10022-007-0005-5

MECHANICAL PROPERTIES TO MEASURE RESISTANCE OF FOOD PACKAGING MATERIALS TO EXTERNAL INFLUENCES

Stanislav Zeman

Department of Animal Husbandry and Food Production Mechanization
Slovak University of Agriculture in Nitra

Key words: loading force, modulus in elasticity in tension, tensile strength, relative elongation

Abstract

Resistance of food packaging materials to external influences was studied. Three different film packages made of plastics (TATRAFAN® KX; TATRAFAN® KXP/S) and of a material containing food contact additives used for meat products(KOLAGEN) were analysed for tensile stress, relative elongation (tensile strain), and modulus of elasticity in tension (Yong's modulus) as mechanical properties.

From the results alleged, at packing materials KOLAGEN by implication at deep dispersion measure out valuation. At packing materials TATRAFAN® KX and TATRAFAN® KXP/S on defiance desing fetch by onerons strength of 67 and 40.8 N at relative elongation 177.01 and 122.66% at longitudinal direction, and of 131 and 102.4 N and relative elongation 34.08 and 31.87% in cross direction, respectlively. According to the measured mechanical properties, the conditions of life and resistance to handling damage of food packaging materials can be determined.

WŁAŚCIWOŚCI MECHANICZNE OPAKOWAŃ I ICH ODPORNOŚĆ NA OBCIĄŻENIA ZEWNĘTRZNE

Stanislav Zeman

Słowacki Uniwersytet Rolniczy w Nitrze

Słowa kluczowe: siła obciążająca, rozciąganie, naprężenie graniczne, moduł sprężystości, wydłużenie względne.

Streszczenie

Badano odporność materiałów opakowaniowych na obciążenia zewnętrze, analizując następujące parametry: siłę obciążającą, naprężenia, wydłużenie względne i moduł sprężystości na rozciąganie. Próbki wykonano z substancji spożywczej (KOLAGEN) i tworzyw sztucznych (TATRAFAN® KX i TATRAFAN® KXP/S).

Stwierdzono, że zakres i charakter zmienności przyjętych parametrów przy wzdłużnym i poprzecznym rozciąganiu KOLAGENU były do siebie podobne. W przypadku TATRAFANU®

KX i TATRAFANU® KXP/S zerwanie materiału dla obciążenia wzdłużnego nastąpiło przy sile od 67 do 40,8 N i wydłużeniu względnym 177,01÷122,66% i dla obciążenia poprzecznego przy sile od 131÷102,4 N i przy wydłużeniu względnym 30,08÷31,87%. Uzyskane wyniki pozwalają określić trwałość i odporność opakowań na uszkodzenia oraz warunki manipulacji produktami spożywczymi.

Introduction

Packing material role is to protect the original quality of foodstuff from undesirable external influences.This can be managed thanks to barrier properties of the packing material. Desired protection can be achieved by using simple layer of e.g. polymer, or by using multilayer coat involving various polymers, films or metal leaf.

When deciding about the packing material, all ingredients of the foodstuff and of the packing material must be considered. This is due to the fact, that they can interact with each other in different stock conditions. Since there is not any absolute protection, it is important to adjust properties of the packing to real contitions (Mathlouthi 1994).

Stationery packing materials occupy a leading position in foodstuff packaging as far as quantitative measure is concerned. On the other hand, thanks to its properties, plastics are used for packing of extra wide spectrum of foodstuff. It is given by its barrier properties fluently transiting from full permeability to almost non – permeability for diffferent gas components.

Structural characteristics as well as conditions in which external forces take effect are crucial factors influencing the rise of deffects and dangerous random breakings and crevices in materials. The most important are the speed of loading and environmental influences (temperature, relative air humidity etc.). These factors in their mutual combination state if fast growing of microdeffects together with rising of crevice or slow growing with plastic deformation will take place. Short-term trial describes solidity and deformation behaviour in continuous growth of external forces (Meissner 1987, Kovačič 1971).

Material and methods

Tear off machine – type TIRA 2700 was used for meusuring mechanical properties of packing materials. We had adjusted the test conditions for stress-strain properties to STN ISO 527-1, STN ISO 577-2 and STN ISO 527-3 standard. Measure and evaluation methodology is stated in (Zeman 2001a and Zeman 2001b).

KOLAGEN, packing material often used for filling meat products, was used for measuring. Strength and good permeability for smoke and water vapour are the main qualities of the material. TATRAFAN® KX, packing material, was used as well. It is “biaxial-oriented“, co-extruded, polypropy-

len film, which is resistent against fats, oils and solvents. It has also outstanding mechanical and optical properties, it is healthy publishable and suitable for packaging of foodstuff. The thickness of the wrapping is 35 μm, surface weight is 31.8 g cm^{-2}, and water vapour permeability is 4,0 g m^{-2} d^{-1}. Another material, that was used is wrapping material TATRAFAN® KXP/S – is "biaxial-oriented", co-extruded, pearled polypropylen film. It is turned out by co-extrusion from healthy clean commodities. The film is of pearl colour and it has brilliant glance. It reflects sun rays and therefore it extends durability of wrapped products. The casing is suitable for wrapping sweets and baking products. The thickness of the wrapping is 40 μm, surface weight is 29.9 g cm^{-2}, and water vapour permeability is 3.0 g m^{-2} d^{-1}.

Results and discussion

Matematitical – statistical processing of the rezults of mechanical properties of packing is indicated in table 1.The measuring of tensile properties of the wrapping material KOLAGEN (Fig. 1) allege, that if the external loading force achieved the value of 133 N, the testing sample broke at 1777.23 MPa. These values were achieved for the testing sample, which had been cut out legthwise to the axis of the package. We also studied tensile stress for the same material (Fig. 2), but this time the sample had been cut out crosswise to the axis of the package.The material broke down at loading force 105 N and at relative elongation 13.07%, elasticity modulus achieved value 1998.92 MPa in tensile stress 78.98 MPa. The results achieved show, that the values of tensile stress, loading force and relative elongation that we measured were equal to those stated by Zeman (2001) in case of cut out crosswise to the axis of the package. In case of cut out legthwise to the axis of the package, there were small deviations by 16.1% in tensile stress.

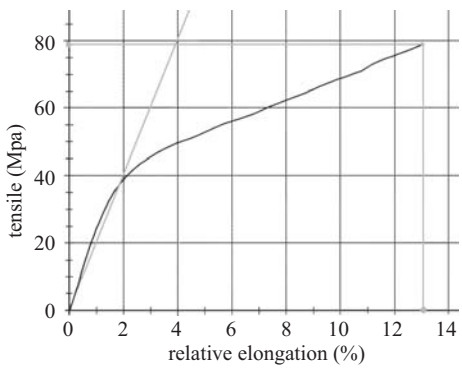

Fig. 1. Course of molulus of elasticity and tensile strenght in packing material KOLAGEN tested in longitudinal direction

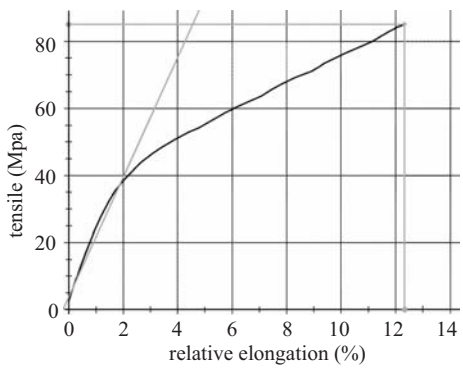

Fig.2. Course of molulus of elasticity and tensile strenght in packing material KOLAGEN tested in cross direction

The results of measuring mechanical properties for wrapping material TATRAFAN® KX (cut out lengthwisely), loaded by external force is shown in Figure 3. Note that the failure of the material arose at loading force 67 N and relative elongation by 177.01%. The tensile stress reached the value of 123.16 MPa and elasticity modulus 1496.42 MPa. Axis of the package can be seen in case of test sample cut out crosswisely (Fig. 4). The failure of the material arised at loading force 131 N and relative elongation by 34.08%. The tensile stress for the test material hit 231.52 MPa and elasticity modulus hit value 3135.44 MPa. Having compared the measured values of tensile

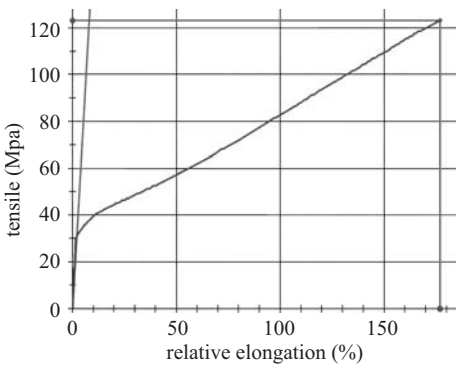

Fig.3. Course of molulus of elasticity and tensile strenght in packing material TATRAFAN®KX tested in longitudinal direction

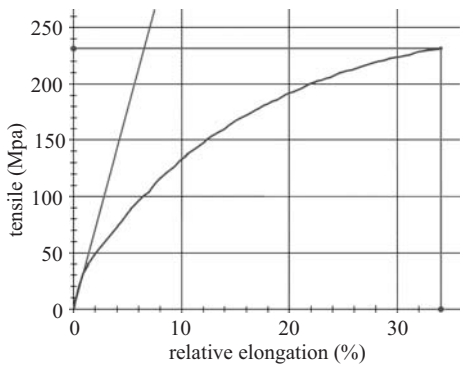

Fig.4. Course of molulus of elasticity and tensile strenght in packing material TATRAFAN®KX tested in cross direction

Table 1

Basic statistical characteristics of observed parameters

Packaging material	Load	Statistical characteristics	Packing thickness mm	Packing width mm	Modulus of elasticity MPa	Tensile MPa	Relative elongation %
KOLAGÉN	longitudinal direction	Φ	0.097	15.00	1777.23	84.99	12.55
		s	0.008	0.00	224.01	10.25	1.29
		v, %	8.240	0.00	11.38	11.06	10.64
	cross direction	Φ	0.097	15.00	1998.92	78.98	13.07
		s	0.010	0.00	316.82	9.7	2.44
		v, %	10.21	0.00	18.46	14.57	21.73
TATRA-FAN®KXP/S	longitudinal direction	Φ	0.035	15.00	1468.61	123.16	177.01
		s	0.000	0.00	121.72	7.46	12.44
		v, %	0.000	0.00	8.29	6.22	7.55
	cross direction	Φ	0.035	15.00	3135.44	231.52	34.08
		s	0.000	0.00	377.05	11.24	4.30
		v, %	0.000	0.00	12.03	4.49	9.72
TATRA-FAN®KX	longitudinal direction	Φ	0.040	15.00	973.27	58.11	122.66
		s	0.000	0.00	31.76	2.57	7.26
		v, %	0.000	0.00	3.41	4.22	5.28
	cross direction	Φ	0.040	15.00	1918.31	138.84	31.87
		s	0.000	0.00	120.92	5.92	3.04
		v, %	0.000	0.00	6.88	4.40	10.32

stress with those stated by the manufacturer we found out, that tensile strength lengthwise is by 8.3% less, crosswisely – correspondence was achieved. The values of unit elongation that we got are by 9% lengthwise and by 36.3% crosswise less than values stated by the manufacturer.

After studying mechanic properties of packing material TATRAFAN® KXP/S, which had been loaded lengthwisely (Fig. 5) we may state, that tensile stress roses steeply, later the course is of curve character until achieving value 27 MPa. After this the course remains linear. The breakthrough arised at force value 40.8 N and relative elongation 122.66%. Tensile stress 58.11 MPa and elasticity modulus 973.27 MPa were touched. Fig.6 shows, that in case of this sample, the value of stress at the strength was 138.84 MPa, with loading force 102.4 N and elasticity modulus 1918.31 MPa.

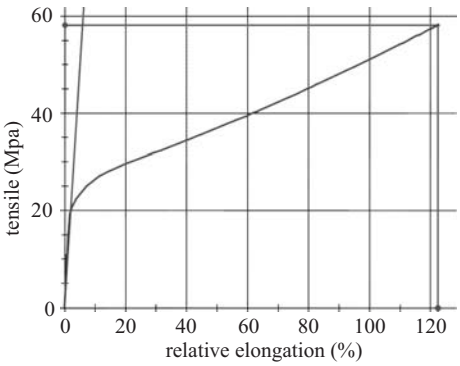

Fig.5. Course of molulus of elasticity and tensile strenght in packing material TATRAFAN®KXP/S tested in longitudinal direction

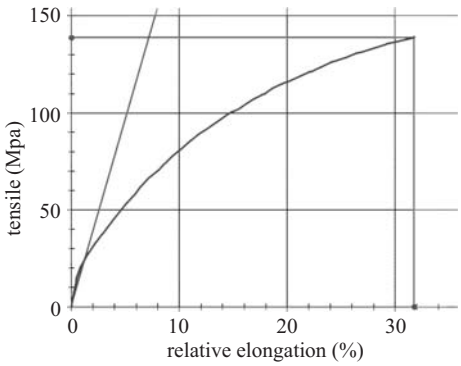

Fig.6. Course of molulus of elasticity and tensile strenght in packing material TATRAFAN®KXP/S tested in cross direction

Conclusion

Based on the experimental measuring results, we can state, that in case of KOLAGEN, manufactured from edible substances, the relative elongation at loading forces is on average equal, divergence arose at stress of the strength by 30,4%.

Emerging from studying tensile stress of TATRAFAN® KX the failure of the test sample arose at loading force 131 N crosswisely, while 67 N were needed lengthwisely. This also influenced a considerable increase in tensile stress and elasticity modulus. Results of measuring TATRAFAN® KXP/S show, that behaviour of this material is similar to the previous one. Having compared the materials mentioned above we found out, that in case of packing material TATRAFAN® KX we need 64.2% more power to breakthrough the sample lengthwisely and 27.9% crosswisely. Based on the variation of force, stress and elasticity modulus it is apparent, that test samples

TATRAFAN® KX and TATRAFAN® KXP/S are more resistant as long as the force works crosswisely. On the other hand, if the force works lengthwisely KOLAGEN is more resistent.

References

ČURDA D. 2001. *Vlastnosti obalu pro balení potravin*. In: *Svět balení*, č. 2, s. 10–12. ISSN 1212–7809

KOVAČIČ Ľ., BÍNA J., KOMÁREK Z. 1971. *Plasty a korózia*. ALFA, Bratislava, s. 460.

MEISSNER B., ZILVAR V. 1987. *Fyzika polymerù*. SNTL, Praha, s. 308.

MATHLOUTHI M. 1994. *Food Packaging and Preservation*. BLACKIE ACADEMIC, London, s. 275. ISBN 0-7514-0182-X.

ZEMAN S. 2001a. *Vplyv mechanických vlastností obalov na plnenie živočíšnymi produktami*. Acta technologica agriculturae, roč. 4, č. 4, s. 102–105. ISSN 1335-2555.

ZEMAN S. 2001b. *Mechanické vlastnosti obalov*. Strojárstvo v hospodárstve a priemysle, roč. 5, č. 7–8, s. 55. ISSN 1335-2938.

Translated by Johana Jakubovičová

Accepted for print 12.06.2007

TECHNICAL SCIENCES
Abbrev.: Techn. Sc., No 10, Y 2007

DOI 10.2478/v10022-007-0006-4

OPTIMIZATION OF THE CONSTRUCTION OF A PRESSURE TANK USING CAD/CAE SYSTEMS

***Jerzy Domański*[1], *Grzegorz Żywica*[2]**

[1]Department of Technical Sciences
University of Warmia and Mazury
[2]Institute of Fluid Flow Machinery
Polish Academy of Sciences

Key words: pressure tank, optimalization of construction, CAD/CAE.

Abstract

The paper presents a method for optimizing the construction of a vertical pressure tank with a given capacity, for specified service conditions. Such tanks are elements of process lines applied in numerous branches of the economy, including the chemical, pharmaceutical, cosmetic and food industry.

The optimization process was carried out using CAD/CAE systems. In order to find the best engineering solution, multi-criteria optimization of the pressure space of a tank was performed. This enabled to choose the optimum construction, with the emphasis on low weight, high producibility and operating comfort.

OPTYMALIZACJA KONSTRUKCJI ZBIORNIKA CIŚNIENIOWEGO Z WYKORZYSTANIEM SYSTEMÓW CAD/CAE

***Jerzy Domański*[1], *Grzegorz Żywica*[2]**

[1]Katedra Mechaniki i Podstaw Konstrukcji Maszyn
Uniwersytet Warmińsko-Mazurski
[2]Instytut Maszyn Przepływowych
Polska Akademia Nauk

Słowa kluczowe: zbiornik ciśnieniowy, optymalizacja konstrukcji, CAD/CAE.

Streszczenie

W artykule przedstawiono metodę optymalizacji pionowego zbiornika ciśnieniowego o ustalonej objętości dla określonych warunków eksploatacji. Zbiorniki tego typu są elementami linii technologicznych stosowanych w wielu gałęziach gospodarki, m.in. w przemyśle chemicznym, farmaceutycznym, kosmetycznym i spożywczym.

Optymalizację przeprowadzono z wykorzystaniem systemów CAD/CAE. W celu znalezienia najlepszego rozwiązania konstrukcyjnego wykonano optymalizację wielokryterialną przestrzeni ciśnieniowej zbiornika. Przeprowadzona analiza pozwoliła na wybór konstrukcji optymalnej, charakteryzującej się małą masą, dużą technologicznością oraz łatwością eksploatacji.

Introduction

The term "tank" describes a wide range of vessels, such as e.g. underground containers with a capacity of around 5000 m^3 used for liquid fuel storage, transportation tanks or process equipment and devices designed for various production branches. The present paper focuses on tanks which are elements of process lines, applied in numerous branches of the economy, including the chemical, pharmaceutical, cosmetic and food industry. Their capacity usually varies between several and several dozen cubic meters. Depending on the function they perform in technological processes, these can be storage tanks, buffer tanks, mixing tanks, reactors, manifolds, filters, etc. Due to the physical and chemical processes taking place inside such vessels, their construction should ensure the occurrence of internal overpressure.

The design, production and conformity assessment of pressure tanks available in the European Union are specified in the Directive of the European Parliament and the Council of the European Union 97/23/WE of May 29, 1997 on the harmonization of the national legislation of the Member States relating to pressure equipment. The objective of this Directive is to ensure the free movement and circulation of pressure equipment within the European Union as well as to lay down the essential safety requirements.

The main structural units of pressure vessels are thin-walled shells. To simplify the design process and to reduce the costs of construction, the shells take the simplest geometrical shapes: they may be flat, cylindrical, conical or spherical. The body of a pressure tank is usually a combination of these components (Konopko 1998). It follows that the design of pressure vessels consists primarily in determining the dimensions of the above components. The selection of the appropriate computational model and its simplification should enable to take into consideration at least the key characteristics of a real object. The rapid development of computational techniques observed today permits the generation of complex theoretical models as well as a more adequate assessment of the properties of real objects. The traditional methods employed for strength analysis are based on computations resulting from the adoption of analytical solutions and idealized theoretical models. Such computations are performed for particular components of a pressure tank, i.e. the blanket, heads and supports. The application of digital computational methods (CSD) enables to perform a strength analysis for the entire construction, without the division into components. These methods allow to examine objects characterized by complex shapes, at various boundary conditions. Due to the fact that computer-aided techniques are much less time-consuming, it is possible to analyze many constructional variants and choose the optimum one.

Shell optimization methods

Thin shell optimization involves searching for the optimum shape of a central surface and wall thickness (MAGNUCKI 1998). Two groups of optimization methods are applied for this purpose, i.e. variational and parametric. The variational methods are based on search for a function, and are limited to non-classic problems of variational calculus, most often isoperimetric problems. A detailed description of variational calculus applied to mechanics may be found, among others, in a monograph by H. Lippmann (LIPPMANN 1972). Parametric shaping consists in search for the dimensions of structural units of the shell, such as shell thickness, the distance between ribs, the cross-section of reinforced ribs, the distribution of supports, etc.

The problems of the optimization of shell components are still widely discussed by numerous authors (MAZURKIEWICZ, NAGÓRSKI 1986, MAGNUCKI 1993). Due to their diversity, the problems of shell optimization cannot be analyzed by one method or described in a simple way (MAGNUCKI 1998). There are many approaches to this problem and the choice of a given method depends on the complexity of a task, the nature of a feasible set and the accuracy required to determine the optimum.

The paper presents a method for optimizing the construction of a pressure tank, taking into account not only strength conditions but also other aspects affecting the production and operation of such equipment.

Methods for determining the thickness of components of pressure vessels

As already mentioned, the main components of pressure vessels are thin-walled shells. Generally speaking, a shell is defined as a body limited by two surfaces placed close to each other and an edge (MAGNUCKI 1998). Thickness h of a shell is the distance between these surfaces, and the geometric loci of the points equally distant from these surfaces are referred to as the central surface of a shell. The value that allows to differentiate between thin and thick shells is the boundary value $20 \cdot h \cong R_{\min}$, where $R_{\min}$ is the minimal radius of the central surface curvature. The shells for which the value of the product $20 \cdot h$ is less than $R_{\min}$ are considered thin, whereas those for which this value is greater than $R_{\min}$ are considered thick.

The thickness of thin shells can be determined based on various theories, including the momentless theory of rotation shells, the theory of boundary disturbances of rotation shells and the general linear theory of thin shells. These theories were formulated and developed by Gauss (1777–1855), Lame (1795–1870), Codazzi (1824–1873) and Weingarten (1836–1910). All of these

theories are described in detail in literature on the subject (GALIMOV 1975, OLSZAK 1980, MAZURKIEWICZ, NAGÓRSKI 1986, MAGNUCKI, SZYC 1987, MAGNACKI 1998).

The problems of solid body mechanics may be also solved using numerical methods. The finite element method is the most popular among them. It is also applied to solve problems related to thin-walled constructions and shells. The finite element method is associated with approximate solutions of differential equations (ŁODYGOWSKI, KĄKOL 2003). It requires the selection of approximating functions which must take into account boundary conditions and the specific properties of materials, as well as to describe the geometry of the area under analysis. The mathematical basis and a description of the finite element method can be found in many papers (ZIENKIEWICZ 1980, ŁODYGOWSKI, KĄKOL 2003, RAKOWSKI, KACPRZYK 2005). Due to the popularization and development of information technology, the finite element method have become a practical and widely applied tool, used also for construction design.

As already said, the essential safety requirements to be satisfied by pressure equipment available on the EU market are specified in the Pressure Equipment Directive (PED) 97/23/WE. The Directive lays down general guidelines for the design and production of pressure equipment and assemblies. Detailed guidelines are established by regulations, provisions and standards in force in the Member States, which comply with the above Directive. An example of such norms are EN-13445, AD 2000–Merkblätt or WUDT/UC 2003. According to PED, pressure equipment can be designed using two different methods, i.e. a computational method or an experimental method (for specified service conditions). The computational method may involve design based on formulas related to the theories mentioned above, or design based on analysis performed using numerical methods. In the present paper the thickness of walls of pressure vessels was determined using one of numerical methods – the finite element method.

Optimization of the construction of a pressure tank

Various types of pressure equipment are manufactured today. They may have one or many blankets, but the key role in such constructions is always played by pressure spaces. The fittings to pressure vessels (e.g. connecting pieces, inspection openings, hatches, valves) are designed for specified service conditions. In this way series of types of the most common components, to be used within specified pressure and temperature ranges, are developed. The main task to be carried out by a designer is to design the pressure space of a pressure tank, equipped with appropriate sub-assemblies.

Characteristics of a pressure tank

The present paper deals with the optimization of the pressure space of a vertical tank, composed of the most common structural components, i.e. a cylindrical unit and two press-formed heads. The working capacity of the tank was 8 m^3 and the internal overpressure was equal to 6 bar at a temperature of 100°C. The tank was designed for fluid density of 1000 kg m^{-3}. These parameters correspond to those of pressure tanks manufactured at one of the production plants in Olsztyn. Table 1 presents the technical data for the pressure vessel analyzed in the study.

Table 1

Technical data of pressure tank

Parameter	Value	Unit
Working capacity	8	m^3
Degree of filling tank	90	%
Max. allowable pressure PS	6	bar
Max. allowable temperature TS	100	°C
Density of working medium	1 000	kg m^{-3}
Coefficient of welds	1	–
Material	1.4404	–

Construction material. The construction material used in the study was stainless, austenitic chromium-nickel steel 1.4404 (Polish Standard PN-EN 10088-1:1995). This material is commonly applied for constructing equipments for the chemical and food industry. Steel 1.4404 is weldable and has very good plastic properties. The properties of steel were adopted based on the Standard EN 10028-7:2000. Permissible stresses for the above material were determined in accordance with Annex I to the Directive 97/23/WE: "Essential Safety Requirements". In the case of austenitic steel for which ultimate elongation (at rupture) exceeds 35%, as well as in the case of the domination of steady load and temperatures beyond the range of considerable creep, reduced stress cannot exceed the value calculated from the following relationship:

$$\min\left[\frac{R_{1,0/t}}{1,2};\frac{R_m}{3}\right] \tag{4.1}$$

For steel 1.4404 used at the highest admissible temperature TS = 100°C, permissible stresses cannot exceed 143.3 MPa.

Heads of the tank. The results of supplementary studies (Żywica 2005) showed that the capacity to weight ratio is much more desirable for ellipsoidal heads than for basketwork ones. Therefore it was assumed that the optimized pressure space will be limited by ellipsoidal heads at the bottom

and at the top, according to the Standard DIN 28013. During the technological processes of pressing and spinning, the thickness of such heads decreases by about 10%, as compared with the thickness of semi-finished steel. That is why both technological allowance and metallurgic deviation were taken into account in the calculations (cf. PN-EN 10029:1999).

Cylindrical unit. During plastic forming the thickness of the cylindrical unit decreases by about 5%. The thickness of the blanket is also affected by metallurgic deviation, which for steel sheets is specified in the Polish Standard PN-EN 10029:1999. Te minimal thickness of the blanket was adopted for calculations, taking into consideration both these factors.

The foundation of the tank. It was assumed that the tank has three tubular legs. Such a shape has numerous advantages, including easy availability of semi-finished steel, easiness of finishing and after-machining, the smallest possible external surface exposed to external effects, and good buckling properties. The presence of three legs eliminates the occurrence of unloaded legs, which increases the stability of the tank and makes it possible to use the so called weight-leg. The tube is connected to the pressure space with a washer 10 mm thick, which enables to reduce localized stresses in the bottom head, resulting from support. While selecting the cross-section of a support we should take into account not only the loads resulting from tank weight and content, but also the possibility of occurrence of extra forces. These can be loads caused by wind blast, service platforms, etc. It was assumed that the legs of the tank were made of tubular steel profile, 219.1 mm in diameter and 3 mm in thickness. Additional studies were performed in order to correctly place the legs on the head of the tank (Żywica 2005). The stresses generated in the supported head served as a criterion for choosing the optimum place for support location. It was assumed that the optimum distance (measured from the central axis of the head) between the legs is half of the outer radius of the head.

Computational model

The computational model of a pressure tank was generated using one of the popular CAD systems, equipped with the CAE module. Several such applications are available on the market today. Autodesk Inventor Professional and SolidWorks/CosmosWorks are most popular in small and medium-sized enterprises. The advantage of such programs is the possibility to perform a quick analysis of a part under design without the need to examine the details of the theory of the finite element method, which is extremely time-consuming. On the other hand, their disadvantage is that they have certain limitations when compared to the professional packages of the finite element method.

For the purpose of this study we created a parametric model of a pressure vessel. The model was developed in the assembly context, which means

that its parts have external references and require time-related operations. While creating parts in the assembly context, the geometry of one component may be used to define another component. Models are then fully matched and any changes introduced into the reference component are followed by the update of dependent components. Various configurations of components were applied to rebuild the model.

Due to the fact that the tank had three supports composed of three identical segments, the computational model was simplified and only one third of this part of the tank was analyzed, under appropriate symmetry conditions. The use of symmetry for model building contributes to lower costs and higher accuracy of calculations (ZAGRAJEK et al. 2005). The transformation into the simplified model of a pressure tank is illustrated in Figure 1.

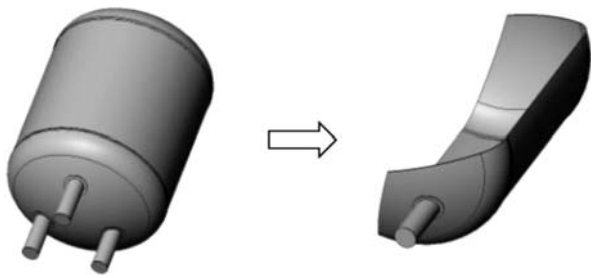

Fig. 1. Simplification of the computational model

The number of finite elements in the MES model was increased until it was found that its further increase did not considerably improve the results anymore. This operation was aimed at minimizing the risk of the discretization error (RAKOWSKI 1996), and enabled to obtain a network composed of elements whose number ensured conformity of results and numerical efficiency. In consequence, the model made up of about 80 000 elements was adopted for further analysis. The application discussed permits the division of a given geometric shape into tetrahedral elements only, so such elements were used in the study. Figure 2 presents ten-node tetrahedral elements of the Solid187 type. Each node of the Solid187 element has three translational

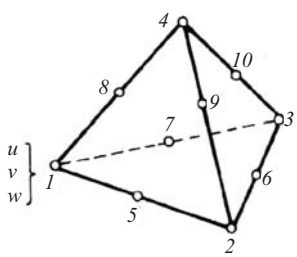

Fig. 2. Solid187 element

degrees of freedom. The displacement area between nodes is approximated with a quadratic function of shape.

The main advantage of the above elements is the possibility to discretize any three-dimensional geometry. That is why they are universally applied in programs based on the finite element method, designed for automatic structure division (Rakowski, Kacprzyk 2005).

Boundary conditions. The following boundary conditions were applied: in the nodes of lower planes of the supports displacements were blocked in all directions, whereas in the nodes of division planes displacements were blocked in the directions perpendicular to the division planes (Figure 3).

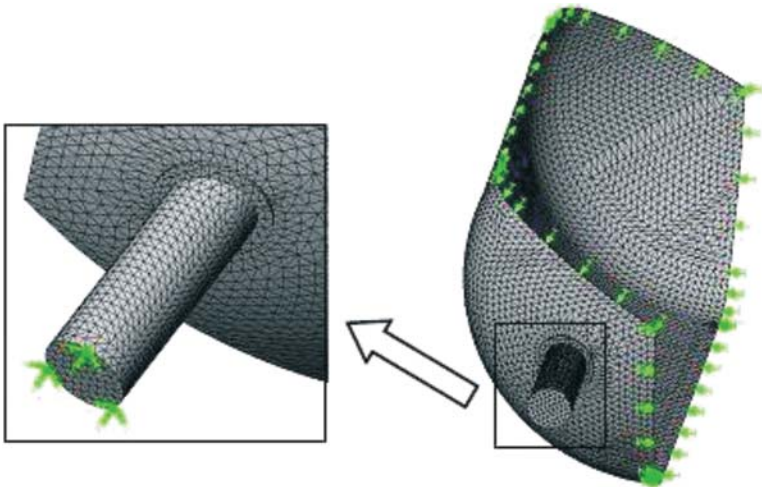

Fig. 3. Boundary conditions

The model of a pressure vessel was exposed to internal surface load whose value was determined as the sum of THE highest permissible pressure and the maximal hydrostatic pressure that could affect a given part of the pressure space. It follows that the value of the pressure applied was different for the bottom head, top head and blanket of the tank. The gravity force was also taken into account in the calculations.

Mathematical optimization model

Parameters. The following parameters (variables with specified values) describing the model were adopted:
– the highest permissible pressure – PS = 6 BAR,
– the highest permissible temperature – TS = 100°C,
– total capacity of the tank – V_c = 8.9 m^3,
– permissible stresses for steel 1.4404 f = 143.3 MPa,

– shape of ellipsoidal heads according to the Standard DIN 28013 $R = 0.8D_z$ and $r = 0.154D_z$,
– distance form the top of the bottom head to the ground 0.5 m,
– three legs made of tube Ø219.1x3.

The other parameters were: design of the tank, values of the material properties of steel 1.4404, load and fastening of the pressure tank.

Decision variables. The following decision variables were adopted:
– outer diameter of the heads D_z ,
– height of the cylindrical part of the tank H_C,
– thickness of particular components of the pressure space g_{DD}, g_P, g_{DG}.

The vector of the above decision variables has the form:

$$x = (D_Z, H_C, g_{DD}, g_P, g_{DG}) \in R^5$$

All decision variables may only take discrete values.

Feasible set. The feasible set includes all solutions fulfilling the conditions below:
– strength condition $\sigma_{HM} \leqslant f$,
– geometric condition $1400 \leqslant D_z \leqslant 2800$,
– volume condition $V \geqslant V_c$.

According to the Huber-Mises hypothesis, reduced stresses σ_{HM} depend on thickness g_{DD}, g_P, g_{DG}. Their values can be determined by the finite element method. The geometric condition ($1400 \leqslant D_z \leqslant 2800$) limits the mean values of the heads, and in this way also the tank diameter. The minimum value (1400 mm) is assumed to limit the height of the blanket, provide the possibility of mounting various fittings and accessories on the heads and ensure the stability of the entire construction. The maximum value (2800 mm) permits rail or road transportation of the ready-made pressure vessel (Ziółko 1995). The volume condition specifies the minimal height of the blanket, which cannot be less than V_C, including the heads.

The feasible set can take the form:

$$\phi = \phi(x) = \phi(D_Z, H_C, g_{DD}, g_P, g_{DG}) \subset R^5 \tag{4.3}$$

Optimization criteria. In order to choose the best solution from the set of feasible solutions, the following optimization criteria were established:

a) Weight criterion:

Lightweight constructions contribute to reducing the production costs, which is of primary importance in the case of expensive materials, such as stainless steel. Lightweight machines are easier to manufacture, assemble and transport. That is why the mass of the pressure space of a tank was taken into consideration.

b) Producibility criterion:

Producibility consists in adjusting the construction to the technical requirements (Osiński, Wróbel 1995). A machine should be easy to manufacture, and the production costs should be low (Dietrich 1999). The production capacity of a given production plant is also very important, especially in the

case of series production, where certain facilitations applied in many devices bring good economic results. The most labor-consuming part of the production of pressure vessels is connecting components of their working spaces. The length of welds and the thickness of steel sheets is of great significance during the production of pressure equipment. Lower thickness of steel sheets facilitates their plastic forming. Lower length of welds increases their safety and reliability. In order to obtain the numerical value of the objective function, during the optimization process the producibility criterion was expressed as the cross-section of the minimal number of welds necessary to join components of the pressure space.

c) Operating comfort criterion:

If a machine is to perform functions for which it was designed, it must be easy to operate. This concerns everyday operation, maintenance and repairs. Therefore, the machine must be adjusted to the needs and possibilities of the man operating it. Because in tanks used for technological purposes many fittings and accessories are placed on the top head (e.g. stirrers, inspection opening, safety valves, hatches, etc.), their height should be as low as possible. Taking this into account as well as considering the fact that this criterion is difficult to describe using numbers, it was assumed that the height of the pressure space of a tank is a measure of maintainability.

The above criteria are not the only ones, but were found to be the most important in our study. The objective function (F_c) can take the following form:

$$F_c(x) = (f_1(x) + f_2(x) + f_3(x)) \tag{4.4}$$

where stand for the criteria of weight, producibility and operating comfort respectively.

Methods

The aim of the first stage of the study was to find the height of the cylindrical unit of the tank, belonging to the set of feasible solutions. This height was determined using the spreadsheet Microsoft Excel and the mathematical dependences included in the Standard DIN 28013 concerning ellipsoidal heads. The height of the cylindrical unit was dependent on the thickness and diameter of heads, whose values were selected based on the Standard DIN 28013. The values of the diameters had to remain in the range specified by the geometric condition $1400 \leq D_z \leq 2800$. The total capacity of the pressure space had to fulfill the volume condition. Figure 4 shows a comparison of three variants of a tank of identical capacity.

The aim of the next, main stage of the study was to find the minimal thickness of components of the pressure space. The strength analysis was

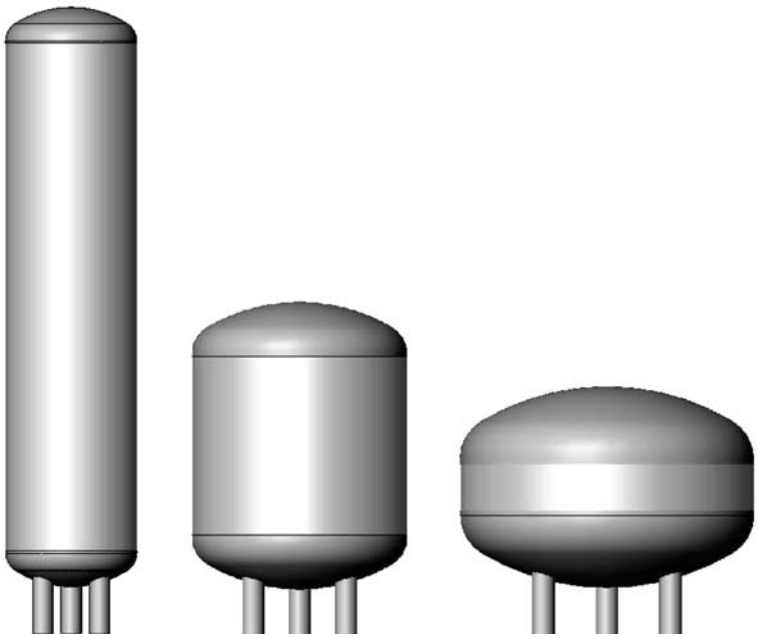

Fig. 4. Comparison of different variants of a pressure tank

carried out using the finite element method. Subsequent variants of the tank were generated in the CAD system, using a table of configurations. This enabled prompt restructuring of the computational model. For each variant the wall thickness was selected so as to meet the strength condition $\sigma_{HM} \leqslant f$. Then the minimal section of welds was calculated, and the mass and height of the pressure space were checked.

The last stage of optimization included the estimation of the values of the objective function for all variants belonging to the set of feasible solutions. Knowing the value of the objective function it was possible to choose the best engineering solution.

Results

This part of the paper presents the results of calculations. Table 2 shows the heights of cylindrical units of tanks as dependent on the diameter of their heads. All these variants represent the set of feasible solutions.

Figure 5 illustrates the reduced stresses obtained as a result of computations by the finite element method. Since the strength condition is fulfilled, i.e. the maximal reduced stresses do not exceed the permissible values, the variant present below belongs to the set of feasible solutions. The thickness

Table 2

Value of diameter and height cylindrical part of pressure tank

External diameter of tanks (mm)	Height of cylindrical part (mm)	External diameter of tanks (mm)	Height of cylindrical part (mm)
1400	5410	2200	1600
1500	4610	2300	1360
1600	3960	2400	1140
1700	3400	2500	950
1800	2930	2600	780
1900	2530	2700	620
2000	2170	2800	460
2100	1870		

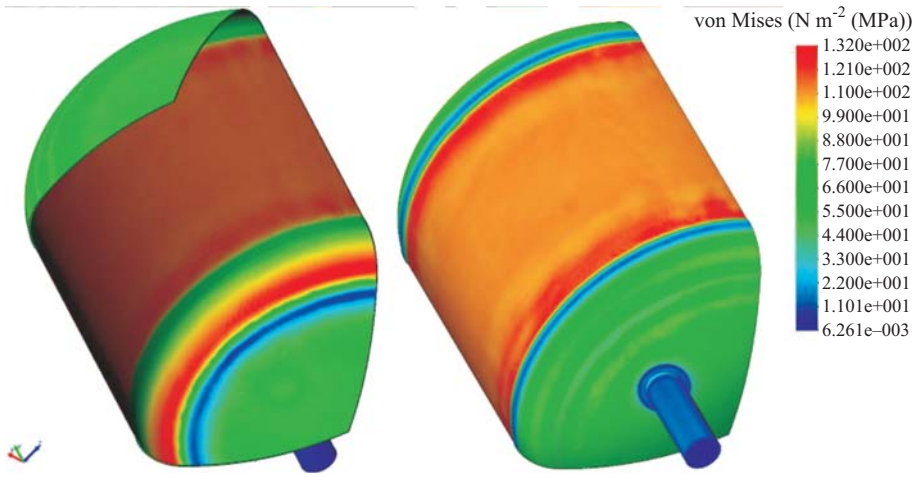

Fig. 5. Reduced stress on the internal and external surfaces of a pressure tank

of walls of the other tanks with known diameters was determined in a similar way (Table 2).

Table 3 summarizes the nominal thicknesses of components of the pressure space of tanks, belonging to the set of feasible solutions.

Table 3

Nominal thickness of pressure space elements

External diameter of tanks (mm)	Nominal thickness of lower bottoms (mm)	Nominal thickness of upper bottoms (mm)	Nominal thickness of cylindrical parts (mm)
1400	8	8	4
1500	8	8	5
1600	10	10	5
1700	10	10	5
1800	10	10	5
1900	10	10	6
2000	12	12	6
2100	12	12	6
2200	12	12	6
2300	12	12	6
2400	14	14	6
2500	14	14	8
2600	14	14	8
2700	14	14	8
2800	16	16	8

Selection of the optimum construction

Table 4 contains the values of particular criteria. Since we deal with the problem of multi-criteria optimization, it is necessary to apply one of the polyoptimization methods. The method of multipliers, also referred to as the method of scalarizing function or the method of pseudopolyoptimization, was employed. The significance of particular criteria was determined using weight coefficients – their values are given in Table 5.

All criteria were standardized so as to make them remain in the range [0,1]. Table 6 presents the standardized values of particular criteria.

The objective function, taking into account all optimization criteria, has the form:

$$F_c = \sum_{i=1}^{3} \rho_i q_i^* \tag{4.5}$$

and considering the values of weight coefficients:

$$F_c = 0{,}3 \cdot q_1^* + 0{,}3 \cdot q_2^* + 0{,}4 \cdot q_3^* \tag{4.6}$$

According to each of the criteria, various models of a pressure tank are the optimum constructions. According to the weight, producibility and operating comfort criteria, the best models are those of a diameter of 1500 mm, 1400 mm and 2800 mm respectively. Table 7 and Figure 6 present the values

Table 4

Data value for particular criterion of optimization

External diameter of tanks (mm)	Weight of pressure space (kg)	Cross-section of welds (mm^2)	Height of pressure space (mm)
1400	1060.8	91610	6178
1500	1024.2	116795	5428
1600	1081.2	94727	4841
1700	1071.0	103799	4332
1800	1068.9	111072	3912
1900	1189.8	137577	3563
2000	1322.4	147879	3276
2100	1343.1	115220	3026
2200	1368.0	119950	2807
2300	1398.6	124620	2618
2400	1621.5	134744	2460
2500	1791.0	172880	2321
2600	1839.3	178787	2202
2700	1890.3	184661	2093
2800	2193.6	197363	2005

Table 5

Value of scale coefficient for particular criterion of optimization

Mass criterion	Producibility criterion	Simplicity of exploitation criterion
0.3	0.3	0.4

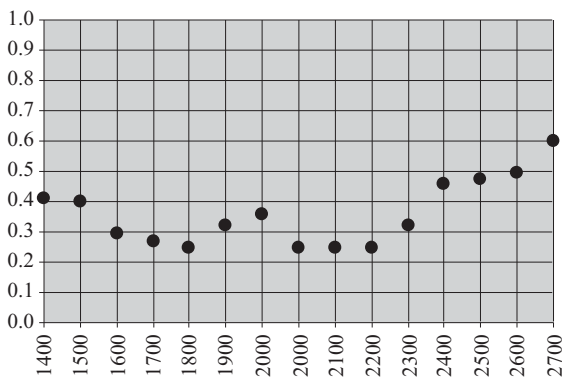

Fig. 6. Values of the objective function (axis of abscissae – tank diameter, axis of ordinates – values of the objective function)

Table 6

Normalized data value for particular criterion of optimization

External diameter of tanks (mm)	Weight of pressure space	Cross-section of welds	Height of pressure space
1400	0.031	**0.000**	1.000
1500	**0.000**	0.238	0.820
1600	0.049	0.029	0.680
1700	0.040	0.115	0.558
1800	0.038	0.184	0.457
1900	0.142	0.435	0.373
2000	0.255	0.532	0.305
2100	0.273	0.223	0.245
2200	0.294	0.268	0.192
2300	0.320	0.312	0.147
2400	0.511	0.408	0.109
2500	0.656	0.768	0.076
2600	0.697	0.824	0.047
2700	0.741	0.880	0.021
2800	1.000	1.000	**0.000**

Table 7

Value and sequence of aims function

External diameter of tanks	Values of aims function $-F_c$	Sequence values of aims function
1400	0.409	11
1500	0.400	10
1600	0.295	6
1700	0.270	5
1800	0.249	4
1900	0.322	8
2000	0.358	9
2100	0.247	2
2200	**0.245**	1
2300	0.248	3
2400	0.319	7
2500	0.458	12
2600	0.475	13
2700	0.495	14
2800	0.600	15

and courses of the objective function for a substitute criterion. Since our task was to minimize the objective function, the best design solution is a tank of a diameter 2200 mm (Figure 7). However, there are also some other solutions belonging to the feasible set, for which the values of the objective function are only slightly higher. These are tanks with a diameter of 1800, 2100 and 2300 mm. Taking into account the adopted criteria, the least desirable model is that of a tank whose diameter is equal to 2800 mm. This tank guarantees operating comfort, but is the heaviest and least producible.

Fig. 7. Optimum construction of a pressure tank at a capacity of 8 m^3

Summary and conclusions

In the age of the uniform market it is not enough for a product to simply perform the functions it was designed for. It should be also characterized by a broadly understood quality. The quality of machines and technical equipments is shaped already at the design stage, which has a profound impact on their final form. Numerous factors must be taken into account during the design process, the most important being safety, reliability, producibility and low weight as well as ergonomics, ecology and economics. All of these factors affect the competitiveness of the ready-made product, and their significance is decided about during the optimization process. The design of modern and competitive constructions requires the use of appropriate computer techniques, enabling to conduct detailed analysis.

The paper presents a method for optimizing the construction of a vertical pressure tank, for specified parameters, according to the adopted optimiza-

tion criteria. The optimization process was carried out using CAD/CAE systems, which allowed to do calculations for many variants of a tank within a relatively short period of time. The optimum construction, i.e. a tank 2200 mm in diameter, was selected based on strength and geometric analysis. This construction, chosen from among other feasible and technologically justified solutions, is characterized by low weight, high producibility and high operating comfort. It should be also noted that if the method of multipliers is applied during the optimization process, the choice of the best construction is strongly affected by the values of weight coefficients. Even a slight change in their values may make the designer choose a given solution.

It should be also stressed that our aim was to present an example of an algorithm of multi-criteria optimization of the construction under analysis, using the applications available to small and medium-sized enterprises. The method used for strength analysis as well as the theoretical model proposed in the study may be modified depending on software and the required accuracy of computations. Other optimization criteria may be also adopted, if they are considered of greater significance under certain conditions.

References

DIETRICH M. 1999. *Podstawy konstrukcji maszyn.* Tom 1. WNT, Warszawa.

GALIMOV K. 1975. *Osnowy nelinejnoj teorii obolocek.* Izd. Kazan. Univ., Kazan.

KONOPKO H. 1998. *Podstawy konstruowania urządzeń przemysłu chemicznego i spożywczego.* Wyd. Politechniki Białostockiej, Białystok.

LIPPMANN H. 1972. *Extremum and Variational Principles in Mechanics.* CISM Udine, Springer Verlag, Wien – New York.

ŁODYGOWSKI W., KĄKOL W. 2003. *Metoda elementów skończonych w wybranych zagadnieniach mechaniki konstrukcji inżynierskich.* Alma Mater, Poznań.

MAGNUCKI K. 1993. *Niektóre problemy optymalizacji konstrukcji prętowych i powłokowych z uwzględnieniem stateczności sprężystej.* Wyd. Politechniki Poznańskiej, Poznań.

MAGNUCKI K. 1998. *Optymalizacja konstrukcji i wytrzymałość zbiorników ciśnieniowych.* PWN, Warszawa – Poznań.

MAGNUCKI K., SZYC W. 1987. *Wytrzymałość materiałów w zadaniach.* PWN, Warszawa – Poznań

MAZURKIEWICZ Z., NAGÓRSKI R. 1986. *O pewnym kształcie powłok obrotowych obciążonych obrotowo-symetrycznie.* Prace naukowe Inst. Inż. Ląd. Politechniki Wrocławskiej, Wrocław.

OLSZAK W. 1980. *Thin Shell Theory: New Trends and Applications.* CISM Udine, Springer-Verlag, Wien –- New York.

OSINSKI Z.,WRÓBEL J. 1995. *Teoria konstrukcji.* PWN, Warszawa.

RAKOWSKI G. 1996. *Metoda elementów skończonych. Wybrane zagadnienia.* Oficyna Wydawnicza Politechniki Warszawskiej, Warszawa.

RAKOWSKI G.,KACPRZYK Z. 2005. *Metoda elementów skończonych w mechanice konstrukcji.* Oficyna Wydawnicza Politechniki Warszawskiej, Warszawa.

ZAGRAJEK T., WRZESIŃSKI G., MAREK P. 2005. *Metoda elementów skończonych w mechanice konstrukcji.* Oficyna Wydawnicza Politechniki Warszawskiej, Warszawa.

ZIENKIEWICZ O.C. 1980. *Metoda elementów skończonych.* PWN, Warszawa.

ZIÓŁKO J. 1995. *Konstrukcje stalowe.* Część 2. *Wytwarzanie i montaż.* WSiP, Warszawa.

ŻYWICA G. 2005. *Optymalizacja konstrukcji zbiornika ciśnieniowego przy wykorzystaniu systemów CAD/CAE.* Katedra Mechaniki i Podstaw Konstrukcji Maszyn UWM Olsztyn (praca magisterska).

Standards Referred to in the Paper:

Blachy stalowe walcowane na gorąco grubości 3 mm i większej – Tolerancje wymiarów, kształtu i masy. PN-EN 10029: 1999

Ellipsoidal dished ends. DIN 28013

Stale odporne na korozję – Gatunki. PN-EN 10088-1

Wyroby płaskie ze stali na urządzenia ciśnieniowe – Część 7: Stale odporne na korozję PN-EN 10028-7:2000

Accepted for print 26.01.2007

TECHNICAL SCIENCES
Abbrev.: Techn. Sc., No 10, Y 2007

DOI 10.2478/v10022-007-0007-3

POSSIBILITIES OF APPLICATION OF STOCHASTIC PROCESS THEORY IN EVALUATION OF TRIBOLOGICAL EXPERIMENT

Ján Pršan, Marian Kučera

Department of Mechanics and Engineering
Slovak University of Agriculture in Nitra

Key words: statistical dynamics, stochastic process, power spectral density, autocorrelation function, tribologic experiment.

Abstract

Mathcad 11, a software product of Mathsoft, was used for random numbers generation. The program enables generating sets of random numbers of various statistical properties. We used random distribution for our application. The set of random numbers had undergone statistical analysis using statistical dynamics methods. We applied low-permeable numeric filter. After filtration, the statistical analysis results have shown, that the power spectrum is relatively low. This has been confirmed also by the Fisher test. There are 15 important frequencies total, ranging in interval of 0.5 Hz – 6.2 Hz. Statistically, the most signifficant frequency is 0.5 Hz. Evaluated and described courses with their frequency spectrums can be used as input parameters of rationalizing and optimizing methods of tools‘ and machinery‘s design modification. They can be also used as input data of load in adhesive wear testing within tribologic experiments.

MOŻLIWOŚCI WYKORZYSTANIA TEORII PROCESÓW STOCHASTYCZNYCH DO OCENY EKSPERYMENTU TRIBOLOGICZNEGO

Ján Pršan, Marian Kučera

Słowacki Uniwersytet Rolniczy w Nitrze

Słowa kluczowe: dynamika statystyczna, proces stochastyczny, gęstość spektralna, autokorealcja, eksperyment trybologiczny.

Streszczenie

Do wygenerowania zbioru liczb przypadkowych zastosowano produkt Mathcada 11 firmy Mathsoft. Program pozwala na generowanie liczb przypadkowych o różnych właściwościach statystycznych. Na potrzeby eksperymentu przyjęto podział przypadkowy. Zbiór liczb przypadkowych poddano analizie statystycznej z zastosowaniem metod dynamiki statystycznej. W analizie zastosowano dolnoprzepuszczalny filtr liczbowy. Po filtracji analiza statystyczna

wykazała, że realizacyjne spektrum częstotliwości jest relatywnie niskie, co potwierdzono również w teście Fishera. Istotnych jest tylko 15 częstotliwości w zakresie 0,5÷6,2 Hz. Statystycznie najbardziej istotna jest częstotliwość 0,5 Hz.

Opisywane funkcje i ich spektra częstotliwościowe mogą być wykorzystane jako wstępne parametry metod optymalizowania konstrukcyjnego narzędzi i maszyn, a także jako wstępne parametry obciążeń w badaniach trybologicznych związanych z adhezyjnym zużyciem materiałów.

Introduction

In practice, it is normally continuous random process that occur. Random process analysis by digital computer assumes numeric formulation of the examined problem. Several operations go before the analysis.

First of all it is scanning the examined process. Concerning non-electrical process, it is tranformed into electrical signal. Normally, direct real-time analysis of the process is not executed, but it is recorded on an appropriate data carrier. It is possible to replay the record anytime. Using A/D converter, data are regularly scanned from the stochastic process application which is analysed. These data are expressed numerically. This is what we call sampling of the stochastic process realization. Throughout the whole process several errors may occur. Errors may affect correctness of the analysis results. These errors may be caused by inertia, non-linearity of the elements used in measuring sequence, additive noise etc. For the process analysis to be successful, all the errors must be negligible. We pay great attention to errors that occur during sampling.

Checking the pattern of the process is a part of the whole scanned process analysis. We mean by this the stacionarity test, detection of periodical components and normality test. Single steps of the analysis give us answers to these questions.

Ergodicity of the process is advantageous for its analysis. Single realization of the examined process is sufficient as a source of information about it. We may eliminate errors caused by sampling the continuous realization of the random process into numeric data by convenient choice of interval between moments of sampling to negligible value. Sampling period Δt is chosen so that the limiting frequency f_m will be bigger than the maximum value of the frequency $f_{\max}$ contained in sampling signal spectrum (of the realization). Usually, $f_m = (1.5 \div 2) f_{\max}$ is chosen with reserve.

Random process can be reached by experimental measuring of the particular device (certain nodes) in real working conditions, or by generating a group of random numbers with defined statistical features. For our application we used standard distribution with following defined arguments: number of figures with corresponding distribution, mean value - median, standard deviation.

We adjusted the generated group of random numbers using digit filter. We filtered off frequencies over 10 Hz. Adjusted group was analysed within the correlation theory.

Specific working conditions of agricultural machinery interact its working life, which is often relatively short, as a result of heterogenous modes of loading and subsequent deterioration of its components and their surface. In agriculture, from 70% to 90% of all damaged components are inactivated because of an abnormal wear. Tribologic node:
– pivot or shaft
– slide bearing, shaft seal etc.
– grease cap
– environment
ranks among frequent nodes in agricultural machinery and plays an important role in transmitting the power from driving unit to functional parts of adapters. The wear and loss of functional capacity of node‘s parts is a result of relative motion and load.

Real tribologic node of an agricultural device in work is a subject to complex dynamic stress of working load. Generators of the work load are variable values of power effects, deformations and motion acceleration of functional parts of the device, which determine its operation reliability. Therefore it is necessary to pay attention to such random processes. Using statistical dynamics in evaluation of values measured in tribologic experiment conditions it is possible to gain information revealing hidden relations between single values and between various statuses of the examined system.

Material and methods

Weight-loss of the samples within tribologic experiment were simulated as a demonstration of exploitation facilities of the random process theory. It was executed using random number generator with defined statistical parameters. Simulated procedures of realization after the transformation of data to PC were adjusted by specific program technique (filtration, basic deterministic parameters of random realization, stacionarity test, trend test for mean value and dispersion, histogram, distribution function).

After the accumulation of the set of digitalized parameters in the PC memory the following values have been defined:

Mean value dependent on time:

$$m(t_i) = \frac{1}{N_i} \cdot \sum_{i=1}^{N_i} p(i) \qquad (1)$$

where:

$N_i = \frac{N}{I}$ is longitude of the chosen interval

N is number of p values in realization
I is number of values in the chosen interval

Centred values of the process

$$p^{\circ}(i) = p(i) - m(t_i) \tag{2}$$

Dispersion of the random value

$$\mu_2 = \int_{-\infty}^{\infty} (x - m_x)^2 f(x)dx = D(x) \tag{3}$$

Standard deviation of the random value

$$\sigma_x = \left|\sqrt{D(x)}\right| \tag{4}$$

After the calculation of the basic statistical characters it is necessary to determine the stationarity or non-stationarity of the process applying an appropriate test. For the advisement on the stationarity of the process within the correlation theory it is sufficient to deal with attributes of the mean value, dispersion and autocorrelation function only. If we prove that mean value and dispersion are constant along the whole evaluation stage of the process and that the autocorrelation function depends only on the difference of two periods $\tau = t_2 - t_1$, the process is stationary.

Autocorrelation function for discrete data will be:

$$R_p(r) = \frac{1}{N-r} \sum_{n=1}^{N-r} p^{\circ}(n) \cdot p^{\circ}(n+r) \tag{5}$$

where: $r = 0,1,2, \ldots, m$

Spectral power density is defined by the basic relation

$$S_p(\omega) = \frac{2}{\pi} \int_0^{\infty} R_p(\tau) \cos \omega\tau d\tau \tag{6}$$

After adjusting we get equation, that can be used in computer algoritm

$$S_p\left(\frac{\pi \cdot l}{m \cdot \Delta t}\right) = \frac{\Delta t}{\pi}\left[R_p(0) + 2\sum_{r=1}^{m-1} R_p(\tau) \cos \frac{\pi \cdot l}{m} \cdot r + R_p(m) \cos(\pi \cdot l)\right] \tag{7}$$

where: $l = 0,1,2, \ldots, m$.

Having been prepared, these functions were graphically visualized and evalueated in terms of stationarity, ergodicity and significance of the power spectrum in relation to relevant frequencies.

The calculation of spectral density function is needed to the determination of the spectrum of the stochastic process. The significance of detected frequencies was confirmed by Fisher test in the process.

Function $I(\lambda)$ is determineed for the sequence of random values by the following formula:

$$I(\lambda) = \frac{1}{2\pi N}\left|\sum_{T=1}^{N} x_t e^{-it\lambda}\right|^2, \quad -\pi \leqslant \lambda \leqslant \pi \tag{8}$$

Function $I(\lambda)$ stands for periodicity chart of sequence $x_1, \ldots, x_n$.

For the statistical attributes of the periodicity chart to be examined in an easier way, another Figures of the formula (8) have been derived:

$$C_k = \frac{1}{N}\sum_{T=1}^{N-k} x_t \quad x_{t+k}, \quad k = 0,1,\ldots,N-1 \tag{9}$$

then

$$I(\lambda) = \frac{1}{2\pi}(C_0 + 2 \quad \sum_{k=1}^{N-1} C_k \cos k) \tag{10}$$

The periodicity chart shows high values in points corresponding frequencies $\lambda_1, \ldots, \lambda_p$. R. A. Fisher derived a test that can be used to discover the statistical significance of high values of the periodicity chart.

This way we determine significant frequencies $\lambda_1, \ldots, \lambda_p$ of the periodicity chart.

Design of the conditions of the experiment

Tribologic qualities of the friction couples are often checked using different devices repecting methods of the specific test room. Based on the experiment we would like to point out possibility and also necessity of using statistical dynamics in this field.

The wear test of selected types of material can be executed on one of devices of TE 97/A type – Figure 1, which ranks among “pivot-disk” test devices with area contact of the frictional-node elements. The test device is suitable for comparative tests of selected materials. The core of the test is imprinting the samples of the forms of pivot to front area of the spinning disk by constant power using hydraulic cylinder. The result of the test is a comparison of wear resistance of single types of material in conditions of the given experiment.

Parameters of the test were derived from the parameters of the adhesive wear test without lubrication used in tribologic laboratory VÚZ Bratislava. They were chosen in order to enable the best possible comparison of tribologic qualities of provided samples. Parameters of the test are following:

- pressure in hydraulic circuit (simulated) 1.47 MPa

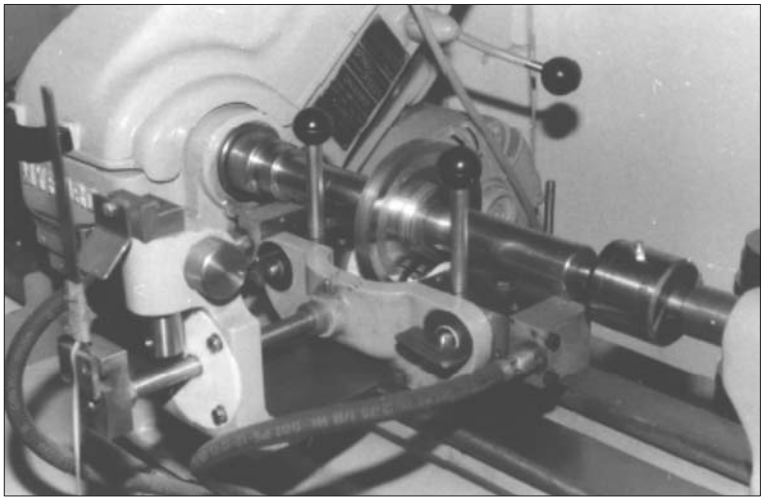

Fig. 1. The view of active part of equipment TE 97/A

- adherence pressure on pivot (simulated) 74.3 N
- circumferential velocity at the test radius 3.2 m.s^{-1}
- exposure time 15, 30, 45, 75s
- material of the companion part steel 12 020
- dimension of the sample 10 x 50 mm

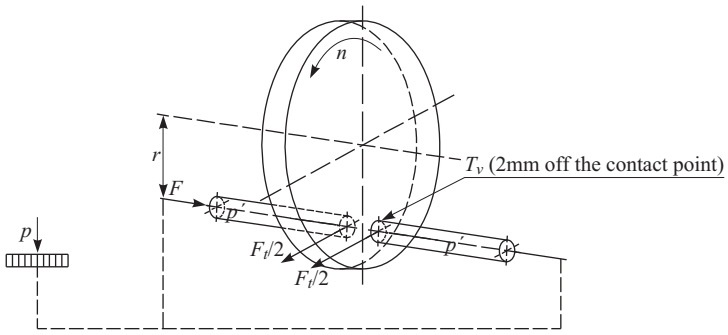

Fig. 2. TE 97/A appliance diagram

Table 1

Fisher test

j	$\lambda(j)$	$T(j)$	$I(\lambda)\cdot 10^6$	W	W_{crit}	Frequency Hz	Number
5	0.01267	495.800	1440487.63	0.0189	0.0095	0.5042	1
41	0.10392	60.463	1411544.50	0.0189	0.0095	4.1347	2
16	0.04055	154.938	1227834.13	0.0168	0.0095	1.6136	3
24	0.06083	103.292	1209192.63	0.0168	0.0095	2.4203	4
33	0.08364	75.121	1082818.63	0.0153	0.0095	3.3280	5
2	0.00507	1239.500	992838.13	0.0142	0.0095	0.2017	6
30	0.07604	82.633	951267.13	0.0138	0.0095	3.0254	7
27	0.06843	91.815	921187.69	0.0136	0.0095	2.7229	8
45	0.11406	55.089	893927.88	0.0134	0.0095	4.5381	9
15	0.03802	165.267	849326.75	0.0129	0.0095	1.5127	10
11	0.02788	225.364	826285.63	0.0127	0.0095	1.1093	11
31	0.07857	79.968	732318.69	0.0114	0.0095	3.1263	12
22	0.05576	112.682	688170.50	0.0108	0.0095	2.2186	13
62	0.15714	39.984	667185.81	0.0106	0.0096	6.2525	14
37	0.09378	67.000	633632.13	0.0102	0.0096	3.7313	15

Results and discussion

Figure 3 shows the course of the generated set with determined statistical characteristics. This set was filtered out by means of low-permeable numeric filter and it was centered to a zero mean value. Adjusted course has undergone the stationarity test. Iteration test and of the trend test for mean value and dispersion were executed. Iteration tests have shown, that this process is stationary in mean value and dispersion, which is proven by histogram showing the distribution of frequency of the centered realization. Its course is similar to standard frequency distribution.

Figure 3 also shows autocorrelation function describing the form of the spectrum of generated numbers in the course of time. After evaluation we detect its standard course, drop from high value and gradual damping.

Frequency analysis of this process is introduced by spectral power density. From the course of the spectral power density it is obvious, that there are several significant frequencies in the generated set. Fisher test proves the above. The most significant frequency of all is the frequency of 0.5 Hz, which is number 5. The corresponding periodicity chart is illustrated in Figure 3.

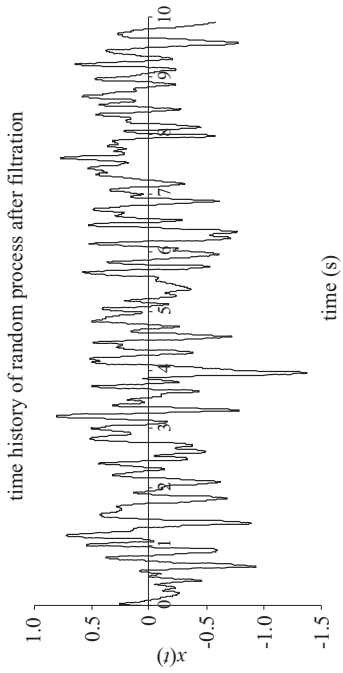
time history of random process after filtration
x(t)
time (s)

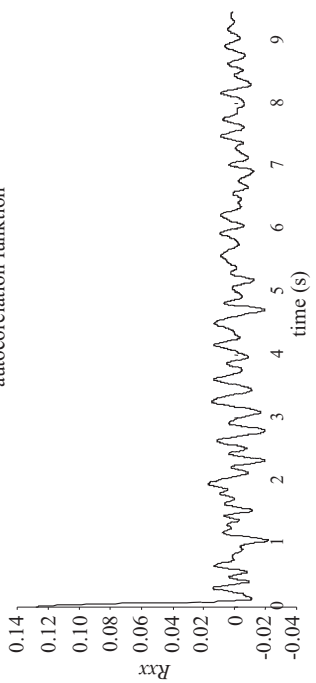
autocorelation funktion
Rxx
time (s)

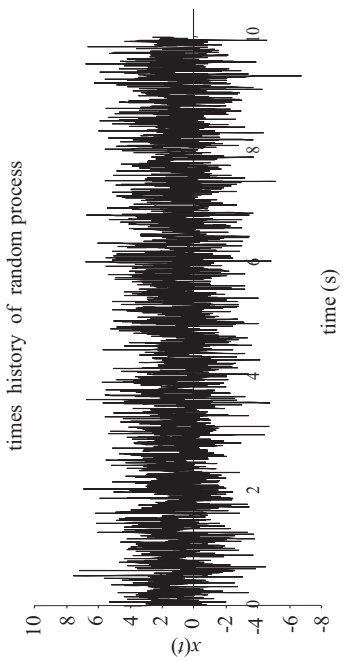
times history of random process
x(t)
time (s)

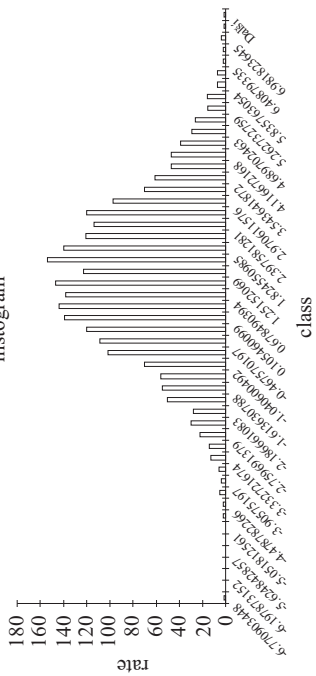
histogram
rate
class

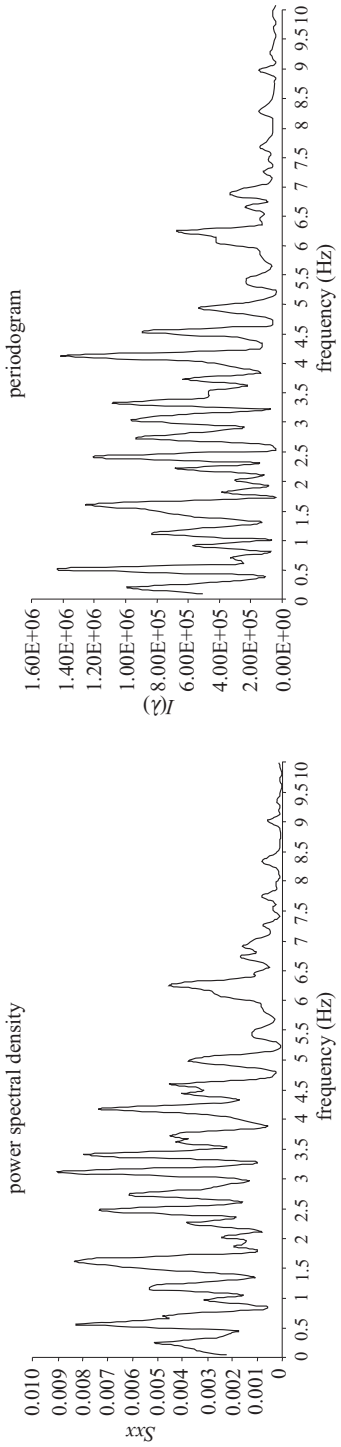

Fig. 3. Random data with defined statistical properties

Conclusion

We applied statistical dynamics methods for evaluation of random realization of the generated set of random numbers.

Evaluated and described courses with their frequency spectrums may be used as input parameters of rationalizing and optimizing methods of tools' and machinery's design modification. They may also be used as input data of load in adhesive wear testing of various types of material.

References

ANDĚL J. 1976. *Statistical analysis of time series*. Praha: SNTL, 1976, 253 s.

BAJLA J., PRŠAN J., BENDA I., ŚTRBA M. 2005. *The evaluating of random processes at the measurement of penetrate resistance of soil.* Scientific Proceedings. Neww Trend in Design and Technical Documentation Creation. Nitra. ISBN 80-8069-517-2.

KUČERA M. 2004. *Analysis of the information from the test of tribological characteristics of selected materials. Scientific Proceedings. Neww Trend in Design and Technical Documentation Creation*. Nitra. ISBN 80-8069-362-5.

ČAČKO J., BÍLÝ M., BUKOVECZKÝ J. 1984. *Measurement, evaluation a simulation of working stochastic processes.* Bratislava, Veda, 210 s.

MATYÁŠ V. 1976. *Measuring, analyzing and creating stochastic processes*. Praha: SNTL, 160 s.

RYDLO P., VANĚČEK A. 1980. *Evaluation of dynamic measurement*, Praha, NADAS, 272 s.

ŠESTÁK J. 1992. *Utilization of the Fisher test in frequency analysis of the stochastic process.* Acta technol. agric., XXXIII, s. 53 – 72. VŠP, Nitra.

Accepted for print 21.09.2007

TECHNICAL SCIENCES
Abbrev.: Techn. Sc., No 10, Y 2007

DOI 10.2478/v10022-007-0008-2

AN ALGORITHM FOR HANDLING EXPERIMENTAL DATA OF PERIODICAL PROCESSES WITH MICROSOFT EXCEL

Jurij Dobriański, Michał Duda

Chair of Electrics and Power Engineering
University of Warmia and Mazury in Olsztyn

Key words: periodical processes, data filtering, data handling, experimental data, periodical processes, measurement noise.

Abstract

This paper describes an algorithm for handling experimental data of periodical processes with Microsoft Excel. Thanks to this method, it is possible to prepare experimental results for analysis with the use of simple, easily available tools. The algorithm filters data and removes what is called measurement noise. This makes it possible to more precisely identify the trends in the analysed data.

ALGORYTM OPRACOWANIA W EXCELU DANYCH EKSPERYMENTALNYCH PROCESÓW OKRESOWYCH

Jurij Dobriański, Michał Duda

Katedra Elektrotechniki i Energetyki
Uniwersytet Warmińsko-Mazurski w Olsztynie

Słowa kluczowe: procesy okresowe, filtrowanie danych, opracowanie danych, dane eksperymentalne, procesy okresowe, szum pomiarowy.

Streszczenie

Opisano algorytm opracowania w Excelu danych eksperymentalnych procesów okresowych. Zaprezentowana metoda pozwala, za pomocą prostych, łatwo dostępnych narzędzi, przygotować wyniki pomiarowe do analizy. Algorytm filtruje dane, usuwając tak zwany szum pomiarowy. Dzięki temu staje się możliwe bardziej precyzyjne zauważenie trendów analizowanych danych.

Introduction

The results of measurements obtained in experimental practice are frequently distorted by measurement noise. The noise is caused by external interfering factors or by excessive sensitivity of the recording equipment. Correct filtering of measurement results enables the retrieval of data, which are sometimes obtained at quite a high cost. Conventional methods of filtering measurement results are onerous and their outcome depends on subjectively adopted parameters (Talar i in. 2003).

Analysis of such measurement data, obtained in experiments, is frequently onerous, and sometimes impossible. Properly conducted pre-analysis of such data, based on filtering algorithms, should reveal more or less generalised trends in the data being analysed. Meanwhile, the additional noise contained in the measurements should be eliminated. This means that the de-noised data enable constant differentiation of the interpolated results and their further analysis is much easier (Rauch i in. 2004).

There are currently many techniques of data filtering. Each of the existing algorithms has advantages and disadvantages, but none of them can be considered universal, which means that it cannot be applied in the smoothing of various types of data containing measurement noise of various characteristics (Rauch, Kusiak 2005).

The problem of data filtering is in fact one of appropriate approximation of measurement points, which in a one-dimensional case are contained in a curve (Buades i in.). Currently, there are many algorithms of approximation, the most popular of them are polynomial approximations, weighted average, neuronal networks, wavelet analysis and Fourier transform. Some methods are accurate but require costly calculations (polynomial approximations), others include speed of action among their characteristics (weighted average), though it is impossible to establish the appropriate condition for the algorithm to discontinue. Like trigonometrical functions in the Fourier transform, wavelet analysis is a mathematical function determined within a certain interval. Consequently, they can be hardly comprehensible for less advanced users and their application may be troublesome. Neuronal networks are even more complex, but they provide much better results. However, the crucial flaw of the method is its low degree of universality (Kusiak i in. 2001).

With an absence of the appropriate filtering measures, a low degree of noise in experimental data, a low frequency of periodical runs, a lack of a universal and simple algorithm of data filtering, it is justified to attempt to apply the simplest logical functions, even those available in spreadsheets.

Formulating the problem

In order to calculate the characteristic features of cyclic processes, it is necessary to determine the minimum and maximum values of parameters which fluctuate periodically during the experiment.

With a considerable number of cycles (at least close to a hundred), handling data placed in measurement tables is best done with the use of computers; this ensures error-free repeated application of the same data handling technique, increases the reliability of the final results and saves the time needed to handle the data.

Obstacles and problems encountered during data handling are caused by the following properties of measurement data sets. The most important of them are:

– so-called "measurement noise", i.e. random, short-lasting deviations of the parameter values, unrelated to the basic changes occurring in the object. It causes the appearance of small extrema which, when data are handled with the use of a computer, can be treated as the extrema of the object operation, while not being such; they should be eliminated;

– digital data transmission sometimes shows the results of rounding the transmitted values, which is typical of all digital methods and is expressed by replacing close values by identical ones. This, in turn, makes it impossible to determine the trends of a parameter change, makes it difficult to determine the extrema if only a limited number of the elements of a measurement series.

Examples of such properties are shown in Figure 1.

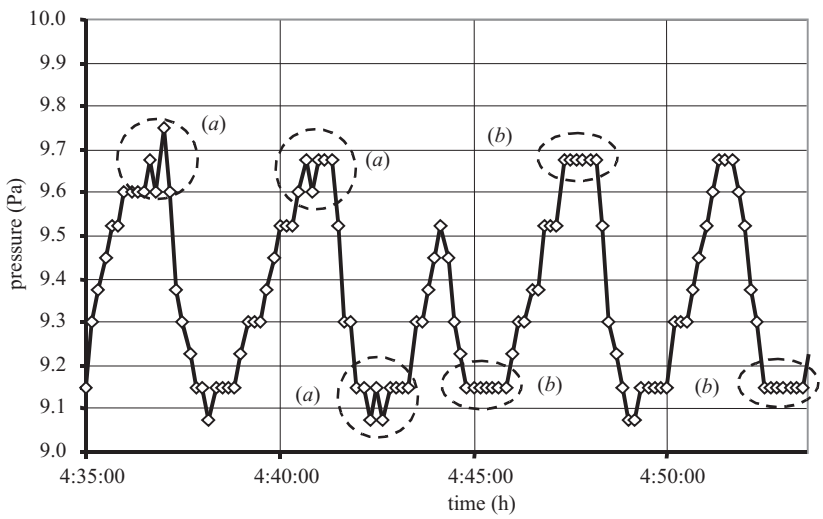

Fig. 1. Examples of additional, "noise-related" maxima and minima (a) and series of identical values (b) in measurement data transmitted with the use of digital techniques

Selection of a data handling method

Selection of data handling method depends not only on the capabilities offered by the software, but also on how advanced the user is in operating it.

Spreadsheets, especially Microsoft Excel, provide high level of calculation capabilities and convenient tools for graphic data presentation. In addition, they are commonly used by many users. Therefore, Microsoft Excel can be a good and easily available tool for experimental data handling. Excel is not intended as a tool for creating complex algorithms; this is related to significant limitations of certain of its functions and should be taken into account when selecting a method of data handling.

One of the significant limitations of Excel is that its logical function IF has only two variants of response: TRUE or FALSE. This in turn makes it necessary to apply additional levels of embedding a function within a function, which is limited to 7 levels of embedding. This affects the overall length of algorithm in a cell. When standard functions are used, it is indeed limited. Nevertheless, Excel's calculation capabilities can ensure the required level of data handling without using specialised programming languages. An example of such an application is presented in this paper.

Algorithm of elimination of minimum and maximum caused by measurement noise

Measurement noise causes sharp increase in the value of the measurement parameter, followed immediately by a return to the values close to the average. In practical terms, it shows as a pair of maximum-minimum which are situated next to or close to each other, as in Figure 1a. Therefore, an algorithm intended for elimination of such interferences should not take into account many consecutive measurement values – it could be two-three values before and after the analysed item. A block diagram of the algorithm, based on the logical function IF, is shown in Figure 2.

The rhombus elements of the block diagram contain the indexes of comparable measurement elements. The index of an analysed cell is marked by *i*. Over the lines connecting the diagram's elements are symbols (lines and dots). A dot in a symbol means the current position, while lines – possible meanings of other measurement values in relation to the current value, which have been analysed at this place in the algorithm. The following text of the Excel function describes the algorithm:

```
=IF(C9=B10;B10;IF(C9>B10;IF(C8>=C9;IF(C7>=C8;B10;IF(B10>=B11;B10;B9));IF(B10=
B11;IF(B11>=B12;B10;B9);IF(B10>B11;B10;B9)));IF(C8<=C9;IF(C7<=C8;B10;IF(B10<=
B11;B10;B9));IF(B10=B11;IF(B11<=B12;B10;B9);IF(B10>B11;B9;B10)))))
```

According to the algorithm text, the processed measurement value will be written into the C10 cell. Data for comparison are taken from previous

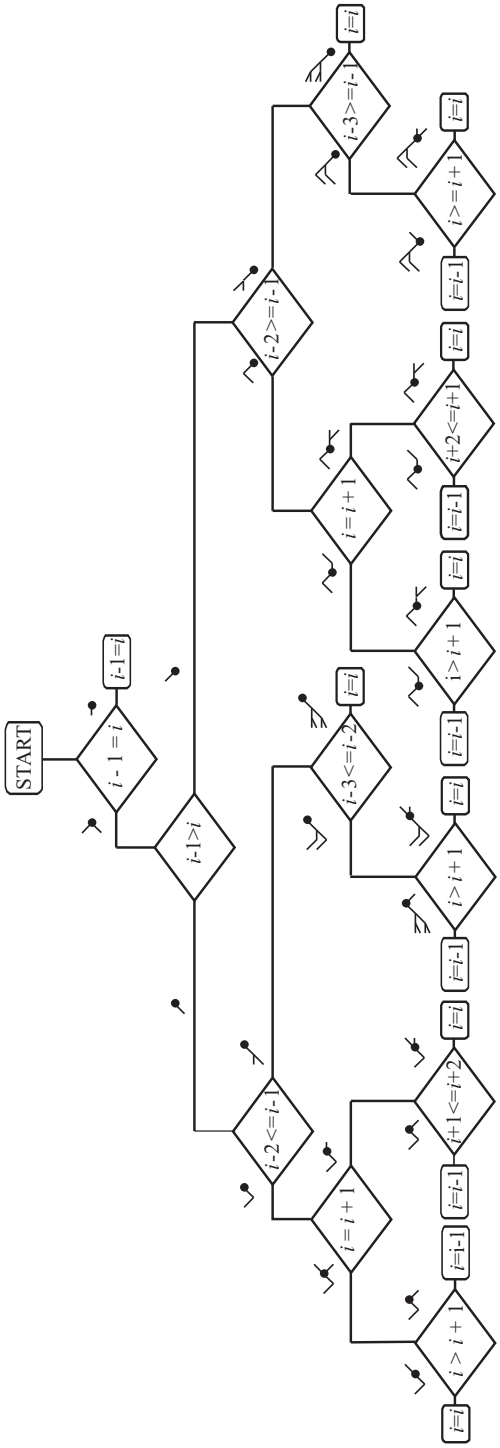

Fig. 2. A block diagram of an algorithm used to eliminate neighbouring minimum and maximum, caused by measurement noise

cells of column C and from several cells of column B, whose values have been determined in previous steps of calculation.

The diagram of the positions of cells from which data are taken is shown

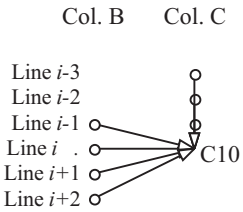

Fig. 3. The diagram of the positions of cells from which data are taken for eliminating the neighbouring minimum and maximum

Table 1

An example of elimination of measurement noise with the use of an algorithm for the 'IF' function in Microsoft Excel

Time, h	The value in the pressure cell before application of the algorithm (Pa)	The value in the pressure cell after application of the algorithm (Pa)
4:35:30	9.450	9.450
4:35:40	9.525	9.525
4:36:00	9.600	9.600
4:36:40	9.675	9.675
4:36:50	9.600	9.675
4:37:00	9.750	9.750
4:37:10	9.600	9.600
4:37:20	9.375	9.375
4:37:30	9.300	9.300
4:37:40	9.225	9.225
4:37:50	9.150	9.150
4:38:10	9.075	9.075
4:38:20	9.150	9.150
4:39:00	9.225	9.225
4:39:10	9.300	9.300
4:39:40	9.375	9.375
4:39:50	9.450	9.450
4:40:00	9.525	9.525
4:40:30	9.600	9.600
4:40:40	9.675	9.675
4:40:50	9.600	9.675
4:41:00	9.675	9.675
4:41:30	9.525	9.525
4:41:40	9.300	9.300
4:42:10	9.150	9.150
4:42:20	9.075	9.075
4:42:30	9.150	9.075

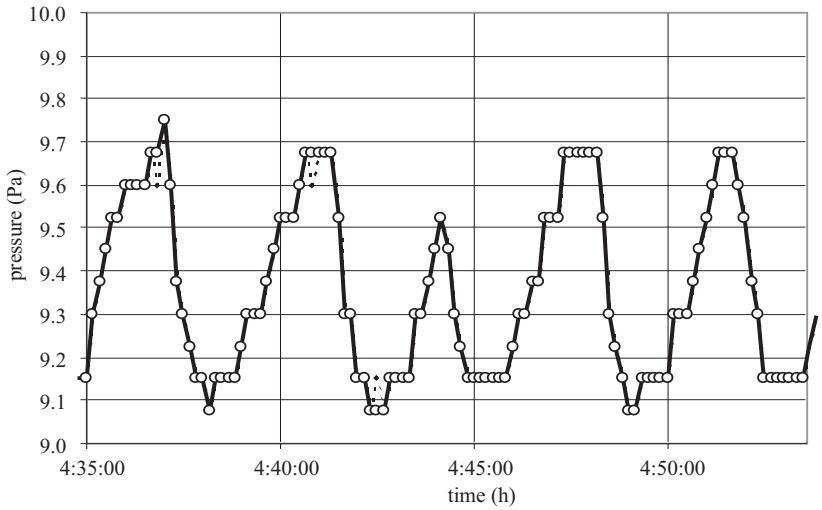

Fig. 4. The result of applying the algorithm of elimination of neighbouring minimum and maximum, caused by measurement noise: the dot line shows the original data

in Figure 3. The calculations produce a column with new, corrected data (Tab. 1). The results of processing, which eliminates the maximum and minimum situated close to each other are shown in Figure 4.

An algorithm for reducing the size of a series of identical measurement values

It is useful to reduce the size of a series of identical measurement values so as to avoid analysing considerable numbers of consecutive values of measurement data. Which in turn causes an increase in the level of embedding of the logical IF functions in one another.

The algorithm provides for checking the character of consecutive measurement data. If a series of values is found of two identical values, then the value on the limit of the series will be replaced with one that is calculated as the mean of the neighbouring cells. In other cases, the values will be assigned with no change. A block diagram of the algorithm is shown in Figure 5; its formula is as follows:

=IF(B9<>B10;IF(B10=B11;(B9+B11)/2;B10);IF(B8=B9;(B9+B11)/2;B10)).

The outcome of the double application of the algorithm is shown in Figure 7.

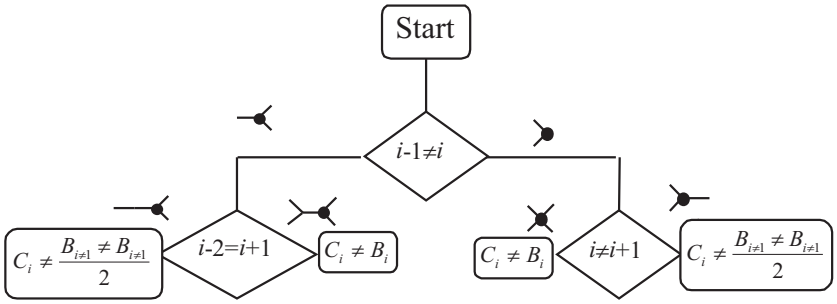

Fig. 5. A block diagram to reduce the size of a series of identical measurement values

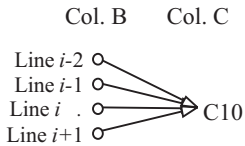

Fig. 6. A diagram of positions of the cells from which data are taken to reduce the size of a series of identical measurement values

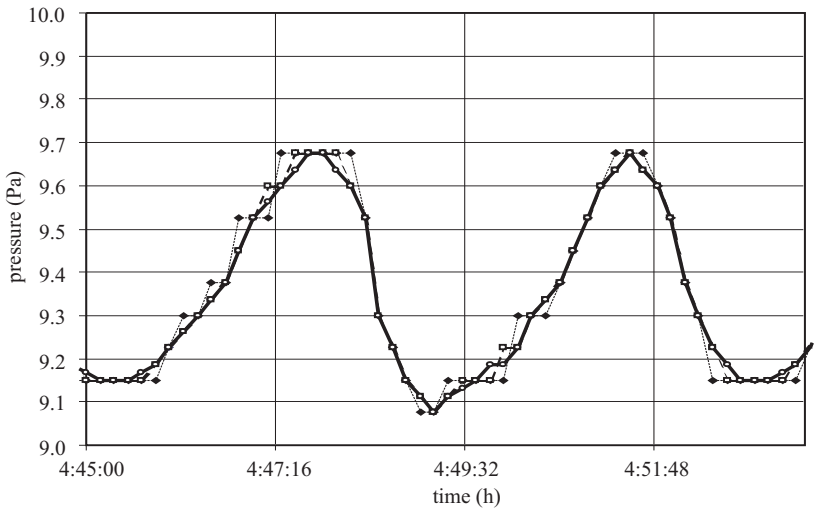

Fig. 7. The outcome of double application of the algorithm for reducing the size of a series of identical measurement values: the stroke line denotes the values before processing

Table 2

An example of applying an algorithm to reduce the size of a series of identical measurement values. The shaded cells indicate the values which have been changed by the algorithm

Time	Pressure	The value of the pressure cell after the application of the algorithm	The value of the pressure cell after the secondary application of the algorithm
1	2	3	4
4:45:00	9,150	9.150	9.169
4:45:10	9,150	9.150	9.150
4:45:20	9,150	9.150	9.150
4:45:30	9,150	9.150	9.150
4:45:40	9,150	9.150	9.169
4:45:50	9,150	9.188	9.188
4:46:00	9,225	9.225	9.225
4:46:10	9,300	9.263	9.263
4:46:20	9,300	9.300	9.300
4:46:30	9,375	9.338	9.338
4:46:40	9,375	9.375	9.375
4:46:50	9,525	9.450	9.450
4:47:00	9,525	9.525	9.525
4:47:10	9,525	9.600	9.563
4:47:20	9,675	9.600	9.600
4:47:30	9,675	9.675	9.638
4:47:40	9,675	9.675	9.675
4:47:50	9,675	9.675	9.675
4:48:00	9,675	9.675	9.638
4:48:10	9,675	9.600	9.600
4:48:20	9,525	9.525	9.525
4:48:30	9,300	9.300	9.300
4:48:40	9,225	9.225	9.225
4:48:50	9,150	9.150	9.150
4:49:00	9,075	9.113	9.113
4:49:10	9,075	9.075	9.075
4:49:20	9,150	9.113	9.113
4:49:30	9,150	9.150	9.131
4:49:40	9,150	9.150	9.150
4:49:50	9,150	9.150	9.188
4:50:00	9,150	9.225	9.188
4:50:10	9,300	9.225	9.225
4:50:20	9,300	9.300	9.300
4:50:30	9,300	9.338	9.338
4:50:40	9,375	9.375	9.375
4:50:50	9,450	9.450	9.450
4:51:00	9,525	9.525	9.525
4:51:10	9,600	9.600	9.600

cont. tab. 2

1	2	3	4
4:51:20	9,675	9.638	9.638
4:51:30	9,675	9.675	9.675
4:51:40	9,675	9.638	9.638
4:51:50	9,600	9.600	9.600
4:52:00	9,525	9.525	9.525
4:52:10	9,375	9.375	9.375
4:52:20	9,300	9.300	9.300
4:52:30	9,150	9.225	9.225
4:52:40	9,150	9.150	9.188
4:52:50	9,150	9.150	9.150
4:53:00	9,150	9.150	9.150

An algorithm for determining the minimum and maximum of the parameters of the process under study

When determining the minimum and maximum, it is necessary to take into account a possibility of remaining a series of identical measurement values at the extreme points of the measurement records. The aim of the function used to determine the minimum and maximum is to ascertain whether the point under examination has the maximum or minimum value as compared with the neighbouring points. It will also check whether the analysed value is situated on an upward or downward section. If the next two neighbouring measurement records have the same value as the one under examination, the analysed point will be marked as ‘unknown’.

The block diagram of the algorithm which determines the extreme values is shown in Fig. 8, and the text of the algorithm function is presented below.

=IF(B9=B10;IF(B11=B10;”0";IF(B11>B10;”g”;”d”));IF(B9>B10;IF(B11=B10;IF(B12=B11;”unknown”;IF(B12>B11;”min”;”d”));IF(B11>B10;”min”;”d”));IF(B11=B10;IF(B12=B11; ”unknown”;IF(B12>B11;”g”;”max”));IF(B11>B10;”g”;”max”))))

A diagram of the cells from which data are taken to determine the extreme values of measurement parameters is shown in Figure 9.

The data processing results in a column with markings in respective lines: min, max, g (upwards), d (downwards) and unknown. The last indicator allows for checking whether there are any series left with repeated (three or more times) data values. The table clearly shows the places where the maxima and minima are situated and enables their calculation.

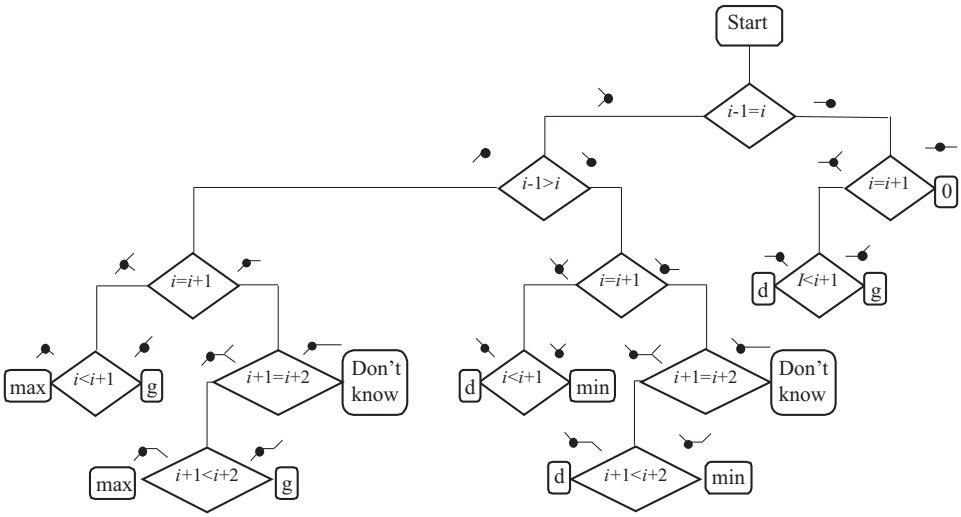

Fig. 8. A block diagram of the algorithm for determining the extreme values of measurement parameters

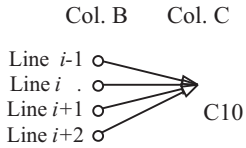

Fig. 9. A diagram of the cells from which data are taken to determine the extreme values of measurement parameters

Table 3

An example of application of an algorithm for determining the minimum and maximum of the process param

Time	Pressure, Pa	Change of Pressure	Min–max	Unknown
0:01:30	7.950	max	7.95	0
0:01:40	7.913	down	0	0
0:01:50	7.875	down	0	0
0:02:00	7.838	down	0	0
0:02:10	7.800	min.	7.8	0
0:02:20	7.875	up	0	0
0:02:30	7.950	max	7.95	0
0:02:40	7.913	down	0	0
0:02:50	7.894	down	0	0
0:03:00	7.875	min.	7.875	0

In order to calculate the periods of parameter change, i.e. the time intervals between the extrema, it is useful to select the lines containing extreme values. To this end, one should apply the 'Data' tool in MS Excel, select the 'Filter' tab, then 'Advanced filter' with options "Copy elsewhere' and 'Only unique records'.

The algorithm proposed here enables finding the minimum and maximum values of the measured parameters; it has been tested and successfully applied in handling the results of experiments to determine the thermal condition of a laboratory model and solar installation in the study conducted at the Faculty of Technical Sciences of the University of Warmia and Mazury in Olsztyn.

Summary

This study is an attempt to analyse measurement data obtained in experimental determination of the thermal condition of a laboratory model and solar installation. The tools contained in Microsoft Excel were used in filtering data. The filtration results presented in tables and figures indicate that the analysis conducted with the use of Microsoft Excel is highly effective in the filtration of data containing interfering signals in the form of measurement noise.

The results show the usefulness of the technique in filtering measurement data and is an example of using Microsoft Excel, while at the same time indicating its high capabilities in processing and analysing large sets of numerical data. Further research should be aimed at assessment of filtration errors.

Reference

Talar J., Rauch Ł., Kusiak J. 2003. *Filtrowanie danych pomiarowych przy wykorzystaniu analizy falkowej i sztucznych sieci neuronowych.* Informatyka w Technologii Materiałów, 3–4: 180–188.

Rauch Ł., Talar J., Zak T., Kusiak J. 2004. *Filtering of termomagnetic data curve using artificial neural network and warelet analysis.* Proc. 7th ICAISC 2004, Conf. Zakopane, Poland, Springer-Verlag, 1093–1098.

Rauch Ł, Kusiak J. 2005. *Filtrowanie danych pomiarowych przy wykorzystaniu metody cząstek dynamicznych*. Przegląd mechaniczny, 7–8: 39.

Buades A., Coll B., Morel J.M. *On image denoising methods.* Centre de Matematiques et de Leurs Applications (http://www.cmla.ens-cachan.fr)

Kusiak J., Pietrzyk M., Gawąd J., Roberts C.M., Wajda W. 2001. F*iltering of the measurement data by ANN approach.* Proc. Conf. "Computer Science in Metals Technology KomPlasTech'2001", eds, Grosman F., Piela A., Kusiak J., Pietrzyk M., Korbielów, ss. 65–70.

Accepted for print 12.10.2007

TECHNICAL SCIENCES
Abbrev.: Techn. Sc., No 10, Y 2007

DOI 10.2478/v10022-007-0001-9

STUDY OF NEGATIVE PRESSURE IN SUCTION PROPELLER AND TUBE AGITATORS

Anatoliy Molchanov, Andrzej Wróblewski

Department of Environmental Engineering
University of Warmia and Mazury in Olsztyn

Key words: suction agitators, negative pressure, velocity, intensity.

Abstract

The paper presents the results of studies on negative pressure generated in propeller and tube agitators. The value of negative pressure depending on the number of agitator revolutions n‹5000 min^{-1} under conditions of the turbulent area (Reynolds number Re_m‹ $2 \cdot 10^5$) was determined.

BADANIE PODCIŚNIENIA W MIESZADŁACH SAMOZASYSAJĄCYCH ŚMIGŁOWYCH I RURKOWYCH

Anatoliy Molchanov[1], Andrzej Wróblewski[1]

Katedra Inżynierii Środowiska
Uniwersytet Warmińsko-Mazurski w Olsztynie

Słowa kluczowe: mieszadła samozasysające, podciśnienie, prędkość, natężenie.

Streszczenie

Przedstawiono wyniki badań podciśnienia, które powstaje w mieszadłach samozasysających – śmigłowym i rurkowym. Określono wielkości podciśnienia w zależności od liczby obrotów mieszadła n‹5000 min-1 w warunkach obszaru turbulentnego (liczba Reynoldsa Re_m‹ $2 \cdot 10^5$).

Introduction and goal of the study

In the processes of biological wastewaters treatment aeration is applied to supply oxygen for aerobic microorganisms and for oxidation of organic compounds. Aeration is also used in various configurations during water preparation processes. Aeration with appropriate compression devices at ca. 0.15 MPa through diffusers or porous plates is commonly used. Such installations are complicated and costly and, as a consequence, it was proposed to apply suction agitators with turbine agitator in modern treatment plants

and in chemical industry (Karcz 2001, Błasiński et al. 1991, Kowal 2001). Such agitators create the radial stream of gas-liquid medium and do not cause uplifting the microorganic sediment from the bottom. Additionally, during the process of mixing air with water in turbine agitator air bubbles of large diameters are formed, which contributes to small contact surfaces between water and air. It is known (Aksielrud 1981, Lewicki 1999) that the speed of mass exchange between the gas bubbles and the liquid increases with increasing the own surface of contact between phases (m^2/m^3) and the speed of sliding of the bubbles in the liquid. There is a possibility of creating conditions for intensification of mass exchange (absorption of air oxygen) through movement of agitator blades with orifices on the surface through which the air is sucked. Under such conditions gas bubbles smaller in diameter than the bubbles formed in the turbine agitator are torn off the rotating surface.

This study aimed at investigating the dependence of negative pressure ΔP on agitator blade surface with orifices and at the end of the tubes of the tube agitator from the revolutions frequency. That negative pressure provides the base for computation of the sucked air velocity W, its flow intensity Q and agitator immersion depth H (Koch 1998):

$$W = \sqrt{\frac{2\Delta P}{\varsigma}}\ , \text{ m/s} \tag{1}$$

$$Q = \frac{\pi d^2}{4} W\ , \text{ m}^3\text{/s} \tag{2}$$

$$H = \frac{\Delta P}{\varsigma g}\ , \text{ m} \tag{3}$$

where:
d – diameter of suction orifice, m/s^2;
g – acceleration of gravity,
ς – air density, kg/m^3

In case of suction agitators at a depth exceeding the H value the air is not sucked and that is why computing the H value from formula (3) on the basis of ΔP determined experimentally is so important. Computing the Q value from formula (2) is needed for computation of technological quantities of oxygen sucked from the air (Lewicki 1999).

Selection of agitator types and experimental parameters

The above information indicates that testing the triple blade propeller agitator designed by the Kiev Institute of Technology (Kowal 2001), that assures movement of the liquid towards the tank bottom raising the active sediment containing microorganisms would be helpful (Fig. 1a).

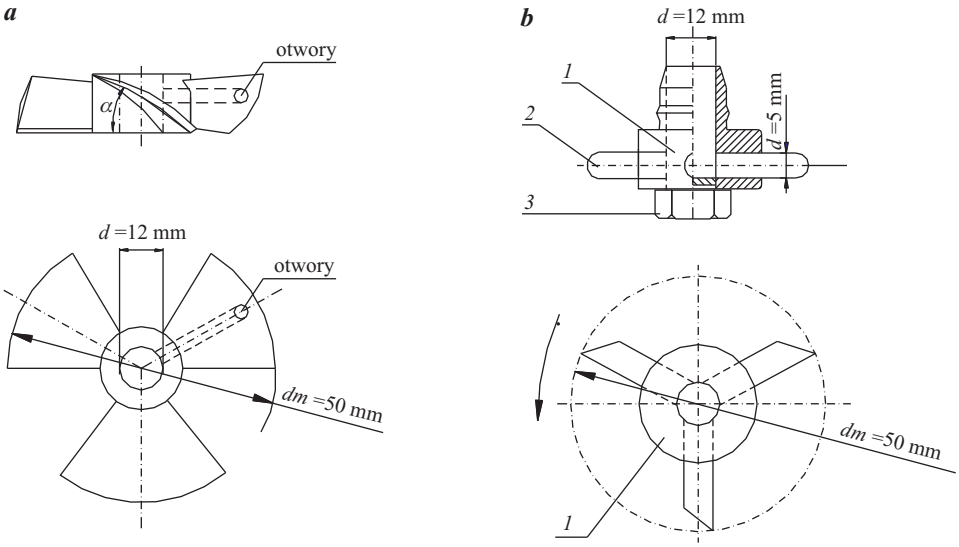

Fig. 1. Scheme of propeller agitator a) and tube agitator b) *1* – casing, *2* – tube, *3* – screw

The diameter of that agitator is d_m= 50 mm. At high revolutions (n<5000 min^{-1}) such an agitator secures generating a turbulent zone, which is generally applied (Koch, Noworyta 1998, Heim et al. 1995) with Re_m:

$$\mathrm{Re}_m = \frac{n d_m^{\,2}}{\nu} \leqslant 2 \cdot 10^5$$

where:
ν – kinematical viscosity coefficient, m^2/s,

The study by Heim et al. 1995 presents the results of studies on tube and disk suction agitators. The oxygen volume penetration coefficient was calculated showing practically equal effectiveness of those agitators. The rube agitator, however, is simpler and cheaper. That is why the triple tube agitator with the diameter d_m = 50 mm was chosen.

Description of the laboratory station and the methodology of experiments

The diagram of the laboratory station is presented in Figure 2. It consisted of a tank in which the agitators in the form of perforated cone or with triple blade agitator with the diameter d_m = 50 mm were mounted (Molchanov 2003).

Electric motor (*1*) is connected through the clutch (*2*) with the shaft (*3*) that is installed on bearings in the case with a flange. The water container

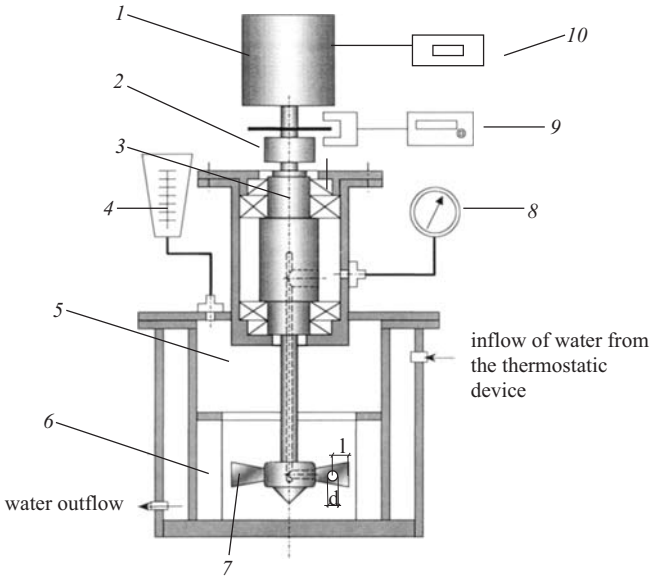

Fig. 2. Diagram of the laboratory test station for the propeller agitator *1* – motor, *2* – clutch, *3* – shaft, *4* – container, 5 – tank, *6* – fins, *7* – propeller agitator, *8* – vacuum meter, *9* – tachometer, 10 – power meter

is made of stainless steel. It possesses a mantle to which a thermostatic device is connected. The propeller agitators are operated at high speeds and as a consequence they can operate without reduction or belt couplings. At high rotation speeds of agitators a funnel forms, which can uncover the entire propeller. In this case the power demand decreases, the suction of air starts and the mixing effectiveness decreases rapidly. To avoid funnel formation 4 fins are mounted on the walls of the tank (*6*). The pressure behind the blade is measured using the vacuum meter (*8*), the revolutions frequency with a tachometer (*9*) and engine power with a wattmeter (*10*).

The methodology of the experiment involves measurement of negative pressure ΔP at various revolutions frequencies of the agitator n. The gases dissolved in the liquid were sucked through the orifices in agitator blades and they accumulated in the container (*4*), from which the water was going to the tank (*5*). Water from the tank (*5*) was filling the lidded container (not shown in Figure 2).

Results and analysis of experiments

The average results from three tests are presented in table 1.

It was determined experimentally that the negative pressure ΔP on agitator blade increases with the increase of propeller and tube agitator

Table 1

Dependence of negative pressure ΔP on revolutions frequency of studied agitators

No.	n min^{-1}	ΔP, KPa for agitators	
		propeller agitator	tube agitator
1	1000	2,5	–
2	2000	15	10
3	3000	27	35
4	4000	35	46
5	5000	38	50

revolutions frequency. On the basis of the determined value of negative pressure ΔP increase the velocity of air sucked and the intensity of its flow Q as well as the agitator immersion depth H can be computed.

Conclusions

On the basis of the examination of negative pressure that is generated in suction propeller and tube agitators:

– a method for computing the immersion depth H for those agitators on the basis of the experimentally determined value of negative pressure ΔP was developed;

– the value of negative pressure depending on the revolutions of the agitator $n < 5000$ min^{-1} under the turbulent zone conditions (Reynolds number $Re_m = nd_m^2/\nu < 2 \cdot 10^5$) was determined;

– it was concluded that although the tube agitator is simpler and cheaper, it creates a radial stream and as a consequence application of a combination of two agitators on a single shaft: at the top an ordinary propeller agitator that forms the vertical stream and a suction tube agitator under it, seems rational.

References

Aksielrud G., Molchanov A. 1981. *Rozpuszczanie ciał stałych*. WNT, Warszawa.

Błasiński H., Michalski H., Rzyski E., Stelmach J., Urbanowicz T. Pat. Polski nr 148476, 1991.

Heim A., Rzyski E., Stelmach J. 1995. *Mieszanie z napowietrzaniem. Mieszadła samozasysające.* Inżynieria i aparatura chemiczna. 2: 20–22.

Karcz J. 2001. *Mieszanie układu ciecz-gaz w aparatach z mieszadłem szybkoobrotowym*. Inżynieria i aparatura chemiczna, 1: 3–13.

Koch R., Noworyta A. 1998. *Procesy mechaniczne w inżynierii chemicznej.* WNT, Warszawa, p. 514.

Kowal O. 2001. *Wpływ kawitacji na charakterystyki reologiczne i hydrauliczne potęgowych płynów nienewtonowskich.* Autoreferat pracy doktorskiej, Politechnika Kijowska, Kiev.

Lewicki P., Lanert A., Kowalczyk R., Połacka Z. 1999. *Inżynieria procesowa i aparatura przemysłu spożywczego*. WNT, Warszawa, p. 468.

MOLCHANOV A., WIŚNIEWSKA A., WRÓBLEWSKI A., JACHNO O., KOWAL O. 2003. *Badanie podciśnienia na łopatce samozasysającego mieszalnika śmigłowego do aeracji wody i ścieków.* Referaty VI Konferencji Naukowo-Technicznej „Aktualne problemy naukowo-badawcze budownictwa", Olsztyn – Kortowo, pp. 241–244.

Accepted for print 26.04.2007

TECHNICAL SCIENCES
Abbrev.: Techn. Sc., No 10, Y 2007

DOI 10.2478/v10022-007-0010-8

RELATIONS AMONG STRENGTH AND STRUCTURE OSTEOPOROTIC AND COXARTHROTIC TRABECULAR BONE

Adam Mazurkiewicz, Tomasz Topoliński

Department Mechanicals Egineering and Mechatronics
Uniwesity of Technology and Life Sciences, Bydgoszcz

Key words: trabecular bone, osteoporosis, coxarthrosis, structure, strength.

Abstract

In the paper presented results of measurement of selected coefficients structure and strength of samples of osteoporotic and coxarthrotic human trabecular bone. Analysis of relationships among coefficients in both groups of samples were executed. Aim the work was description of dependence among coefficients, and qualification them of relationship with compression strength of samples of bone.

RELACJE MIĘDZY WYTRZYMAŁOŚCIĄ A STRUKTURĄ OSTEOPOROTYCZNEJ I KOKSARTRYCZNEJ KOŚCI BELECZKOWEJ

Adam Mazurkiewicz, Tomasz Topoliński

Katedra Podstaw Inżynierii Mechanicznej i Mechatroniki
Uniwersytet Technologiczno-Przyrodniczy w Bydgoszczy

Słowa kluczowe: kość beleczkowa, osteoporoza, koksartroza, struktura, wytrzymałość.

Streszczenie

W pracy przedstawiono wyniki pomiarów wybranych wskaźników opisujących strukturę oraz wytrzymałość na ściskanie ludzkiej osteoporotycznej i koksartrycznej kości beleczkowej. Przeprowadzono analizę wzajemnych związków między wskaźnikami struktury oraz wytrzymałością kości w obu badanych grupach kości. Celem pracy było określenie wzajemnych związków między badanymi wskaźnikami struktury oraz określenie ich związków z wytrzymałością kości beleczkowej.

Introduction

Examining construction of bone on structure level, are able to differentiate following tissues: cortical bone called also compact bone, trabecular bone and articular cartiliage. Cortical bone is external part of all bone,

trabecular bone fills interior of long bone and interior of short bone. Articular cartiliage is external layer of bone in places of contact with other bones – joints. Quality of trabecular bone determines strength of all bones. Loss trabeculaes and disturbances them structures, eg. during osteoporosis, leads to diminish strength of bones. Therefore important problem is estimation of coefficients of structure of trabecular bone, which can be base to indirect estimation strength of bone.

Aim the work

Aim the work is qualification of dependences among selected coefficients structure nad strength samples collected with osteoporotic and coxarthrotic human trabecular bone. Executed also description founded dependences mathematical equations.

Sample of trabecular bone

Trabecular bone is porous tissue, which has anizotropy construction and mechanical properties. In dependences from age, and also of kind of disease structure of bone can be composition plates or trabeculaes. From bone material ie. 42 femoral heads (21 osteoporotic and 21 coxarthrotic) gained in result of hip arthroplasty, in first stage were cut out slice from base of head about thickness 8.5 mm, perpendicularly to the axis of neck of bone. Next, from central region of slice were cut out sample in shape of cylinder, about diameter 10 and heights 8.5 mm. Manner of collect and shape of samples presented in figure 1 a÷c.

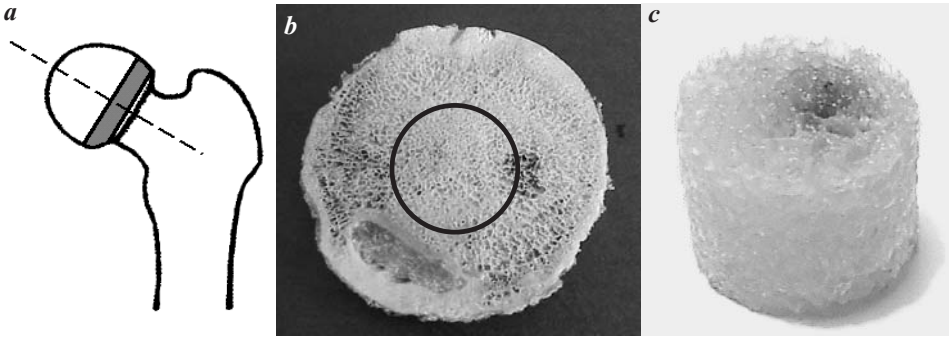

Fig. 1. The schema collect a,b), and shape of samples c)

Coefficients of structure of trabecular bone

To the description of structure of trabecular bone accepted selected coefficients among proposed by Parfitt (Parfitt 1987). The coefficients are universally usaged to estimations of construction of trabecular bone. To investigation accepted following coefficients:

- **Tb.N**, 1/mm – trabecular number – average number continuous trabeculaes on unit area or volume of sample,
- **Tb.Th**, mm – trabecular thickness –average thickness trabecula in sample,
- **Tb.Sp**, mm – trabecular separation – average distance among trabecula in sample (average dimension of pores in sample),
- **TV**, mm^3 – trabecular volume – volume of sample (volume tissue and pores),
- **BV**, mm^3 – bone volume – volume tissue in sample,
- **BS**, mm^2 – bone surface – area tissue in sample,
- **BS/BV**, 1/mm – quotient: bone surface and bone volume,
- **BV/TV**, – quotient: bone volume and trabecular volume,
- **US**, MPa – compression strength.

Methods of the investigations

Measurement of morphological parameters executed at microtomographic system μCT80 at Technological University in Eidhoven - Netherlands. In figure 2 presented typical image of layer of sample of bone received from ěCT80. The device is able to imagining layers of sample distant from oneself about 36 μm. On the base of analysis obtained images and calculations executed at microtographic system obtained values all coefficients with exeption for compression strength. The values of compression strength obtained from mechanical test.

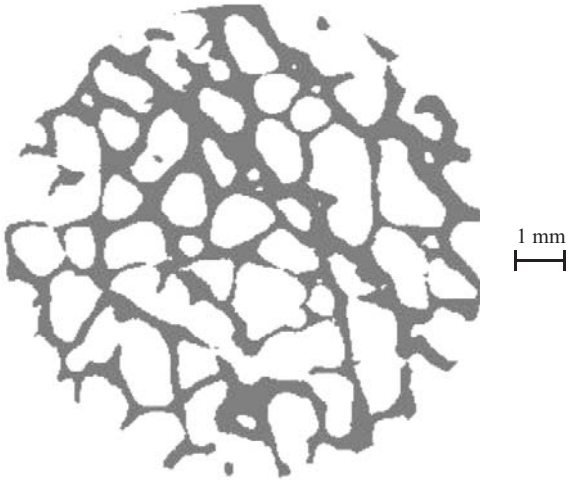

Fig. 2. Typical image of layer of sample obtained from ěCT80 system

Results

In figures 3÷6 presented values of parameters Tb.N, Tb.Th, Tb.Sp and compression strength in function BV/TV. In figures 7÷10 are these same coefficients in function BS/BV. Quotient BV/TV describes ratio content volume of tissue in volume of sample. It is reverse of porosities of sample – porosity is defined as relation of volume of pores to volume of sample. Quotient BS/BV describes ratio extending of structure. If compared two structures about the same tissue volume and different tissue surface can ascertain, that structure about greater surface is structure about smaller thicknesses, but about more extending of architecture. In all figures drew lines of regression, together with equations of regression and values of coefficients of determination.

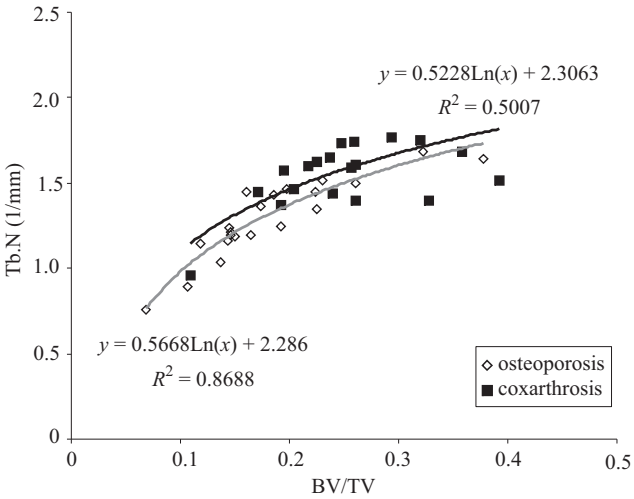

Fig. 3. Graph of values of Tb.N in function BV/TV

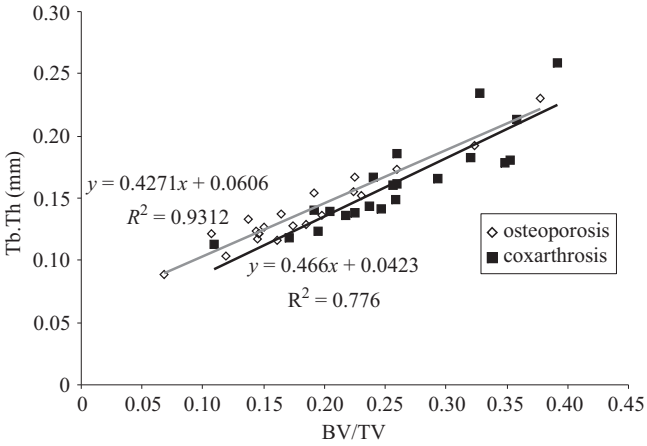

Fig. 4. Graph of values of Tb.Th in function BV/TV

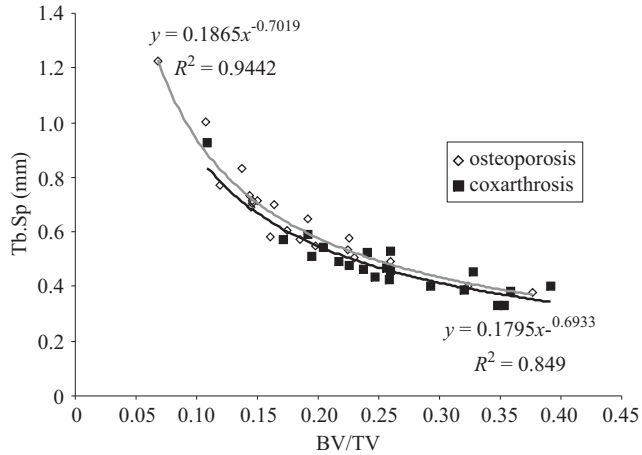

Fig. 5. Graph of values of Tb.Sp in function BV/TV

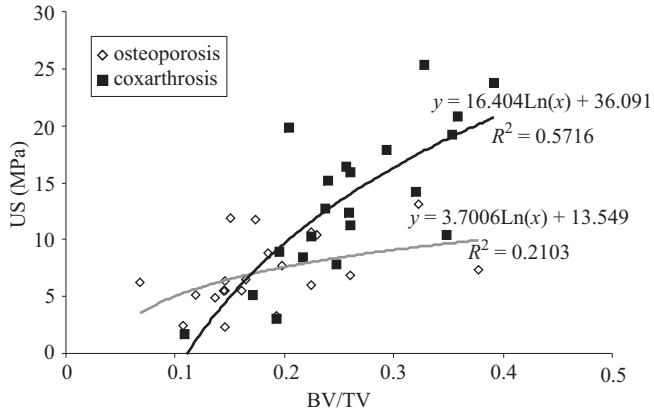

Fig. 6. Graph of compression strength US in function BV/TV

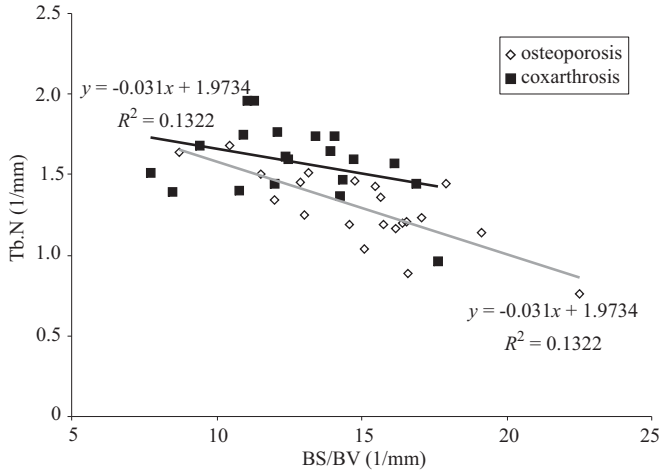

Fig. 7. Graph of values of Tb.N in function BS/BV

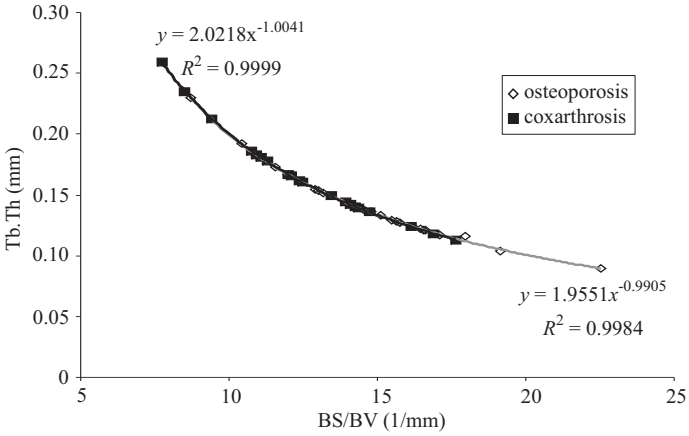

Fig. 8. Graph of values of Tb.Th in function BS/BV

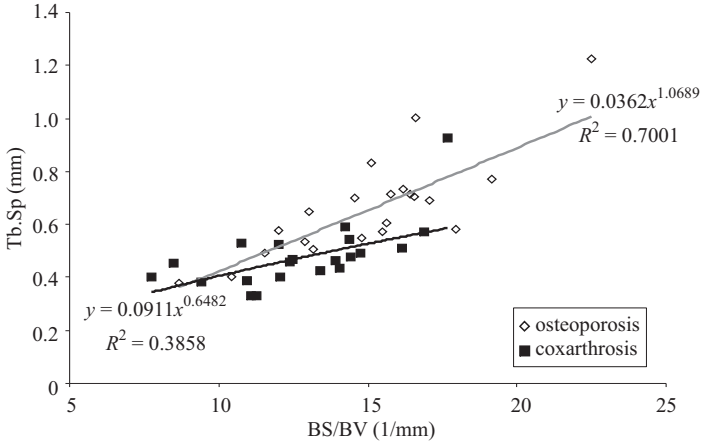

Fig. 9. Graph of values of Tb.Sp in function BS/BV

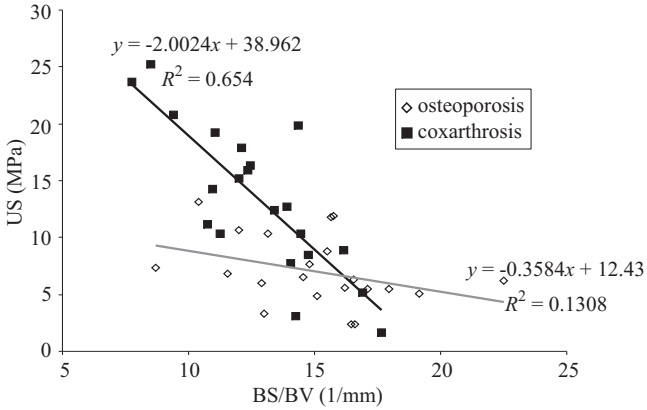

Fig. 10. Graph of compression strength US in function BS/BV

Discussion

Analysing figures 3÷4 are visible distinct relationships among number continuous trabeculaes and average thickness of trabecula for osteoporotic samples. Coefficient of determination achieved value 0.93. For coxarthrotic samples the value are lower, however do not come down below 0.5. In both cases for greater "amount bone in bone" number of trabeculaes is greater – describing equation is logarithmic – and at values BV/TV below 0.2÷0.25 dynamics this grow to diminish. Relationship among thickness of trabecula and "amount bone in bone" was linear in examined material. The results of investigations pointed, that osteoporotic bone has less number continuous trabeculaes at greater average thickness of trabeculae than coxarthotic bone. Simultaneously increase walues of BV/TV marks diminish of distance among trabeculaes, and dynamics this grow to diminishing. Description this relationship about high values of coefficient of determination R^2=0.84 for coxarthrotic samples, R^2=0.94 for osteoporotic samples – is possible to description power function about power less than one – at small differences among osteoporotic and coxarthrotic bone.

Increasing "amount bone in bone" for coxarthrotic bone means increase of strength – drawing 6. For osteoporotic bone about less number continuous trabeculaes and greater distance among trabeculaes in all range of changes BV/TV – is not relationship between strength and BV/TV, at weakly tendency of height of strength at increase BV/TV, and visible difference of between both groups of samples. This ascertainment leading to conclusion about lack of relationship between Tb.N, Tb.Th, Tb.Sp and compression strength of bones.

Considering regular structure can ascertain, that conversion structure from structure about large thicknesses of trabeculaes to structure about greater number and smaller thicknesses of trabeculaes lead to increasing BS/BV, what confirmed results presented in figure 8, for both groups of samples. Osteoporotic damages of structure lead to damages greater numbers of trabeculaes than more the stucture is crumbled – figure 7, in effect lead to increasing distance among trabeculaes – figure 9. In case coxarthrotic bone this relationship don't appeared.

In case coxarthrotic samples increasing values BS/BV lead to decrease of strength – figure 10, described linear equation about coefficient of determination R^2=0.65. For osteoporotic samples don't exist the relationship – coefficient of determination about value R^2=0.13 points on irregularities of damages of structure.

Conclusions

Value of BV/TV gives informations about degree fulfilments of structure called "amount bone in bone" what often is pointed in descriptions and diagnosis of osteoporosis. For examined samples the coefficient has value from above 0.05 to near 0.4. At increasing the value in very similar manner for both examined group of samples increasing linearly Tb.N and Tb.Th and decreasing Tb.Sp. However values above-mentioned of coefficients are similar at these same values BV/TV, strength both kinds of bones can be different. It can be result this, that about strength of samples decides not only values of BV/TV, but also structure and properties trabecular bone in idividual persons. In spite collected of samples from the same place of femoral heads (Mazurkiewicz 2003), difficulty directly to take into account direction trabeculaes structure as individual feature of peoples, which is result for example their life activities.

Value BS/BV gives informations about degree of extending (crumbling) structure of bone. With increasing of crumbling should growing Tb.N diminish Tb.Th and Tb.Sp. Results of investigations not exactly confirm this ascertainment. Decrease Tb.Th is observed, don't observed increase Tb.N and Tb.Sp. It can be result this, that Tb.N is number continuous trabeculaes - having supported two ends. Only such trabeculaes can carrying the loads. In the investigations examined samples of bone collected from people with osteoporosis and coxarthrosis, what causes, that structure of samples is irregular as consequence of the diseases. Even in case crumbling structures number propperly trabeculaes in the sample isn't to large, what causes that distances among them also are large. It is visible on example of osteoprotic samples where, increase Tb.Sp and decrease Tb.N is more distinct, than in coxarthrotic samples. Influence of changes BS/BV on strength isn't easy to interpretation, but is visible, that is more significant for coxarthrotic than osteoporotic samples.

In further analysises, should be use not single coefficients but them double or triple combinations, what should lead to improvement obtained results.

References

Mazurkiewicz A., Pakuła M. 2003. *The estimations of Young's modulus of trabecular bone.* 4th International Conference of PHD Students, Miszkolc – Hungary.

Parfitt M. et. al. 1987. *Bone histomorphometry: Standarization of nomenclature, symbols and units*. Journal of Bone and Mineral Research, 6.

Accepted for print 10.05.2007

TECHNICAL SCIENCES
Abbrev.: Techn. Sc., No 10, Y 2007

DOI 10.2478/v10022-007-0011-7

THE SINGULARITIES AT THE VICINITY OF THE TRIPLE POINT OF CONTACT OF THREE ORTHOTROPIC WEDGES IN PLANE ELASTICITY

Aleksandra Wieromiej-Ostrowska

Department of Technological and Computer Science Education
University of Warmia and Mazury in Olsztyn

Key words: anisotropic elasticity, stress singularities.

Abstract

The particular problem of the order of singularity at the vicinity of the triple point of contact of three wedges made of the same (rotated) materials is considered.

The order of singularity λ changes with the change of the opening angle φ and the wedge rotation angle ψ of at least one material. Relations λ–φ for different sets of elastic constants corresponding to the composites of the epoxy resin and kevlar fiber, epoxy resin and boron fiber and the real metallic cubic crystal (aluminium and tungsten) have been studied. The real solutions were taken into considerations only.

General cases of the lack of symmetry were considered. Modes of stress distribution for different values of λ were found. It is not difficult to notice that neither of them describes symmetric nor skew-symmetric stress field.

RZĄD OSOBLIWOŚCI W OTOCZENIU WIERZCHOŁKA POTRÓJNEGO PUNKTU KONTAKTU TRZECH KLINÓW W PŁASKIM ZAGADNIENIU TEORII SPRĘŻYSTOŚCI

Aleksandra Wieromiej-Ostrowska

Zakład Edukacji Technicznej i Informatycznej
Uniwersytet Warmińsko-Mazurski w Olsztynie

Słowa kluczowe: anizotropia sprężysta, osobliwości pól naprężeń.

Streszczenie

W pracy rozpatrzono problem rzędu osobliwości λ w otoczeniu wierzchołka potrójnego punktu kontaktu trzech klinów wykonanych z tych samych (obróconych) lub rożnych ortotropowych materiałów linowo sprężystych. Zbadano przebiegi zmienności rzędu osobliwości λ ze zmianą kąta rozwarcia klina φ przy różnych kątach obrotu ψ przynajmniej jednego z materiałów i dla różnych kombinacji stałych sprężystych odpowiadających takim materiałom, jak: kompozyt żywicy epoksydowej i włókna kewlarowego, kompozyt żywicy epoksydowej

i włókna borowego, rzeczywisty kryształ metaliczny w układzie regularnym (aluminium i wolfram). Poszukiwano rozwiązań o rzeczywistych wartościach λ.

Dla wybranego przypadku niesymetrycznego znaleziono rozkłady naprężeń odpowiadających wartościom λ. Rozkłady te nie wykazywały symetrii ani antysymetrii.

Introduction

Strength of singularity at the tip of the orthotropic wedge embedded into infinite two-dimensional elastic orthotropic body was considered in the Part One of the previous paper (Blinowski and Wieromiej-Ostrowska (2005)). Considerations were restricted to the wedges symmetrically oriented with respect to the axes of orthotropy. They concerned mainly, the relations between the order of singularity and the wedge opening angle and/or elastic properties of materials. Mixed boundary value conditions were assumed: continuity of both, tractions and displacements at the interfaces was demanded.

Two modes of the stress distribution corresponding to different values of λ: symmetric and skew-symmetric were found. For the case of nearly isotropic materials the quantitive results roughly repeated these obtained by the authors for isotropic materials reported in the paper by Blinowski and Wieromiej (2004), where the symmetries of solutions were assumed in advance.

In the Part Two of the mentioned paper the considerations were generalized on the wedges arbitrarily oriented with respect to the axes of orthotropy and on the complex solutions $\lambda = a + ib$ as well.

It was found that the real solutions for λ are solitary in the complex plane, no complex solutions corresponding to the finite elastic energy in the vicinity of the wedge tip ($0 \leqslant \mathrm{Re}\lambda \leqslant 2$) were found.

The particular problem of the order of singularity at the vicinity of the triple point of contact of three wedges made of the same (rotated) materials is considered in the present paper. Solution of such a problem may bring a valuable contribution into understanding of material fatigue process. Mathematical treatment of such a problem does not differ from the used in the previous papers by Blinowski and Wieromiej-Ostrowska (2005) and (2007). The only difference consists in the use of larger 12 x 12 matrices.

Formulation of the boundary value problem

As it has been already mentioned, we shall focus our attention in the present paper on the mixed boundary value problem assuming continuity of displacement fields as well as the normal and tangential stresses at the interfaces in the vicinity of the point of contact of three wedges.

We shall consider the general non-symmetric problems: compare Figure 1. All quantities in the domain of the first material will be noted using the

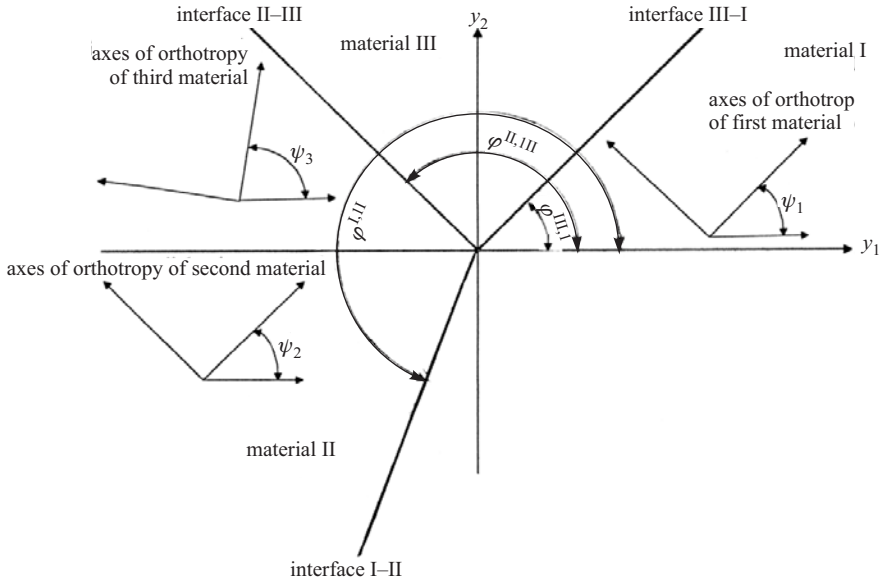

Fig. 1. Orientation of the triple point of contact of three wedges made of the same (rotated) or different materials with respect to the observer frame axes
– ($\varphi^{I,II} - \psi^{I}$) the angle between the first material axis of ortothropy and I–II interface
– ($\varphi^{I,II} - \psi^{II}$) the angle between the second material axis of ortothropy and I–II interface
– ($\varphi^{II,III} - \psi^{II}$) the angle between the second material axis of ortothropy and II–III interface
– ($\varphi^{II,III} - \psi^{III}$) the angle between the third material axis of ortothropy and II–III interface
– ($\varphi^{III,I} - \psi^{III}$) the angle between the third material axis of ortothropy and III–I interface
– ($\varphi^{III,I} - \psi^{I}$) the angle between the first material axis of ortothropy and III–I interface.

Roman number one (I), while for the second and third material indices II and III will be used.

The complete set of the boundary value conditions must be taken as follows:

$$\left.\begin{aligned} u^{I}_{rI,II} - u^{II}_{rI,II} = 0 \\ u^{I}_{\varphi I,II} - u^{II}_{\varphi I,II} = 0 \end{aligned}\right\} \text{– displacement continuity for I–II interface}$$

$$\left.\begin{aligned} \sigma^{I}_{\varphi\varphi I,II} - \sigma^{II}_{\varphi\varphi I,II} = 0 \\ \sigma^{I}_{r\varphi I,II} - \sigma^{II}_{r\varphi I,II} = 0 \end{aligned}\right\} \text{– traction continuity for II–I interface}$$

$$\left.\begin{aligned} u^{II}_{rII,III} - u^{III}_{rII,III} = 0 \\ u^{II}_{\varphi II,III} - u^{III}_{\varphi II,III} = 0 \end{aligned}\right\} \text{– displacement continuity for II–III interface} \quad (1)$$

$$\left.\begin{aligned}\sigma^{II}_{\varphi\varphi II,III}-\sigma^{III}_{\varphi\varphi II,III}=0\\ \sigma^{II}_{r\varphi II,III}-\sigma^{III}_{r\varphi II,III}=0\end{aligned}\right\}\text{– traction continuity for II–III interface}$$

$$\left.\begin{aligned}u^{III}_{rIII,I}-u^{I}_{rIII,I}=0\\ u^{III}_{\varphi III,I}-u^{I}_{\varphi III,I}=0\end{aligned}\right\}\text{– displacement continuity for III–I interface}$$

$$\left.\begin{aligned}\sigma^{III}_{\varphi\varphi III,I}-\sigma^{I}_{\varphi\varphi III,I}=0\\ \sigma^{III}_{r\varphi III,I}-\sigma^{I}_{r\varphi III,I}=0\end{aligned}\right\}\text{– traction continuity for III–I interface}$$

where $\sigma_{\varphi\varphi}$ and $\sigma_{r\varphi}$ are the transversal and tangential stresses in polar coordinates, while u_r and u_φ denote the radial and transversal components of the displacement field.

Conditions (1) and relations (29) from the paper of Blinowski and Wieromiej-Ostrowska (2005) generate the following homogenous system of twelve equations for the determination of the unknown multipliers in the linear combinations of four particular solutions (A_1, A_2, B_1, B_2) for the all three materials I, II, III.

$$\underline{\mathbf{A}}\ \underline{\mathbf{x}}=0 \tag{2}$$

where $\underline{\mathbf{x}}=\begin{bmatrix}A_1^I\\ B_1^I\\ A_2^I\\ B_2^I\\ A_1^{II}\\ B_1^{II}\\ A_2^{II}\\ B_2^{II}\\ A_1^{III}\\ B_1^{III}\\ A_2^{III}\\ B_2^{III}\end{bmatrix}$

Regarding the terms of the matrix **A** – see Appendix.

Results and conclusions

As one can expect the order of singularity λ changes with the change of the wedge opening angle φ and of the wedge rotation angle ψ of at least one material. Calculations have been done for different values of the elastic constants corresponding to some composites: epoxy resin and kevlar fiber, epoxy resin and boron fiber and for the real metallic cubic crystal (aluminium and tungsten). The real solutions only were taken into considerations.

Some particular problems were solved. For the first of them the elastic properties of material corresponded to the composite of the epoxy resin and kevlar fiber. The wedge opening angle φ_1 of the first material varied within the interval $\varphi_1 \in \left(0, \frac{\pi}{2}\right)$. For the second material the opening angle was taken $\varphi_2 = \pi$, for the third material the opening angle varied corresponding to change of the first one ($\varphi_1 + \varphi_3 = \pi$)[1]. The first material was symmetrically oriented with respect to the symmetry plane of the body, the second material of the wedge was rotated by the angle $\psi_2 = \frac{2}{3}\pi$, while the third material was rotated by the angle $\psi_3 = -\frac{2}{3}\pi$. For given angles of rotation a single solutions only for the wedge opening angles φ_1 within the interval $\left(\frac{\pi}{12}, \frac{\pi}{2}\right)$ was found, while no solutions for φ_1 within interval $\left(0, -\frac{\pi}{12}\right)$ was observed, see Figure 2.

Similar problem for the same material and different angle $\psi_1 = \frac{\pi}{2}$ was studied. No solution was observed in this case.

The same problem was considered for composite of epoxy resin and boron fiber and no results were obtained.

For the case of the boron-epoxy composite and the geometry corresponding to the first problem double solution for the wedge opening angles $\varphi_1 \in (0.18, 0.7)$ were found. For $\varphi_1 \in (0.04, 0.18)$ and $\varphi_1 \in (0.18, 0.7)$ single solutions were found while no solutions were observed at the remaining part of the interval $\left(0, \frac{\pi}{2}\right)$, see Figure 2.

---

[1] We adopt the following notation:
$\varphi_1 = \varphi^{I,II} - \varphi^{I,III}$, $\varphi_2 = \varphi^{I,II} - \varphi^{II,III}$, $\varphi_3 = \varphi^{II,III} - \varphi^{I,III}$.

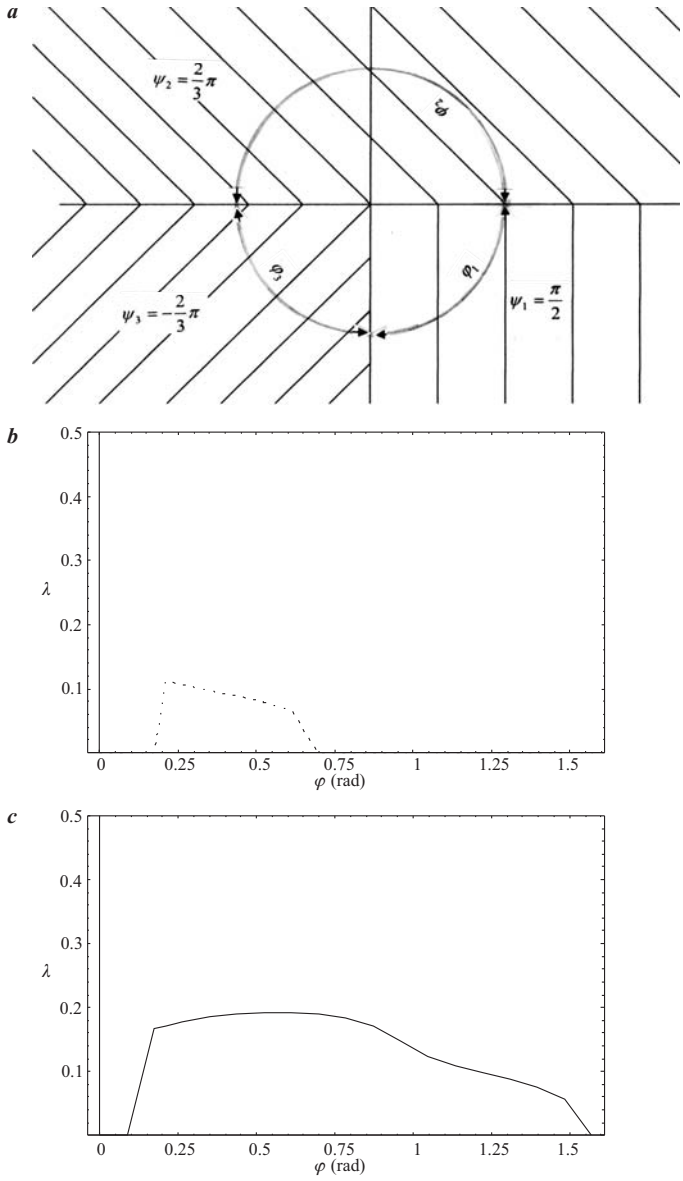

Fig. 2. The point of contact of three wedges made of the same (rotated) materials corresponding to the composite of the epoxy resin and boron fiber, compare Table 1.
The order of singularity λ versus opening angles φ, and given wedge rotation angles ψ.

Tabel 1

Elastic constans	E_1	E_2	γ_1	γ_2	γ_3
Material I	266.9	16.6	1.05	3.79	2.82
Elastic constans	E_1	E_2	γ_1	γ_2	γ_3
Material II	66.5	9	0.6	4.51	3.27

For the same case with the first material rotated by $\frac{\pi}{2}$, the results were qualitatively similar: compare Figure 3. This makes a difference with respect to the case of kevlar-epoxy composite, where solutions disappeared under such a rotation.

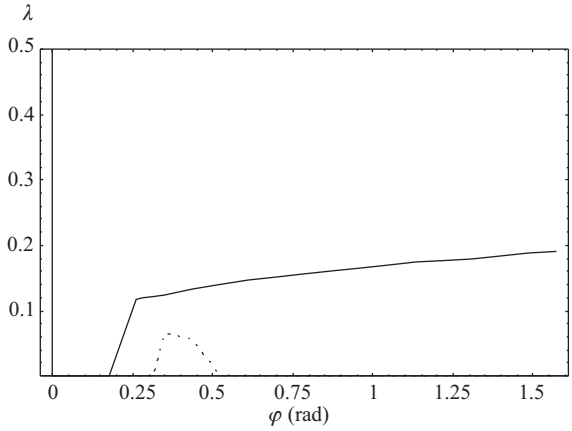

Fig. 3. The point of contact of three wedges made of the same (rotated) materials corresponding to the composite of the epoxy resin and boron fiber, compare Table 1.
The order of singularity λ versus opening angles φ, and given wedge rotation angles ψ.

For the case of the real metallic cubic crystal (aluminium and tungsten), where the point of contact of three wedges made of the same (rotated) materials was considered, under the same geometry as in the problem depicted in the Figure 4. No real solution for λ from the interval (0,1) corresponding to finite elastic energy was observed.

For the symmetric problems considered in paper Blinowski and Wieromiej-Ostrowska (2005) the symmetric and skew-symmetric distributions of stress have been found, while for the non- symmetric problems (considered in paper Blinowski and Wieromiej-Ostrowska (2007)) two non-symmetric distributions of stress have been found.

In the present paper the lack of symmetry of the boundary value problem yields two non-symmetric solutions as well.

For the case of the point of contact of three wedges made of the same materials corresponding to epoxy-boron composite for the first wedge opening angle $\varphi_1 = \frac{5}{36}\pi$, the second wedge opening angle $\varphi_2 = \pi$ and the first material of the wedge rotated by the angle $\psi_1 = \frac{\pi}{2}$, the second material of the wedge rotated by the angle $\psi_2 = \frac{2}{3}\pi$, while the third material of the

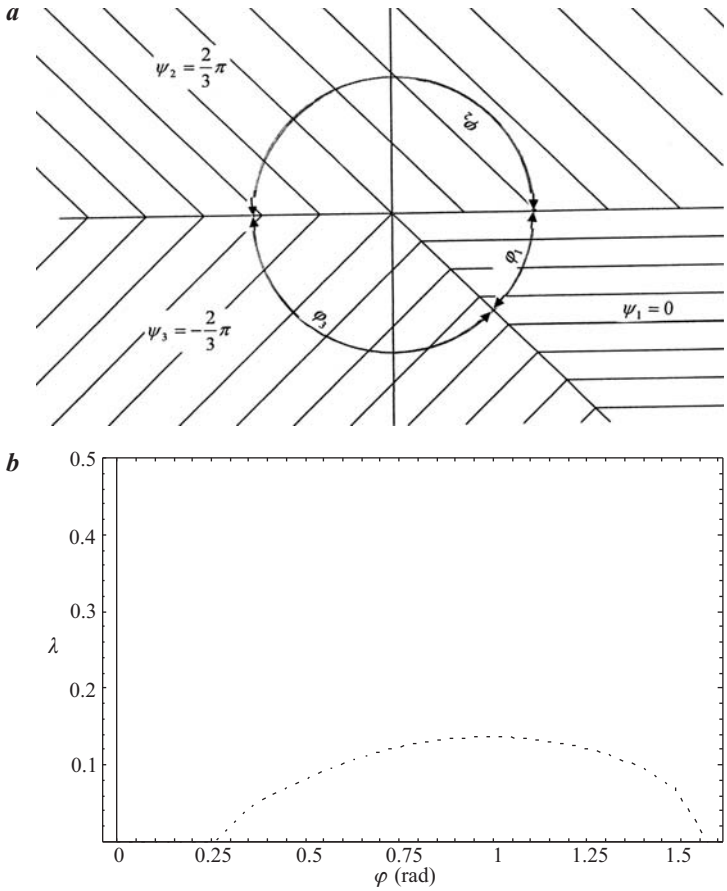

Fig. 4. The point of contact of three wedges made of the same (rotated) materials corresponding to the composite of the epoxy resin and kevlar fiber, compare Table 2.
The order of singularity λ versus opening angles φ, and given wedge rotation angles ψ.

Tabel 2

Elastic constans	E_1	E_2	γ_1	γ_2	γ_3
Material I	91.1	15.87	0.59	4.01	2.92
Elastic constans	E_1	E_2	γ_1	γ_2	γ_3
Material II	91.1	15.87	0.59	4.01	2.92

wedge was rotated by the angle $\psi_3 = -\frac{2}{3}\pi$ one obtains: $\lambda_1 = 0.088$, while the corresponding eigenvector is the following:
$[0.10;-0.58;0.04;-0.006;0.21;-0.17;0.05;0.001;-0.08;-0.74;0.009;-0.002]$[2], for the se-

[2] Zeros at the even positions in eigenvectors of the matrix **A** describe the symmetric stress of distribution, while zeros of the odd positions corresponds to skew-symmetric of the stress field.

cond value of $\lambda_2 = 0.189$ the corresponding eigenvector looks as follows: $[-0.30; -0.47; 0.01; 0.02; -0.56; -0.36; 0.03, 0.012; 0.28; -0.37; -0.02; 0.019]$, compare Figure 3. It is not difficult to notice that neither of them describes symmetric nor skew-symmetric stress field.

From the results mentioned above no firm conclusions concerning the existence and the number of solutions as well as for the strength of the singularities can be formulated at the present stage of study of that subject. For particular combinations of the materials employed in engineering constructions the problems must be separately solved for every case under consideration.

References

Blinowski A., Ostrowska-Maciejewska J. 1995. *On the stress distribution in bending of strongly anisotropic beams,* Engng.Trans., 43: 1–2, 83–89.

Blinowski A., Wieromiej A. 2004. *Singular stress in the vicinity of a sharp inclusion in an elastic matrix,* Techn. Sc., 7: 159–174.

Blinowski A., Wieromiej-Ostrowska *A*. 2005. *On the singularities at the tips of the orthotropic wedges in plane elasticity.* Part One, Techn. Sc., 8: 107–124.

Blinowski A., Wieromiej-Ostrowska *A*. 2006. *On the singularities at the tips of the orthotropic wedges in plane elasticity.* Part Two, Techn. Sc., 9:65–72.

Śleziona J. 1998. *Podstawy technologii kompozytów.* Wydawnictwo Politechniki Śląskiej, Gliwice.

Nye J.F. 1962. *Własności fizyczne kryształów.* PWN, Warszawa.

Seweryn A. 1997. *Kumulacja uszkodzeń i pękanie elementów konstrukcyjnych w złożonych stanach obciążeń.* Białystok.

Seweryn A., Molski K. 1996. *Elastic stress singularities and corresponding generalized stress intensity factors for angular corners under various boundary conditions.* Engineering Fracture Mechanics, 55: 529–556.

Accepted for print 21.09.2007

Appendix

For reference, we shall expose here explicit expressions for the components of the matrix **A.** For the sake of brevity we shall subdivide our matrix into nine square submatrices as follows:

$$\underline{\mathbf{A}} = \begin{bmatrix} \mathbf{A}^1 & \mathbf{A}^2 & 0 \\ 0 & \mathbf{A}^3 & \mathbf{A}^4 \\ \mathbf{A}^5 & 0 & \mathbf{A}^6 \end{bmatrix},$$

For submatrix $\mathbf{A^1}$ one can write:

$$A_{11} = -\begin{bmatrix} \dfrac{-\left(\gamma_1^I\right)^2 + \left(\gamma_2^I\right)^2 - 2\left(\gamma_3^I\right)^2}{\gamma_2^I} \operatorname{Im}\left(\varphi^{I,II} - \psi^I, 1-\lambda, \gamma_1^I\right)\cos\left(\varphi^{I,II} - \psi^I\right) + \\ \gamma_1^I \dfrac{\left(\gamma_1^I\right)^2 - \left(\gamma_2^I\right)^2 - 2\left(\gamma_3^I\right)^2}{\gamma_2^I} \operatorname{Re}\left(\varphi^{I,II} - \psi^I, 1-\lambda, \gamma_1^I\right)\sin\left(\varphi^{I,II} - \psi^I\right) \end{bmatrix} / E^I,$$

$$A_{12} = -\begin{bmatrix} \dfrac{-\left(\gamma_1^I\right)^2 + \left(\gamma_2^I\right)^2 - 2\left(\gamma_3^I\right)^2}{\gamma_2^I} \operatorname{Re}\left(\varphi^{I,II} - \psi^I, 1-\lambda, \gamma_1^I\right)\cos\left(\varphi^{I,II} - \psi^I\right) - \\ \gamma_1^I \dfrac{\left(\gamma_1^I\right)^2 - \left(\gamma_2^I\right)^2 - 2\left(\gamma_3^I\right)^2}{\gamma_2^I} \operatorname{Im}\left(\varphi^{I,II} - \psi^I, 1-\lambda, \gamma_1^I\right)\sin\left(\varphi^{I,II} - \psi^I\right) \end{bmatrix} / E^I,$$

$$A_{13} = -\begin{bmatrix} \dfrac{\left(\gamma_1^I\right)^2 - \left(\gamma_2^I\right)^2 - 2\left(\gamma_3^I\right)^2}{\gamma_1^I} \operatorname{Im}\left(\varphi^{I,II} - \psi^I, 1-\lambda, \gamma_2^I\right)\cos\left(\varphi^{I,II} - \psi^I\right) + \\ \gamma_2^I \dfrac{-\left(\gamma_1^I\right)^2 + \left(\gamma_2^I\right)^2 - 2\left(\gamma_3^I\right)^2}{\gamma_1^I} \operatorname{Re}\left(\varphi^{I,II} - \psi^I, 1-\lambda, \gamma_2^I\right)\sin\left(\varphi^{I,II} - \psi^I\right) \end{bmatrix} / E^I,$$

$$A_{14} = -\begin{bmatrix} \dfrac{\left(\gamma_1^I\right)^2 - \left(\gamma_2^I\right)^2 - 2\left(\gamma_3^I\right)^2}{\gamma_1^I} \operatorname{Re}\left(\varphi^{I,II} - \psi^I, 1-\lambda, \gamma_2^I\right)\cos\left(\varphi^{I,II} - \psi^I\right) \\ -\gamma_2^I \dfrac{-\left(\gamma_1^I\right)^2 + \left(\gamma_2^I\right)^2 - 2\left(\gamma_3^I\right)^2}{\gamma_1^I} \operatorname{Im}\left(\varphi^{I,II} - \psi^I, 1-\lambda, \gamma_2^I\right)\sin\left(\varphi^{I,II} - \psi^I\right) \end{bmatrix} / E^I,$$

$$A_{21} = \begin{bmatrix} \dfrac{-\left(\gamma_1^I\right)^2 + \left(\gamma_2^I\right)^2 - 2\left(\gamma_3^I\right)^2}{\gamma_2^I} \operatorname{Im}\left(\varphi^{I,II} - \psi^I, 1-\lambda, \gamma_1^I\right)\sin\left(\varphi^{I,II} - \psi^I\right) - \\ \gamma_1^I \dfrac{\left(\gamma_1^I\right)^2 - \left(\gamma_2^I\right)^2 - 2\left(\gamma_3^I\right)^2}{\gamma_2^I} \operatorname{Re}\left(\varphi^{I,II} - \psi^I, 1-\lambda, \gamma_1^I\right)\cos\left(\varphi^{I,II} - \psi^I\right) \end{bmatrix} / E^I,$$

$$A_{22} = \begin{bmatrix} \dfrac{-\left(\gamma_1^I\right)^2 + \left(\gamma_2^I\right)^2 - 2\left(\gamma_3^I\right)^2}{\gamma_2^I} \operatorname{Re}\left(\varphi^{I,II} - \psi^I, 1-\lambda, \gamma_1^I\right)\sin\left(\varphi^{I,II} - \psi^I\right) + \\ \gamma_1^I \dfrac{\left(\gamma_1^I\right)^2 - \left(\gamma_2^I\right)^2 - 2\left(\gamma_3^I\right)^2}{\gamma_2^I} \operatorname{Im}\left(\varphi^{I,II} - \psi^I, 1-\lambda, \gamma_1^I\right)\cos\left(\varphi^{I,II} - \psi^I\right) \end{bmatrix} / E^I,$$

$$A_{23}=\begin{bmatrix}\dfrac{\left(\gamma_1^I\right)^2-\left(\gamma_2^I\right)^2-2\left(\gamma_3^I\right)^2}{\gamma_1^I}\operatorname{Im}\left(\varphi^{I,II}-\psi^I,1-\lambda,\gamma_2^I\right)\sin\left(\varphi^{I,II}-\psi^I\right)- \\ \gamma_2^I\dfrac{-\left(\gamma_1^I\right)^2+\left(\gamma_2^I\right)^2-2\left(\gamma_3^I\right)^2}{\gamma_1^I}\operatorname{Re}\left(\varphi^{I,II}-\psi^I,1-\lambda,\gamma_2^I\right)\cos\left(\varphi^{I,II}-\psi^I\right)\end{bmatrix}/E^I,$$

$$A_{24}=\begin{bmatrix}\dfrac{\left(\gamma_1^I\right)^2-\left(\gamma_2^I\right)^2-2\left(\gamma_3^I\right)^2}{\gamma_1^I}\operatorname{Re}\left(\varphi^{I,II}-\psi^I,1-\lambda,\gamma_2^I\right)\sin\left(\varphi^{I,II}-\psi^I\right)+ \\ \gamma_2^I\dfrac{-\left(\gamma_1^I\right)^2+\left(\gamma_2^I\right)^2-2\left(\gamma_3^I\right)^2}{\gamma_1^I}\operatorname{Im}\left(\varphi^{I,II}-\psi^I,1-\lambda,\gamma_2^I\right)\cos\left(\varphi^{I,II}-\psi^I\right)\end{bmatrix}/E^I,$$

$$A_{31}=-\gamma_1^I\operatorname{Im}\left(\varphi^{I,II}-\psi^I,2-\lambda,\gamma_1^I\right),$$

$$A_{32}=-\gamma_1^I\operatorname{Re}\left(\varphi^{I,II}-\psi^I,2-\lambda,\gamma_1^I\right),$$

$$A_{33}=-\gamma_2^I\operatorname{Im}\left(\varphi^{I,II}-\psi^I,2-\lambda,\gamma_2^I\right),$$

$$A_{34}=-\gamma_2^I\operatorname{Re}\left(\varphi^{I,II}-\psi^I,2-\lambda,\gamma_2^I\right),$$

$$A_{41}=\left[\left(\gamma_1^I\right)^2\operatorname{Re}\left(\varphi^{I,II}-\psi^I,1-\lambda,\gamma_1^I\right)\cos\left(\varphi^{I,II}-\psi^I\right)-\gamma_1^I\operatorname{Im}\left(\varphi^{I,II}-\psi^I,1-\lambda,\gamma_1^I\right)\sin\left(\varphi^{I,II}-\psi^I\right)\right],$$

$$A_{42}=-\left[\left(\gamma_1^I\right)^2\operatorname{Im}\left(\varphi^{I,II}-\psi^I,1-\lambda,\gamma_1^I\right)\cos\left(\varphi^{I,II}-\psi^I\right)+\gamma_1^I\operatorname{Re}\left(\varphi^{I,II}-\psi^I,1-\lambda,\gamma_1^I\right)\sin\left(\varphi^{I,II}-\psi^I\right)\right],$$

$$A_{43}=\left[\left(\gamma_2^I\right)^2\operatorname{Re}\left(\varphi^{I,II}-\psi^I,1-\lambda,\gamma_2^I\right)\cos\left(\varphi^{I,II}-\psi^I\right)-\gamma_2^I\operatorname{Im}\left(\varphi^{I,II}-\psi^I,1-\lambda,\gamma_2^I\right)\sin\left(\varphi^{I,II}-\psi^I\right)\right],$$

$$A_{44}=-\left[\left(\gamma_2^I\right)^2\operatorname{Im}\left(\varphi^{I,II}-\psi^I,1-\lambda,\gamma_2^I\right)\cos\left(\varphi^{I,II}-\psi^I\right)+\gamma_2^I\operatorname{Re}\left(\varphi^{I,II}-\psi^I,1-\lambda,\gamma_2^I\right)\sin\left(\varphi^{I,II}-\psi^I\right)\right],$$

The elements of remaining submatrices can be obtained easily by the following modifications of matrix $\mathbf{A^1}$:

- for matrix $\mathbf{A^2}$ variables E^I ψ^I, γ_1^I,γ_2^I should be replaced with E^{II} ψ^{II}, $\gamma_1^{II},\gamma_2^{II}$ and signs of all terms should be changed;
- matrix $\mathbf{A^3}$ can be obtained from $\mathbf{A^1}$ by replacing variable $\varphi^{I,II}$ with $\varphi^{II,III}$ and variables E^I ψ^I, γ_1^I,γ_2^I should be replaced with E^{II} ψ^{II}, $\gamma_1^{II},\gamma_2^{II}$;

- for $\mathbf{A^4}$ one should replace in $\mathbf{A^2}$ variable $\varphi^{I,II}$ with $\varphi^{II,III}+2\pi$ and variables E^{II} ψ^{II}, γ_1^{II}, γ_2^{II} should be replaced with E^{III} ψ^{III}, γ_1^{III}, γ_2^{III};
- matrix $\mathbf{A^5}$ can be obtained from $\mathbf{A^1}$ by replacing variable $\varphi^{I,II}$ with $\varphi^{III,I}$;
- matrix $\mathbf{A^6}$ can be obtained from $\mathbf{A^2}$ by replacing variable $\varphi^{I,II}$ with $\varphi^{III,I}$ and variables E^{II} ψ^{II}, γ_1^{II}, γ_2^{II} should be replaced with E^{III} ψ^{III}, γ_1^{III}, γ_2^{III}.

Reviewers

Janusz Badur, Jan Bagieński, Oleh Klyus, Marek Matczyński,
Janusz Podleśny, Tadeusz Rawa, Dagmara Tejszerska,
Zdzisław Wójcicki